Signaling mechanisms and developmental function of fibroblast growth factor receptors in zebrafish

Dissertation

zur Erlangung des akademisches Grades
Doctor rerum naturalium (Dr. rer. nat.)

vorgelegt
der Fakultät Mathematik und Naturwissenschaft
der Technischen Universität Dresden

von
Maria Elzbieta Kolanczyk
geboren am 06.02.1980 in Gdansk, Polen

Gutachter: Prof. Dr. Michael Brand
Prof. Dr. Matthias Hammerschmidt
Dr. Suzanne Eaton

Eingereicht am: 19.02.2009
Tag der Verteidigung:

Table Of Contents

Index Of Figures

Acknowledgements

First of all I would like to thank my supervisor Michael Brand for the opportunity to work in his lab and to learn about zebrafish development, science and life. Now I know that PhD, doctor of philosophy, is called like this for a reason. I should also thank my thesis advisors, Suzanne Eaton and Petra Schwille for their feedback and being great role models of women in science.

I would like to extend my gratitude to all those who helped me greatly during my time in the lab. I thank Alexander Picker for introducing me into the world on zebrafish embryology and for his criticism, which allowed me to critically assess my work but also made me tougher. I would like to thank Matthias Nowak for all discussions and smiles, and for critically reading this thesis. Big thank you to Heiner Grandel, whose contagious enthusiasm and undying curiosity were both, an inspiration and a motivating force in my studies.

I would like to thank my colleagues from Tubingen, Nicolas Rohner and Mathew Harris for their openness, trust and harmonious collaboration.

I would like to thank Stefan Hans and Marta Luz for a lot of help, discussions and support during the last phases of my work. My heartfelt thanks go also to Rachel Yu and Anja Machate, my benchwork companions, for all their help, sharing reagents and their experience with me.

I would especially like to thank Julia Ganz and Volker Kroehne for being such supportive friends all these years, for putting up with my mood swings and for keeping my spirit up even in most difficult times.

To all my Dresden friends, especially Julia, Natalya, Mikolaj, Philipp, Jens, Matthias, Alex and Violeta – thank you for all the laughs, dances, deep and shallow discussions, support and love I could count on every step of the way. You guys are an amazing bunch!

I wouldn't be here and I wouldn't be the person I am without my loving family. I would like to thank my mother for inspiring a scientist in me, for teaching me about myself and about the nature of people's minds. I thank my father for his unconditional love, support and for teaching me some important lessons about tolerance and consequence in relations with other people. I would like to thank my little brother for his love and support and my big brother for his guidance and protection. Without you, Mateusz, and your beautiful family, I wouldn't be whole.

I would like to thank Eron for all his love, monkey dances and his self-deprecating sense of humor, which reliably distanced me to all the problems of this world.

I dedicate this work to the memory of my grandfather Jerzy, who had a strong influence on my life, my interest in nature and my confidence that anything's possible.

Summary

Fibroblast growth factor (Fgf) signaling plays multiple inductive roles during development of vertebrates (Itoh 2007). Some Fgfs, such as Fgf8, are locally secreted and signal over a long range to provide positional information in the target tissue (Scholpp and Brand 2004). Fgf ligands signal in a receptor-dependent manner via tyrosine kinase receptors, four of which have been so far identified. Fgf8 signaling was shown to depend both on receptor activation as well as endocytosis. The specificity of Fgf ligands and receptors as well as the function of receptors in the control of the Fgf signaling range have been, however, largely unclear. In order to address the function and signaling mechanisms of Fgfrs in development I have systematically analyzed fgfr TILLING and morpholino knockdown mutants. I have primarily focused on Fgfr1, which was a candidate for Fgf8 signaling partner.

I describe here, some insights into the function of Fgfr1, which as we find, is duplicated in zebrafish and other teleosts. The functions of Fgfr1a and b appear to overlap during early development and to diverge at postembryonic stages. Analysis of Fgfr1a TILLING mutant fish as well as Fgfr1a and b morpholino knockdowns revealed that those two similarly expressed genes act redundantly during development, thereby producing only mild morpholino phenotypes when knocked down independently. Simultaneous knockdown of both genes results in progressive loss of posterior mesodermal body structures, which is consistent with Fgfr1a knockdown in medaka (Yokoi et al. 2007). The role in promotion of mesoderm formation by two fgfr1 genes is paralleled by similar phenotype in Fgf8/Fgf24 double mutants providing functional link between those receptors and ligands (Draper et al. 2003). Two Fgfr1a mutants, being presumptive loss-of-function and hypomorph alleles show dermal skeleton defects in adults, which reveal different functions of two paralogous fgfr1 genes during late development. The zebrafish scale phenotype resembles the morphology of a scaleless mirror carp. In carp, this phenotype was also linked to Fgfr1 mutations, demonstrating how morphological features can be shaped in evolution through modifying common molecular pathways.

Observation of Fgfr1a in the embryo at subcellular level provided some information about the endocytosis and intracellular trafficking of the activated receptor in vivo. Fluorescently tagged Fgfr1a (being one of presumptive receptors for Fgf8 (Scholpp et al. 2004; Trokovic et al. 2005; Yokoi et al. 2007)) is found in overlapping subcellular structures with Fgf8GFP. Fgfr1a is primarily taken up via clathrin-dependent endocytosis and to a lesser degree by caveolin-dependent endocytosis, and it is mostly directed to degradation. Analysis of two mutant Fgfr1a constructs, Fgfr1a^{Y753STOP} and Fgfr1a^{Y753F}, revealed the requirement of Y753 for endocytosis as well as Fgf signaling in context of the whole embryo. Overexpression of Fgfr1a^{Y753F} results in dramatic ligand-dependent expansion of target gene induction in gastrulating embryos. This suggests that receptor endocytosis, as well as the rate

of trafficking is involved in the correct setup of Fgf signaling during early embryo development.

Preliminary analysis of the Fgfr2 TILLING mutant, Fgfr2^{L545STOP}, showed that homozygous mutants presumably lose Fgfr2 function through non-sense mediated decay and the disruption of the protein function. Homozygous mutants are viable but dwarfish, harboring many skeletal defects and are infertile. The phenotypes are consistent with the phenotypes observed in FGFR2 knockout mice, except limb growth, which is abolished in knockout mice and appears normal in mutant Fgfr2^{L545STOP}-/- zebrafish (Arman et al. 1998; De Moerlooze et al. 2000; Yu et al. 2003).

The analysis of Fgfr4 loss-of-function in zebrafish, in contrast, showed unexpected fin induction defects, which suggests differences between the developmental functions adopted by Fgfr2 and Fgfr4 in zebrafish compared to higher vertebrates. Fgfr4 morpholino knockdown embryos display a composite of early and late embryonic defects, including reduced eye growth, cell death and edema of the hindbrain, deformation of the facial skeleton, lack of pectoral fins and curved body axis. Analysis of early inductive events in pectoral fin growth revealed that Fgfr4 is required for the induction of the fin field at early segmentation stages and that it acts downstream of retinoic acid signaling in the hindbrain, spinal cord and lateral plate mesoderm (from which pectoral fins arise). Taken together, Fgfr4 knockdown, expression pattern and protein structure analysis suggest that Fgfr4 is essential in early Fgf signaling during zebrafish development and it apparently lost many of its functions during tetrapod evolution (FGFR4 knockout mice are viable and show no defects (Weinstein et al. 1998)).

Abbreviations

Ab	antibody
AER	apical ectodermal ridge
A-P	anterior-posterior
C	degrees Celsius
CDE	clathrin dependent endocytosis
C-terminus	carboxyl terminus (of a peptide)
Da	Dalton
DAB	diaminobenzidine
DEAB	4-(Diethylamino)-benzaldehyde
DIG	digoxygenin
DNA	deoxyribonucleic acid
Dpf	days post fertilization
D-V	dorsal-ventral
ECM	extracellular matrix
Fgf	fibroblast growth factor
Fgfr	fibroblast growth factor receptor
GFP	green fluorescent protein
GPI	glycosylphosphatidylinositol
Hpf	hours post fertilization
HRP	horseradish peroxidase
HSPG	heparan sulphate proteoglycan
Hyb	hybridisation buffer
IP	immunoprecipitation
ISH	in situ hybridisation
K	kilo
Kb	kilobase
mAb	monoclonal antibody
MESAB	3-aminobenzoate-methanesulphonate salt
MetOH	methanol
MHB	midbrain-hindbrain boundary
mM	milimolar
MO	morpholino
mUb	monoubiquitin
mz	maternal zygotic
NCE	non-clathrin mediated endocytosis
N-terminus	amino-terminus (of a peptide)
nt	nucleotide

ORF	open reading frame
PBS	phosphate buffered saline
PBST	phosphate buffered saline with Tween 20
PBSTx	phosphate buffered saline with Triton X
PCR	polymerase chain reaction
PFA	paraformaldehyde
Pol	polymerase
PTU	1-phenyl-2-thiourea
pUb	polyubiquitin
RA	retinoic acid
RFP	red fluorescent protein
RNA	ribonucleic acid
RT	room temperature
SDS	sodium dodecylsulphate
TILLING	Targating Induced Local Lesion IN Genomes
Ub	ubiquitin
UTR	untranslated region
WT	wildtype
YFP	yellow fluorescent protein

1. Introduction

Pattern formation during vertebrate development is an absorbing topic of research and although several processes and genetic control of early development have already been understood many questions still remain open. Fgf signaling has been shown to play a pivotal role in early vertebrate development but the mode of Fgf morphogen signaling and Fgf in vivo receptor specificity still need to be elucidated.

Some cell biological aspects of Fgf signaling have been studied in tissue culture. However, they were never verified in the context of the embryonic tissue. Although the role of Fgf receptors in development has been studied to some extent in loss-of-function studies and tissue culture the regulation of receptor activity during tissue patterning in vivo has not been fully addressed. We now have an opportunity to focus on those issues using zebrafish embryos which are numerous, easy to manipulate and accessible to imaging at all stages of development.

In this study I used high-resolution confocal microscopy in order to address Fgf receptor signaling and trafficking in vivo in response to Fgf8. I also used available gene tools in order to investigate the role of Fgf receptors (Fgfrs) in zebrafish development. I investigated the regulation of receptor endocytosis in Fgf8 signaling as well as the receptor specificity during early zebrafish development. I trust that the theoretical background provided in this chapter will be sufficient to follow this study and emerging conclusions.

1.1. Zebrafish as a model organism

Zebrafish is a well-established model vertebrate. Zebrafish embryos are easily accessible to observation and manipulation thanks to ex utero development. Translucent tissue and a relatively fast rate of embryonic development make the zebrafish an excellent model organism for studies of tissue patterning, morphogenesis and cell biology. Imaging techniques available to this point made zebrafish the model organism of choice to study phenomena bridging developmental and cell biology. The genome has been sequenced (started in 2001), however due to sequence repeats and non-coding DNA its assembly is not finished yet. With many genes annotated, some still require manual search for their paralogous duplicates or genomic organization. Nevertheless, extensive EST databases and the progressively completed genome database make zebrafish a convenient model organism for many biological fields.

1.1.1. Embryonic development of zebrafish

The zebrafish embryo develops ex utero in a protective chorion, which can be easily removed for microscopy. The development of zebrafish can be divided into seven periods: zygote, cleavage, blastula, gastrula, segmentation, pharyngula and hatching period. This work will be focusing mainly on stages from blastula to segmentation, when most patterning and cell fate determination processes take place. The illustration below (Figure 1.1) indicates some of the stages of early embryonic development.

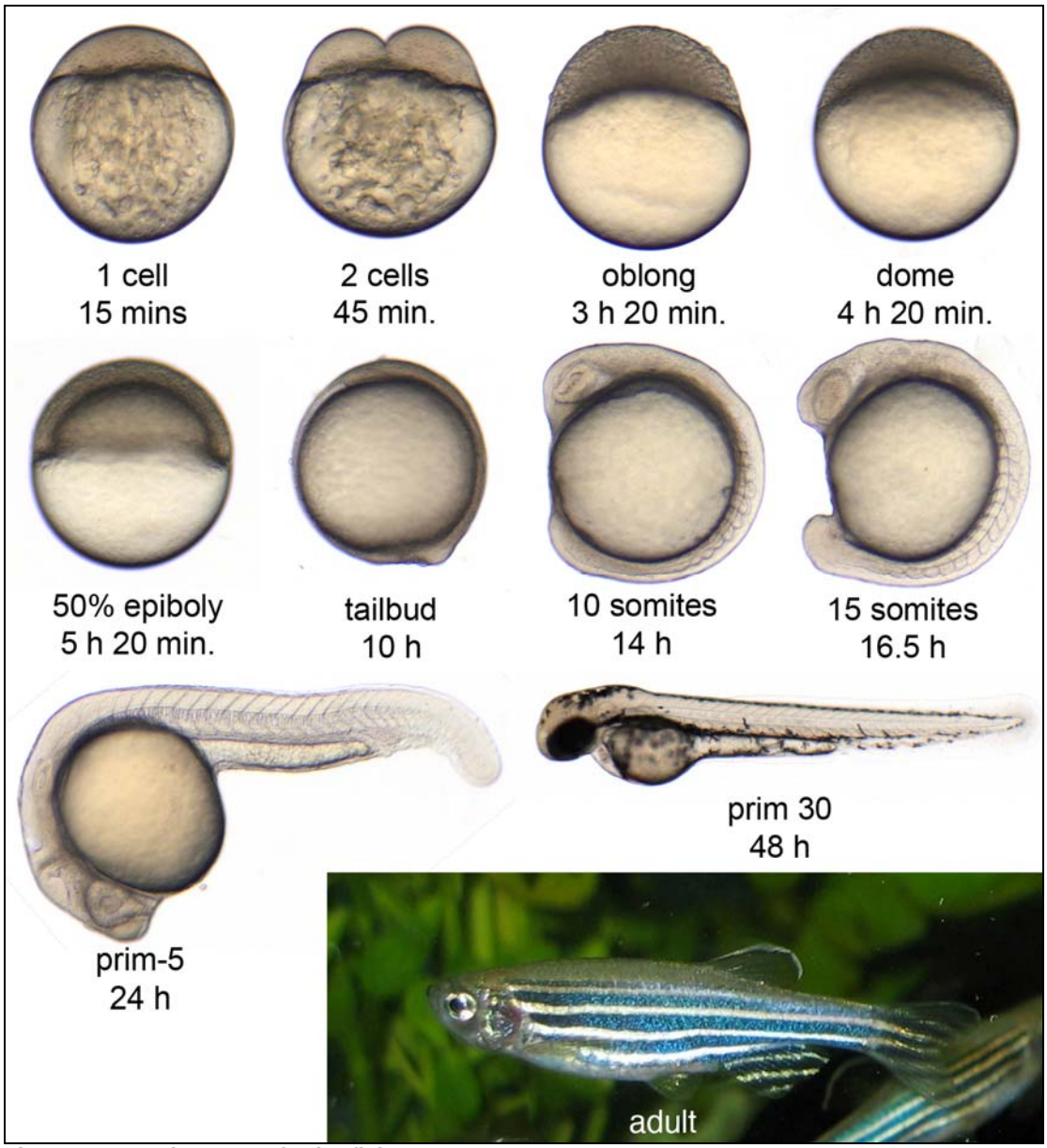

Figure 1.1 Development of zebrafish
The stages of zebrafish development are named after morphological features. Percent epiboly describes the extent to which the epiblast covers the yolk during gastrulation. Hours are given for development at 28,5 °C. All embryos are shown in lateral view, dorsal side to the right for embryos or top for older fish.

Developmental stages described in this work are named according to the convention introduced by Kimmel et al. when embryos are raised at 28.5ºC at non-crowded density (up to 10 embryos/ml) (Kimmel et al. 1995). Embryos develop very quickly and establish their basic body plan already after 24 h post fertilization. The larvae hatch at approximately 2 days and start feeding independently after 6-7 days. Zebrafish reach sexual maturity after about 3 months and live up to 3 years long. The short time frame of embryonic development allows processing of transgenic and mutant zebrafish relatively fast, limiting the duration of experiments to one or two days.

1.1.2. Forward and reverse genetic approaches to gene function

High numbers of offspring and low space requirements make zebrafish a convenient genetic tool. As a result, a variety of mutagenesis screens were performed, which gave rise to a relatively large number of available mutants. Accessibility of the embryos at all stages of development creates a unique opportunity to examine the role of genes essential for early development.

Many genes with essential and unique functions in development of e.g. brain, midline, somites, muscles etc. have been identified through forward genetic mutagenesis screens identifying genes (Haffter et al. 1996). Most forward genetic screens have been done with use of the methylating agent ethylnitrosourea (ENU), a mutagen with high mutation efficiency. The F2 progeny of the mutated parent fish were raised for phenotypic analysis. Identified mutant fish are analyzed through complementation tests and gene mapping in order to find the position of genes responsible for the phenotype (Rawls et al. 2003; Geisler et al. 2007).

Another screening technology made use of retroviral insertional mutations, which can be easily identified thanks to molecular tags encoded at the site of lesion (Amsterdam and Hopkins 2006). Recently, another step has been taken in forward genetics to identify genes involved in growth of adult structures like dermal skeleton or defects in wound healing, behavior etc. (http://www.zf-models.org/workpackages/wp1.html).

To increase the chance of linking single genes with their functions, researchers begun to explore gene functions using reverse genetics. Because knockouts of genes in zebrafish cannot be generated by homologous recombination ES cell manipulation, other methods for targeted gene modification have been suggested. Among those TILLING mutagenesis became popular due to the organized effort of the zebrafish community to share and identify as many mutants as possible (http://www.zf-models.org). The details of this method will by described in further sections of the introduction.

However, due to the limitations of the mentioned methods another technique was developed very recently to create targeted mutations in genes of interest. The method is based on custom designed zinc finger proteins, which introduce double strand DNA breaks in specific sequences (Durai et al. 2005). Such DNA breaks are usually repaired by non-

homologous endjoining, which leads to mutations. The method is still in the phase of development, however, it is very promising for future studies of functions of interesting genes (Ekker 2008; Meng et al. 2008).

Transient gene inactivation is based on the morpholino knockdown technique, also described in detail below. Morpholinos, being synthetic drugs are injected into fertilized eggs at the one-cell stage for uniform distribution of the blocking agent in the embryo.

1.2. Reverse genetic approach to generating FGFR knock out zebrafish

1.2.1. Targeting Induced Local Lesions in Genomes – TILLING

TILLING is used in zebrafish and other organisms (yeast, fly and C.elegans) to identify individuals harboring a mutation in the gene of interest (Till et al. 2003; Henikoff et al. 2004; Winkler et al. 2005; Bokel 2008). Male fish are mutagenized using ENU, which in successful screens resulted in 1 mutation in every 150 Mb (Figure 1.2). The mutagenized sperm is then used to fertilize wildtype eggs and the resulting fish are raised and kept as a living library for sequence screening of genes of interest. Exons in those genes are amplified from DNA (each fish separately) and analyzed for heterozygous mutations. Heterozygous single nucleotide changes can be detected by CelI digestion of the PCR product or direct sequencing (Stern et al. 2005; Amsterdam and Hopkins 2006).

Identified carriers of specific mutations are outcrossed for several generations against wildtype fish to dilute out background mutations. The mutant phenotype is then analyzed in an incross of such genetically “cleaned up” animals. In case of early phenotypes one can confirm gene-specificity by morpholino injection. Gene specificity of the phenotype can be tested by non-complementation of different alleles or, if no other alleles are available, by morpholino knockdown (Araki and Brand 2001).

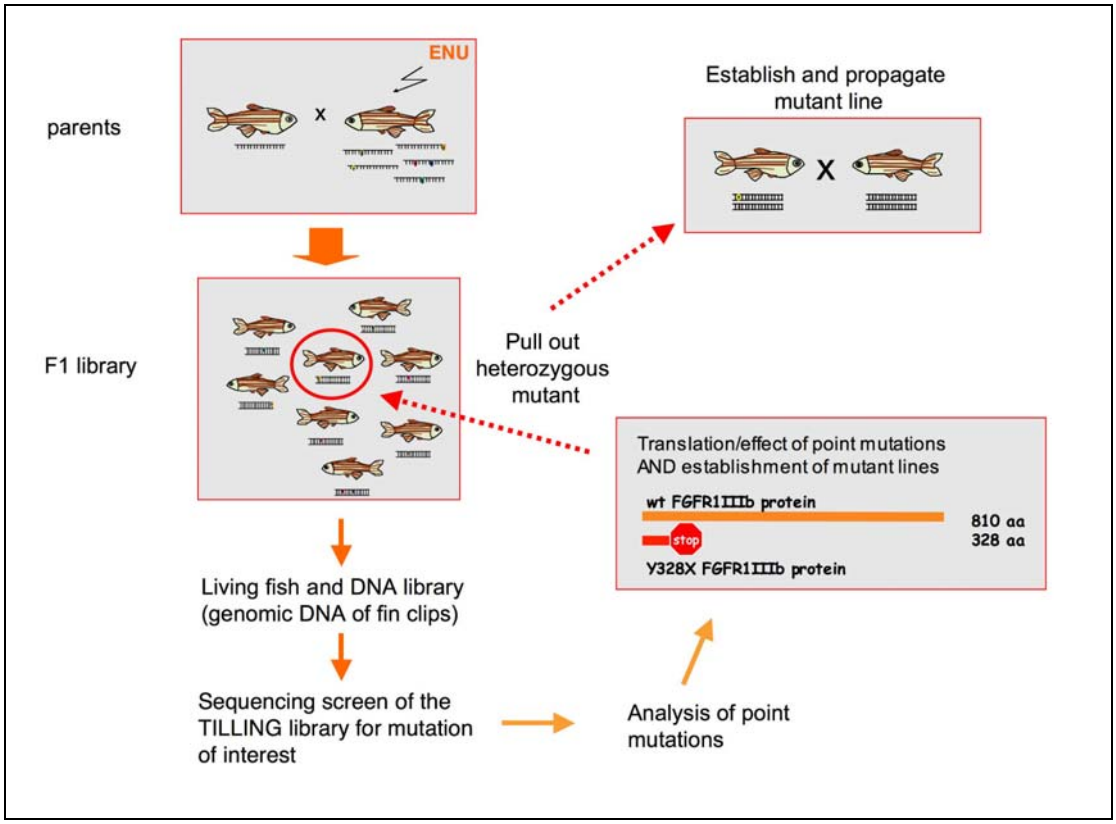

Figure 1.2 TILLING
Targeting-induced local lesions in genomes - a reverse genetic approach to obtain mutants. This flowchart scheme of the TILLING procedure outlines the ways from mutagenesis, through sequencing screen for mutations of interest to establishment of a mutant zebrafish line.

1.2.2. Morpholino mediated gene knock-down

Morpholinos (MOs) are synthetic antisense oligonucleotides of about 25 units, which are analogous to RNA or DNA, except that they have a mopholine ring instead of a ribose ring (Summerton and Weller 1997). They can be delivered to zebrafish embryos by injection at one cell stage for uniform distribution, and are stable for several days. Morpholinos specifically bind to complementary sequences and block mRNA function in two ways.

1.2.2.1. Types of morpholinos

Translation blocking morpholinos are targeted against the 5' untranslated region of an mRNA or the beginning of the open reading frame, which can efficiently abolish translation. Proof of principle morpholino experiments showed that MO mediated-knockdown can phenocopy well characterized mutant phenotypes. For instance, Fgf8 morpholino phenocopies the genetic Fgf8 mutant, acerebellar (ace) (Araki and Brand 2001).

A different morpholino based approach, which allows quantification of the knockdown efficiency, was developed to block pre-mRNA splicing instead of its translation. Splice

blockers are complementary to splice acceptor or donor sites in the unspliced RNA, thereby competing with the splicing machinery for the binding site. MO binding leads to either erroneous exon excision or intron retention. PCR analysis of the RNA from morpholino-injected embryos (morphants) provides information about the efficiency of the gene knockdown (Draper et al. 2001).

1.2.2.2. Controlling morpholino experiments

Unfortunately, morpholinos also often confer toxicity to the cells and off-target effects (Eisen and Smith 2008). Morpholino can cause stress induced cell death in the central nervous system and somites by p53-mediated apoptosis. Although morpholinos act in a sequence specific manner, there is always a chance of blocking also other genes containing similar sequences.

In order to assess these components of the morpholino phenotype, one has to perform a variety of control experiments. As mentioned before, comparison with an existing mutant is optimal, however, seldom available. To check MO efficacy it is good to check the protein loss on a Western Blot or in whole mount tissue staining. However, this is often limited due to unavailability of zebrafish specific antibodies.

To control off target effects, one can try using multiple morpholinos, which independently should induce the same phenotype. In turn co-injecting them together can lead to dilution of off-target effects while preserving the cumulative specific gene knockdown phenotype. Additionally, the specific MO phenotype is most convincing if it is possible to rescue through mRNA injection. Also, one can control for unspecific effects by injecting a mismatch morpholino – a oligonucleotide similar but different by at least 5 units to the working morpholino. Such a modified agent should be unable to bind to its target and hence, cause no gene knockdown phenotype.

1.3. FGF ligand family

1.3.1. FGF conservation

Fgfs are a family of secreted signaling molecules that act as ligands for transmembrane high affinity tyrosine kinase receptors. Fgf binding to the extracellular domains of FGF receptors cause their dimerization and subsequent phosphorylation of specific tyrosines in their cytoplasmic kinase domains (Eswarakumar et al. 2005). This launches cascades of signal transduction inside cells leading to diverse responses like cell proliferation, migration, survival and differentiation.

Human Fgf	Zebrafish Ortholog	Ortholog II
Fgf1	Fgf1	
Fgf2	Fgf2	
Fgf3	Fgf3	
Fgf4	Fgf4	
Fgf5	Fgf5	
Fgf6	Fgf6b	Fgf6a
Fgf7	Fgf7	
Fgf8	Fgf8a	Fgf8b (former 17a)
Fgf9	-	
Fgf10	Fgf10a	Fgf10b
Fgf11	Fgf11	
Fgf12	Fgf12	
Fgf13	Fgf13	
Fgf14	Fgf14	
Fgf16	Fgf16	
Fgf17	Fgf17b	
Fgf18	Fgf18a	Fgf18b, Fgf24
Fgf19	Fgf19	
Fgf20	Fgf20b	Fgf20a
Fgf21	Fgf21	
Fgf22	Fgf22	
Fgf23	Fgf23	

Table 1 List of human Fgfs and zebrafish orthologs (after (Itoh 2007))

Although Fgfs are well conserved during evolution, the number of Fgf genes in organisms varies due to repeated genome duplications and subsequent gene losses. Thus, C.elegans and D. melanogaster have only two and three Fgf genes, respectively, whereas mouse and human have 22 Fgf ligands.

The functions of the Fgf system became complemented with every round of gene duplications and the functions of individual genes became specified in many processes of development, growth and adult homeostasis. Currently there are 27 fgf genes discovered in zebrafish, suggesting an additional duplication event before teleost radiation. The gain of genes was probably followed by a rapid gene loss, because only 20% of zebrafish fgf genes have been found to have a functional paralog (Itoh and Ornitz 2004; Itoh and Konishi 2007).

Gene	Mouse Phenotype		Zebrafish Phenotype
Fgf1	Viable	None identified	Differentiation of erythrocytes
Fgf2	Viable	Mild cardiovascular, skeletal, and neuronal defects	nd
Fgf3	Viable	Mild inner ear, tail, and CNS defects	Various CNS defects, pharyngeal arched defects, specification of epibranchial placodes
Fgf4	Lethal, E4—5	Inner cell mass proliferation	Development of tooth
Fgf5	Viable	Long hair, angora mutation	nd
Fgf6	Viable	Subtle, muscle regeneration	nd
Fgf7	Viable	Hair follicle growth, ureteric bud growth	nd
Fgf8	Lethal, E8	Gastrulation defect, CNS and limb development	Fgf8a - Lack of MHB and cerebellum, enlarged tectum, eye patterning, slight segmentation defect, pharyngeal arches and heart development Fgf8b - unknown
Fgf9	Lethal, PD0	Lung mesenchyme, heart, gastrointestinal tract, skeleton, testes development	nd
Fgf10	Lethal, PD0	Multiple organ development (limb, lung, adipose tissues, etc.)	10a – development of swim bladder, fin and hepatopancreatic ductal system; 10b - unknown
Fgf11	-	nd	nd
Fgf12	Viable	Neuromuscular phenotype	nd
Fgf13	-	nd	nd
Fgf14	Viable	Neurological phenotype	nd
Fgf15	Lethal, E13.5-PD21	Cardiac outflow tract development	(Zf Fgf19) – lens and retina development
Fgf16	Viable		Pectoral fin development
Fgf17	Viable	Cerebellar development	Fgf17b - Early patterning, redundant with Fgf3 and Fgf8
Fgf18	Lethal, PD0	Skeletal and lung development	Unknown for both Fgf18 a and b
Fgf20	-	nd	Essential for initiating fin regeneration
Fgf21	Viable	Not clear	Heamatopoiesis
Fgf22	-	nd	nd
Fgf23	Lethal, PW4—13	Growth retardation, phosphate and vitamin D metabolism	nd
Fgf24	No mouse equivalent	nd	Fin development, pancreas development together with Fgf10 Posterior mesoderm development together with Fgf8a

Table 2 List of murine Fgf knockout phenotypes. Note that mouse FGF15 and human (and zebrafish) FGF19 are orthologous. Nd – not determined (table modified after (Ornitz and Itoh 2001).

Using phylogenetic sequence analysis FGFs can be clustered into 8 sub-families, which share increased homology and synteny (grouped in further sections of this chapter in Table 4). Their functions, however, vary within subfamilies, as revealed by multiple loss-of-function studies in mice and other model organisms (Ornitz and Itoh 2001). FGF functions include patterning of the nervous system, limb formation and skeletal growth. The summary of phenotypes resulting from FGF knockouts in mice and the corresponding loss-of-function phenotypes in fish is presented in the Table 2 above.

1.3.2. FGF responsive genes

Fgf signaling induces sef, family of sprouty and related to them spred genes, family of mkp genes and ETS transcription factors. Fgf responsive genes are mostly negative feedback regulators, except for transcription factors, which are induced to activate Fgf response. Fgfs and other receptor tyrosine kinase dependent factors are both necessary and sufficient to induce these factors.

Sef (similar expression to Fgf) is a putative transmembrane inhibitor of the Fgf function, which binds MEK kinase in the cytoplasm, thereby blocking its translocation into the nucleus. Therefore, it blocks MAPK pathway without deactivating its components (Tsang et al. 2002; Bottcher and Niehrs 2005).

The family of four sprouty genes (sprouty 1, 2, 3 and 4), discovered in vertebrates, is believed to be auto-regulated antagonists of receptor tyrosine kinase signaling. They were first identified as inhibitors of Fgf dependent tracheal branching in Drosophila (Casci et al. 1999). Sprouty proteins bind to the adaptor proteins Grb2 and Sos and block the phosphorylation cascade through the MAPK pathway. They can act very effectively as heterodimers by binding both Grb2 and Sos proteins at the same time. However, the mode of action of Sprouty proteins is not fully understood and many opposing ideas are still being tested (Cabrita and Christofori 2008).

Spred proteins (Sprouty-related proteins with Enabled domain) were recently discovered as distant relatives of sprouty genes with a similar RTK inhibitory role (Wakioka et al. 2001). In Xenopus, Sprouty and Spred proteins were shown to modulate different downstream signaling cascades in Fgf signaling (Guy et al. 2003). Spred is blocking the PLCγ pathway and Sprouty is blocking the MAPK pathway in order to jointly regulate cell movement and formation of mesoderm during gastrulation (Sivak et al. 2005). No such mechanism was confirmed in fish or mouse so far and the PLCγ pathway was shown to have little role in response to Fgf signaling when examined in vitro (Cross et al. 2002).

The Mkp (MAP kinase phosphatase) family comprises of dual-specificity phosphatases able to dephosphorylate both tyrosine and threonine residues in activated MAP kinases (Kondoh and Nishida 2007). In zebrafish the family of Mkps (named Dusp in zebrafish, standing for dual-specificity phosphatase) comprises of at least 9 members, some of which have specific and highly restricted expression patterns during development. Dusp6 is a well-studied member of this family, which belongs to the Fgf8 synexpression group (Klock and Herrmann 2002; Tsang et al. 2004; Vieira and Martinez 2005).

The ETS transctiptional factors, Pea3 and Erm, are defined by the evolutionary conserved Ets domain, which mediates DNA binding (Sharrocks et al. 1997). Both are present throughout development and activate gene transcription in response to Fgf. Expression of both pea3 and erm can be abolished through Fgfr inhibition at embryonic stages and both can be activated by Fgf8 at a long range. Fgf8 overexpression can activate ETS factors ectopically (Raible and Brand 2001).

1.3.3. Function of Fgf8 during development

1.3.3.1. Roles of Fgf8 in gastrulation, MHB maintenance

Fgf8 is expressed very early in vertebrate development and plays important roles in the early patterning events. FGF8 knockout mice die during gastrulation because they fail to develop mesoderm (Meyers et al. 1998). In fish, Fgf8 has been shown to contribute to patterning of dorsal-ventral cell identity together with the bone morphogenetic proteins (BMPs) during gastrulation (Furthauer et al. 1997). However, the zebrafish Fgf8 mutant – acerebellar (ace) shows only a mild DV patterning defect, suggesting redundancy with other growth factors, such as Fgf24, in this process (Draper et al. 2003). Nevertheless, ace mutants display a variety of other phenotypes at later stages, which resemble hypomorphic Fgf8 phenotypes in mice. Fgf8 plays a role in lateral mesoderm patterning, as it is required for induction and establishment of the size of the heart primordium and cell proportion of heart progenitors (Reifers et al. 2000) (Marques et al. 2008). Ace fish display severe brain segmentation defects, characterized by a lack of cerebellum and midbrain-hindbrain boundary (MHB), and enlarged midbrain tectum. The proposed role for Fgf8 in brain is that it is necessary to maintain the MHB and to specify hindbrain identity (Brand et al. 1996; Reifers et al. 1998). In the absence of Fgf8, axon pathfinding in the retinotectal projection and at the forebrain comissures is abnormal (Picker et al. 1999; Shanmugalingam et al. 2000). Fgf8 is also involved in left-right patterning and development of pharyngeal arches (hence, craniofacial skeleton) (Albertson and Yelick 2005).

1.3.3.2. Role of Fgfs in limb development

Vertebrate limb development may be divided into separate stages: specification, induction and maintenance. In chick, FGF8 (and other FGFs) is proposed to act at all these stages (Crossley et al. 1996). However, the involvement of Fgf signaling in forelimb (pectoral fin in fish) development has been largely debated over the last decade. It has been shown in chick that Fgf8 plays a role in early limb development together with retinoic acid signaling. In this model Fgf8 and RA together induce expression of Shh in the limb field, which in turn induces Fgf8 and 10 in the apical ectodermal ridge of the limb bud (AER). The interplay between mesodermal factors and AER expression of Fgfs allows for the outgrowth and polarization of the limb (Crossley et al. 1996).

As mentioned before, FGF8 knockout in mouse is lethal at primitive streak stage (Meyers et al. 1998). This does not allow the study of its function later during limb development. However, conditional knockout mice in which FGF8 was conditionally disrupted in the limb field proved that FGF8 is required for limb induction and patterning (Moon and

Capecchi 2000). However the promoter line used in this study did not allow investigating potential earlier involvement of FGF8 in the limb field specification. The earliest function of FGFs in mouse limb development was associated with FGF10, which acts epistatically upstream of FGF8 in AER (Min et al. 1998).

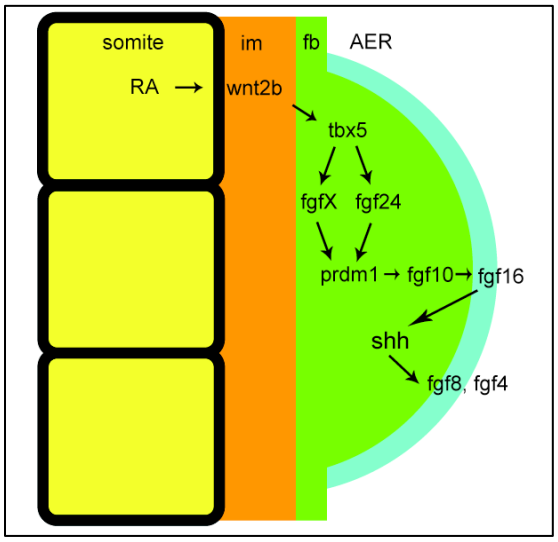

Figure 1.3 Fgf in zebrafish pectoral fin development
A schematic model of Fgf signaling in the development of pectoral fin in zebrafish. Fgf24 is acting downstream of retinoic acid (RA), Wnt2a in the intermediate mesoderm (im) and Tbx5 in the fin bud (fb). Fgf24 and other unknown Fgf induce mesenchymal expression of Prdm1. Prdm1 initiates the cascade of other Fgfs, including Fgf10 in the mesenchyme, which is required for differentiation of the apical ectodermal ridge (AER), which expresses Fgf16, Fgf8 and Fgf4. Expression of Shh is downstream of Fgf16 and is required for the A-P polarization of the limb. Figure reproduced and modified after (Mercader et al. 2006).

The zebrafish fgf8 mutant, acerebellar, develops normal fins, which suggests redundancy between Fgfs. Fgf24 was the earliest Fgf ligand found in the cascade leading to the fin development (see Figure 1.3). It was found to be acting downstream of RA and Tbx5 (the earliest known marker of fin field specification (Rodriguez-Esteban et al. 1999; Tamura et al. 1999)). Fgf24, a zebrafish specific Fgf belonging to the same subfamily with Fgf8, 17 and 18, is involved in the induction of all growth factors expressed in the AER, including Fgf10, Fgf16 and Fgf8 (Fischer et al. 2003; Nomura et al. 2006). Furthermore, Fgf8 in fish was shown to act only at the stage of fin outgrowth and patterning. Whether Fgf signaling is involved in earlier stages of fin development where the tissue gains its competence for fin induction remains to be elucidated.

Previous studies in our and other labs suggest that fin field specification occurs already during gastrulation and early somitogenesis. Inhibition of RA signaling during gastrulation causes a strong delay in Tbx5 expression, whereas prolonged RA inhibitor (4-(Diethylamino)-benzaldehyde, DEAB, blocking activity of RA producing Aldh enzymes) treatment results in complete loss of fins (Grandel et al. 2002). So far, more precise study of RA involvement in this process was hindered by a lack of appropriate markers that would identify prospective fin field at stages earlier than 10 somites.

1.3.4. Fgf8 as a morphogen

Morphogens form a concentration gradient in tissue and induce different responses depending on the distance from the source (Gilbert 2006). There is evidence that Fgf8 fulfills

many criteria of a classic morphogen. It is secreted from a localized source and it is likely to form a gradient of concentration in the receiving tissue to provide positional information in the embryo. The fate of cells is determined by the nested expression of Fgf8 target genes, which suggests the existence of several inductive thresholds of morphogen concentration. Such properties of Fgf8 are best observed during gastrulation, where it is produced at a limited number of cells at the margin and spreads in direction of the animal pole, thereby inducing long and short range genes like Sprouty 4, Pea3 or Erm.

One of the most interesting aspects of developmental biology is to understand the process of morphogen gradient formation. The problem can be split into several sub-processes: morphogen release from the source, the mechanism by which it spreads in the tissue and the mechanism by which it is received by the target cells. Fgf8 is secreted from the producing cells but the mechanism by which it is moves into the receiving tissue was unknown until recently. The regulation of the protein reception is also debated, because of many factors influencing receptor-ligand binding affinities.

There have been many models proposed for the distribution of various morphogens, which are best summarized by (Kornberg and Guha 2007). According to proposed models, proteins can signal over a long range through diffusion, transcytosis, argosomes or cytonemes (Figure 1.4). The latter three models assume an active force, which directionally transports morphogen particles either through extracellular matrix or repeated cycles of endo- and exocytosis. Current evidence suggests that Fgf8 can spread through free diffusion, the simplest of mechanisms (Scholpp and Brand 2004) (Rachel Yu, personal communication). The diffusion model assumes that Fgf8 molecules can move in a random, non-directional way and are not bound to a carrier or actively hindered close to the source.

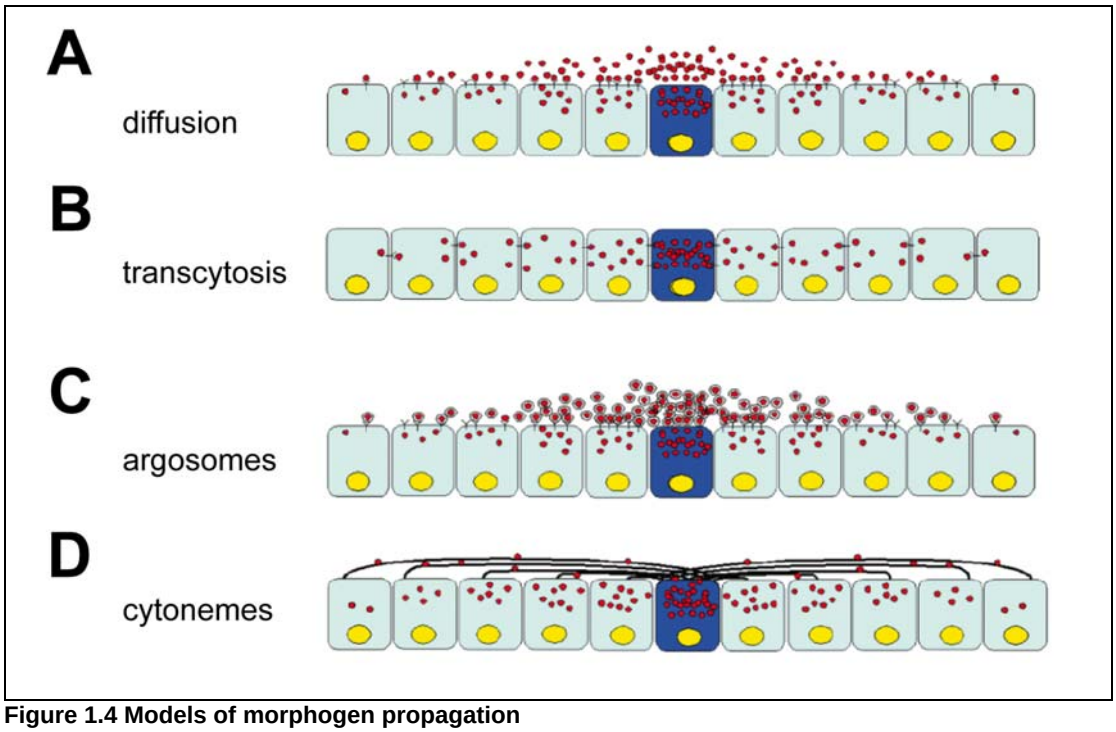

Figure 1.4 Models of morphogen propagation
Four models of morphogen propagation. Morphogen moves (red) from the source (dark blue) to the

receiving tissue (light blue) by free diffusion (A), serial transfer (transcytosis, B), lipoprotein-associated transfer (argosomes, C) or direct cell-cell contact through cell protrusions, cytonemes (D). Figure modified after (Kornberg and Guha 2007).

The random diffusion model leads to an important assumption, that there is a source of Fgf8 and there has to also be “a sink”, i.e. a mechanism of protein decay, which would effectively create a gradient of ligand concentration. Recent studies of Fgf8 endocytosis in the embryo have suggested that the sink mechanism may be dependent on the rate of ligand uptake and intracellular degradation. Inhibition of Fgf8 uptake by overexpressing dominant negative dynamin leads to further range of Fgf8 spreading and target gene induction. Conversely, promoting endocytosis by overexpression of Rab5 causes the opposite effect, shortening the range of Fgf8 signaling and tissue penetration. The evidence based on overall endocytosis manipulation led to a conclusion, that the range of Fgf8 signaling is restricted by the clearance of Fgf8 from the extracellular matrix through endocytic uptake. Hence, the suggested name of the mechanism - restrictive clearance model schematically depicted on Figure 1.5 (Scholpp and Brand 2004).

Many known components of the Fgf signaling pathway are not tested for their function in gradient formation. Firstly, the extracellular matrix (ECM) is rich in heparan sulphate proteoglycans (HSPGs), which have the ability to bind Fgf ligands with high affinity (Allen and Rapraeger 2003). They are also described as important cofactors in the ligand-receptor interactions, possibly regulating the receptor affinity and ligand access to the cell surface (Lin et al. 1999; Park et al. 2000; Pellegrini et al. 2000; Sugaya et al. 2008). Their role in the gradient formation and ligand endocytosis remains to be elucidated. Some glypicans are well studied in the context of other signaling pathways. For instance, the role of Dally in Dpp signaling in the Drosophila wing disc or in tracheal branching, indicated its regulatory importance in protein distribution and receptor binding (Hufnagel et al. 2006; Yan and Lin 2007).

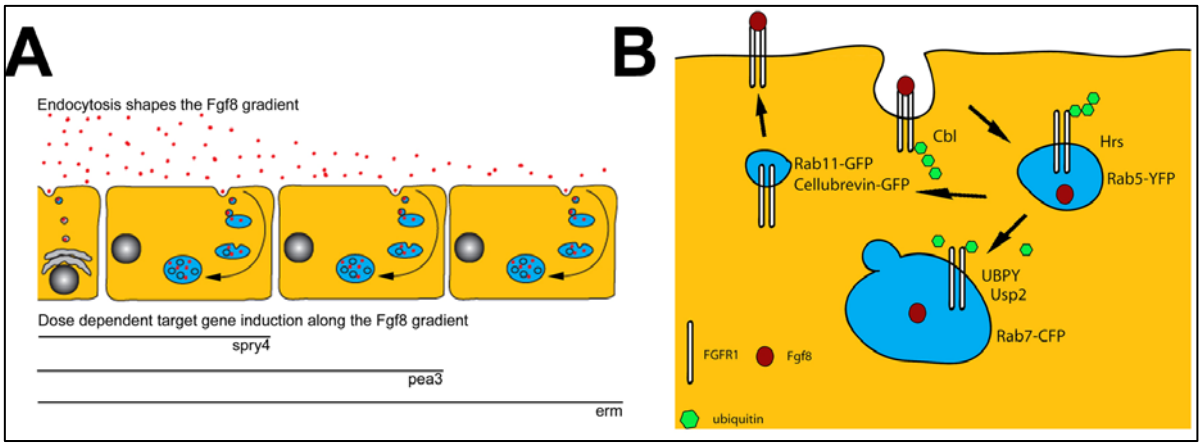

Figure 1.5 FGF8 in restrictive clearance model
Fgf8 as a morphogen (red) induces various target genes depending on its concentration (A). The shape of Fgf8 gradient depends on the rate of endocytosis, i.e. on the receptor mediated uptake and downregulation. Receptor gets endocytosed upon ligand binding, activation and ubiquitylation (B). Schematic modified after (Scholpp and Brand 2004).

Secondly, ligand clearance from the ECM is most likely receptor-dependent. There is, however, little information about receptor specificity and the mechanism by which the endocytosis of the receptor-ligand complex is regulated. Some possible levels of regulation will be discussed in further sections about FGF receptor structure and function.

Finally, during development various tissues may establish Fgf8 gradients in different ways. For instance, fgf8 mRNA produced in presomitic mesoderm undergoes progressive decay in the somites during growth and elongation of the AP axis. This effectively leads to production of a protein gradient proportional to the graded distribution of the mRNA (Dubrulle and Pourquie 2004). This alternative model of gradient formation proves that such processes may depend on the context and the stage of development.

1.4. FGF receptors family

1.4.1. Evolutionary conservation, genome duplication

There are four highly conserved FGF receptors (54-69% of overall homology between human FGFRs) in mice and human and one FGFR-like gene, sharing about 30% similarity with the other four. FGFR genes underwent duplications only in the evolution of vertebrates as organisms like C. Elegans and D. Melanogaster have one and two FGF receptors, respectively (Itoh and Ornitz 2004). However, in vertebrates, FGFRs are alternatively spliced, which leads to production of numerous protein isoforms. The most common isoforms for FGFR1-3 are IIIb and IIIc, the latter being most important (Partanen et al. 1998; Eswarakumar et al. 2005). This results again in an increased diversity in the receptor functions.

In teleosts, despite expectations to find more duplicates of fgfr genes, only fgfrl1 was found to have a paralog (Trueb et al. 2005). In medaka, also Fgfr1 has a paralog. Otherwise, the zebrafish has also 4 Fgfrs and their alternative splice variants seem to be conserved at least for Fgfr1 (Scholpp et al. 2004). Nevertheless, the assembly of zebrafish genome is still under way and there might be more Fgfrs to be found.

1.4.2. Endocytosis and trafficking pathways of receptor tyrosine kinases

1.4.2.1. Paths of endocytosis

Endocytosis is the process in which cells take up matter by a variety of different mechanisms (Conner and Schmid 2003). Cells can take up large particles by phagocytosis

and small liquid particles by various forms of pinocytosis. Sporadically, cells can take up any liquid phase particles in unspecific manner through micropinocytosis. However, the most efficient way of internalizing nutrients and growth factors is mediated by attachment to high-affinity receptors and clathrin-mediated endocytosis (CME). Clathrin facilitated by AP proteins form an invagination in the membrane and recruit the cargo with its receptors into it. The engulfing of nutrients is successful when an invaginated vesicle pinches off into the cytoplasm (Mousavi et al. 2004; Praefcke et al. 2004). Some cargo can also be taken up by cells through caveolin-mediated endocytosis, which is lipid-raft associated and has distinct functions in the cell (Parton and Richards 2003; Pelkmans et al. 2004). Finally, nutrients can be delivered by, so far poorly understood, clathrin and caveolin independent endocytosis as well. Both latter types on endocytosis are refered to as non-clathrin mediated endocytosis (NCE).

Most endocytosis processes require dynamin, which acts as a molecular garrote to pinch invaginated vesicles off the plasma membrane. Expression of dominant negative dynamin almost entirely blocks endocytosis (Henley et al. 1998; Henley et al. 1999; Cao et al. 2007).

In order to allow the endocytosed cargo to reach its destination organelle, vesicles inside cells have to fuse and localize to specific membrane domains on the right endosomal compartments. Trafficking pathways in cells are therefore tightly regulated by membrane organizer proteins, which allow cargo recognition, membrane fusion and bringing endocytosed molecules to degradation, recycling or other destinations. Among such organizers are Rab and SNARE family proteins (McMahon et al. 1993; Chen and Scheller 2001; Zerial and McBride 2001). Because certain Rab proteins are specifically localized to only a restricted pool of vesicles and endosomes inside cells, they are often used as markers for subcellular localization of various cellular components. Rab5, for instance, labels only early endosomes, which is suggesting a recent uptake. Rab7 and Rab9 label late endosomes, which indicates that the cargo is destined to proteasomal degradation. Rab 11 in turn, labels exocytic vesicles, as well as a perinuclear recycling endosomes (Ullrich et al. 1996; Zerial and McBride 2001).

SNARE proteins are implicated in almost all intracellular trafficking processes. SNAREs interact with each other to mediate membrane fusion between vesicles. The active SNARE core complex typically consists of three types of SNARE proteins, namely syntaxin, VAMP (vesicle associated membrane protein) and SNAP-25 (Chen and Scheller 2001; Conner and Schmid 2003). These can also be found in a limited fraction of vesicles and endosomes, hence their use as trafficking markers. For example, Cellubrevin is a member of the VAMP family and is associated with rapidly recycling vesicles in receptor-mediated endocytosis (McMahon et al. 1993).

1.4.2.2. Trafficking of RTKs

Intracellular trafficking of receptor tyrosine kinases is best studied for the EGF receptor. Upon low EGF stimulation the EGFR complex is internalized mostly through clathrin mediated endocytosis (Hanover et al. 1984; Sorkin and Goh 2008). Until recently it was assumed that CME directs the EGFR predominantly to degradation, thereby terminating signaling. However, recently, it has been shown that CME directs receptors to recycling, whereas non-clathrin endocytosis (NCE) leads to receptor degradation. It has also been shown that caveolin-mediated endocytosis increases significantly at high-level EGF stimulation. About 80-90% of those endocytosed complexes are degraded, whereas most CME derived endosomes are recycled. This discovery is significant to our understanding of RTK signal attenuation and downregulation, where early clathrin positive endosomes become more important for signaling than for degradation of the receptor complex (Sigismund et al. 2008).

1.4.2.3. Ubiquitylation

Ubiquitylation is a regulatory post-translational modification, which serves a variety of functions in the cell. Ubiquitin (Ub) moieties are attached by its c-terminus to the lysine residues of its substrate, which is catalyzed by specialized enzymes called ubiquitin E3 ligases. Ubiquitin can be attached to the substrate as a single moiety, but it can also form poly-chains, by serial ubiquitylation of subsequent Ub moieties. There have been many types of chains characterized so far, however, only little is known about their function in the cell. Polyubiquitylation K63 (via ubiquitin lysine 63) and multi-monoubiquitylation (attachment of single moieties on several lysines of the substrate) are known to trigger endocytosis or control gene transcription. Polyubiquitylation K48 in turn is interpreted and a signal to substrate degradation (Dikic 2003; Haglund and Dikic 2005). Ubiquitylation can be controlled in the cell by the presence of debiquitylating enzymes (DUBs), such as AMSH or UBPY. Deubiquitylating enzymes remove ubiquitylation signal from the substrate and change its trafficking along degradation/recycling routes (Naviglio et al. 1998; McCullough et al. 2004).

Both EGFR and FGFR have been shown to be ubiquitylated by the ubiquitin ligase Cbl upon activation (Mori et al. 1995; Dikic 2003). It was, however, unclear so far, what is the role of ubiquitylation in FGFR endocytosis (Monsonego-Ornan et al. 2002). It is known that ubiquitylation is dispensable for EGFR endocytosis but required for its degradation (Soubeyran et al. 2002), whereas in context of TGF receptor it is required for both, endocytosis and degradation (Haglund et al. 2003; Huang et al. 2007) (Kavsak et al. 2000).

1.4.3. FGFR structure and function

Most vertebrate FGFRs consist of two or three immunoglobulin-like (Ig) domains, an acidic box, a short transmembrane domain and a split tyrosine kinase domain on the cytoplasmic end (Fig. 1.6 A). Only zebrafish Fgfr4 has four Ig domains, suggesting different ligand specificity (Thisse et al. 1995). The acidic box located between IgI and igII increases binding affinity to heparin, which in turn promotes ligand-receptor complex formation. The stoichiometry of such a complex (FGFR1-FGF2-heparin) was resolved by crystallography and proposed to be (for a receptor dimer) 2:2:2, i.e. two ligand molecules, two molecules of heparin and 2 receptors (Eswarakumar et al. 2005).

The affinity to FGF ligands is conveyed by the Ig-like domains and binding of cofactors, such as soluble heparans, shed from the cell surface by cleavage. Ligand binding triggers conformational changes of the extracellular domain and subsequent homo- or heterodimerization of the FGFR (Ullrich and Schlessinger 1990) (Bellot et al. 1991). There are at least seven tyrosine residues that can be specifically phosphorylated during receptor activation. Their numbers differ for zebrafish and mouse due to different receptor length, as summarized in Table 3 (after (Mohammadi et al. 1991; Mohammadi et al. 1996)).

Mouse FGFR1	Zebrafish Fgfr1	Function
Y463	Y451	FRS2/Crk interaction
Y583/Y585	Y573/Y575	unclear; dispensable for FGFR1 mediated proliferation and differentiation
Y653/654	Y640/Y641	Regulation of kinase activity, activation
Y730	Y718	unclear; dispensable for FGFR1 mediated proliferation and differentiation
Y766	Y753	PLCγ interaction

Table 3 Comparative list of autophosphorylation sites on mouse and zebrafish FGFR1

Upon receptor activation adaptor molecules are recruited, which launch a cascade of signaling events. A juxtamembrane domain on the FGFR1 associates with FRS2α (Burgar et al. 2002), which in turn recruits Grb2 or Grb2/SOS complexes which directly to activate the MAP kinase cascade. On the other hand, PLCγ binds directly to the phosphorylated Y766 on the receptor (just posterior to the kinase domain) and launches an alternative cascade, leading to calcium store release and shape changes in the cell. Deletion of the last 58 c-terminal amino acids ($FGFR1^{Y766STOP}$) as well as Y766F substitution proved not only to abolish PLCγ interaction but also receptor internalization (Sorokin et al. 1994). It is not clear, however, what triggers receptor endocytosis. It could be activation, ubiquitylation or both.

There are a number of other signaling events that can take place upon FGFR activation, which are summarized in more detail in (Eswarakumar et al. 2005). A simplified diagram below (Figure 1.6 B) shows four levels of possible regulation at the level of receptor dimerization, activation and downstream signaling:

Components of the extracellular matrix alter the likelihood of ligand-receptor interaction (Park et al. 2000).

Plasma membrane co-factors such as FLTR3 and Sef can promote or inhibit FGFR dimerization (Tsang et al. 2002; Bottcher et al. 2004).

On the intracellular side, availability of the adaptor proteins regulate the balance between various cellular responses to the ligand (such as proliferation, migration, differentiation etc.) (Eswarakumar et al. 2005).

Attachment of ubiquitin (Ub) moieties, mediated by ubiquitin ligase such as Cbl, can steer the receptor fate, its trafficking route, its degradation or recycling (Dikic 2003). A set of deubiquitylating enzymes (AMSH, DUB) has been shown to balance the activity of ubiquitin ligases by removing Ub moieties from the substrate (Naviglio et al. 1998; McCullough et al. 2004).

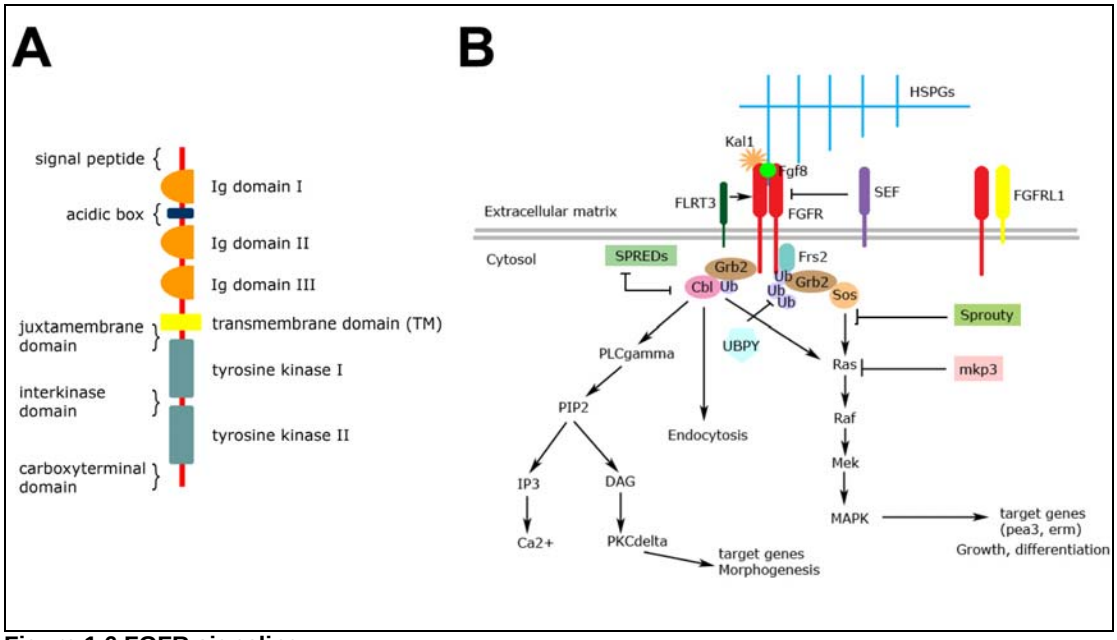

Figure 1.6 FGFR signaling
A prototype structure of FGFR (A). Ig domains affect Fgf binding, affinity and selectivity, acidic box is required for optimal heparin (HSPG) binding, juxtamembrane domain binds FRS2 and PKC, kinase domain binds other adaptor proteins and contains catalytic activity, carboxyterminal domain binds PLC$_\gamma$ and is required for receptor endocytosis.
(B) Fgf8 uptake is receptor dependent and can be regulated on several levels. Components of ECM like HSPGs and transmembrane regulators like FLRT3 or SEF modulate ligand association and dimerization of the receptors. A group of adaptor proteins (FRS2α, Grb2 etc.) form an active signaling complex and facilitate signal transduction via the MAP kinase or PLC$_\gamma$ pathway. Activating the first one leads to proliferation and differentiation, whereas the latter is associated with morphogenesis of the cell. Small modifiers like ubiquitin can alter receptor downregulation and trafficking, effectively influencing the duration of signaling.

1.4.4. Fgfrs in Fgf8 signaling

Fgfs act in a receptor dependent manner as evidenced by experiments in Xenopus, where overexpression of the dominant negative FGF receptor XFD (a form of XlFGFR1, which lacks tyrosine kinase domain) blocks Fgf signaling. In frog, XFD blocks mesoderm

specification (Amaya et al. 1991). Similarly, the use of pan-FGFR inhibitor SU5402, which binds competitively to the tyrosine kinase domain (Mohammadi et al. 1997), results in complete blockage of Fgf signaling. The induction of Fgf specific target genes is stopped and all Fgf-dependent developmental processes fail to proceed (Raible and Brand 2001).

During early zebrafish gastrulation all germ layers in the embryo are competent to respond to Fgf8. However, Fgf8 is produced locally and effectively signals in a limited zone of marginal and dorsal group of cells. The competence of cells to respond to Fgf is mediated by Fgfrs expression on the cell surface. Fgfrs are expressed dynamically during development, and their in vivo specificity to particular ligands is largely unknown. Tissue culture experiments investigated receptor – ligand pairing by testing mitogenic activities of ligands on cells expressing different receptor isoforms (Table 4) (Wang et al. 1994; Ornitz et al. 1996; Zhang et al. 2006). However, these experiments neglected the tissue context (such as presence of ECM components) and expression pattern based associations in the predictions.

Co-expression of ligands and receptors in the same or adjacent cells constitute some circumstantial evidence for functional receptor-ligand pairs. For instance during zebrafish development Fgf8 is expressed at the MHB, where Fgfr1 is the only of Fgfrs present. During gastrulation Fgfr1 is ubiquitous in contrast to other Fgfrs, which are expressed only later in development or in more restricted areas. Therefore, Fgf8 and Fgfr1 act likely in pair during early zebrafish development, despite low comparative binding affinity in vitro.

FGF subfamily	FGF	FGFR activity
Fgf1 subfamily	Fgf1	All FGFRs
	Fgf2	FGFR1c, 3c > 2c, 1b, 4Δ
Fgf4 subfamily	Fgf4 Fgf5 Fgf6	FGFR1c, 2c > 3c, 4Δ
Fgf7 subfamily	Fgf3 Fgf7 Fgf10 Fgf22	FGFR2b > 1b
Fgf8 subfamily	Fgf8 Fgf17 Fgf18	FGFR3c > 4Δ > 2c > 1c >> 3b
Fgf9 subfamily	Fgf9 Fgf16 Fgf20	FGFR3c > 2c > 1c, 3b >> 4Δ
Fgf19 subfamily	Fgf19 Fgf21 Fgf23	FGFR1c, 2c, 3c, 4Δ (weak activity)
Fgf11 subfamity	Fgf11 Fgf12 Fgf13 Fgf14	No known activity

Table 4. Relative mitogenic activities of Fgf subfamilies through various FGFRs after (Zhang et al. 2006)

Another set of evidence is provided through loss of function experiments, which can be matched between ligand and receptors. Table 5 presents mouse knockout phenotypes in FGFRs. Because each FGFR most probably reacts with more than one of the 22 FGF

ligands, receptor phenotypes are usually more complex in nature than those of ligand loss. Phenotypes may result from mutual ligand and receptor redundancy in various developmental processes.

In mouse, analysis of FGF8 and FGFR1 loss-of-function phenotypes reveals some similarities, suggesting interaction. Both genes are involved in mesoderm induction, limb growth and brain patterning. Also in fish, some attempts were made to compare the functions of the two. In medaka, loss of Fgf8 leads to complete loss of mesoderm, however the MHB seems to be preserved. Similarly, the medaka mutant headfish (hdf) carrying a single disrupting mutation in Fgfr1 lacks mesoderm and trunk and forms only head structures. It is believed that the Fgf8-Fgfr1 receptor-ligand pair was conserved through evolution, although its function changed between ray-finned fish like medaka and zebrafish (Yokoi et al. 2007; Shimada et al. 2008). Morpholino experiments in zebrafish align with the mouse phenotypes, in which FGFR1 mutants show reduced MHB fold and abnormal maintenance of this structure. In contrast, Fgfr1 morpholino experiments did not reveal any defects in mesoderm induction (Scholpp et al. 2004).

Gene	Mutations and phenotypes	Reference
FGFR1	FGFR1 null; gastrulation defects, lethal at E8.5-9.5, mesoderm and somites defects	(Yamaguchi et al. 1994) (Deng et al. 1994)
	FGFR1IIIb -/- mutants; no obvious defects, defects in tail development	(Partanen et al. 1998)
	FGFR1 chimeras; defects in migration of mesoderm through primitive streak	(Ciruna et al. 1997)
	FGFR1 hypomorphs, lethal P0; craniofacial, somite and limb defects, abnormal AP patterning	(Partanen et al. 1998)
	FGFR1 hypomorphs; pharyngeal region defects, neural crest migration defects	(Trokovic et al. 2003)
	Conditional FGFR1 knockout at MHB; lack of expected neuronal differentiation in MHB region	(Trokovic et al. 2005) (Jukkola et al. 2006)
FGFR2	FGFR2 null, die at peri-implantation E4.5	(Arman et al. 1998)
	Hypomorhpic FGFR2; lethal E10.5, defective placenta and no limb buds	(Xu et al. 1998)
	FGFR1IIIb isoform disruption; craniofacial and inner ear defects	(De Moerlooze et al. 2000) (Pirvola et al. 2000)
	Conditional inactivation of FGFR2 in mesenchymal condensations; dwarfism, defects in osteoblast proliferation	(Yu et al. 2003)
FGFR3	FGFR3 null; skeletal dysplasia, long bones and inner ear defects	(Deng et al. 1996) (Colvin et al. 1996)
FGFR4	FGFR4 null; no obvious phenotype	(Weinstein et al. 1998)
	FGFR3/FGFR4 double null; late lung defects not observed in single receptor-deficient mice	

Table 5. FGFR loss-of-function effects in mouse

In order to study the function of Fgfrs in Fgf8 gradient formation it is essential to see what are the trafficking routes of the receptor itself. It is important to know, whether Fgfr1 is primarily degraded or recycled in developing embryos and how long in proportion does it occupy early endosome populations, from where it is likely to actively signal. It would be interesting to determine whether the receptor is just removed from the cell surface to undergo degradation or if it recovers and gets recycled together with its cargo (ligand) out into the cell

surface and ECM again. The duration of signaling may tell us something about the speed of clearance and Fgf8 degradation inside cells.

1.4.5. FGF receptors and human disease

In humans, mutations in FGFR1, FGFR2 and FGFR3 cause a variety of skeletal and neurological disorders. Mutations in FGFR1 and FGFR2 cause craniosynostosis (characterized by premature fusion of skull sutures) and syndactyly (webbing of fingers and toes). Mutations in FGFR3 cause hypochondroplasia (dwarfism), achondroplasia, thanatophoric dysplasia and craniosynostosis (Yamaguchi and Rossant 1995). Typically, mutations responsible for these disorders are due to single amino acid changes rendering receptors dominant active. Some of these mutations result in ligand-independent dimerization of the receptors (Eswarakumar et al. 2005). FGFR mutations are believed to arise de novo in the parental germline and in case of mutations in FGFR3 they are found to correlate with aging of the father (Horton et al. 2007). The incidence of FGFR related genetic disorders vary, depending on the syndrome, between 1:25000 and 1:100000 individuals.

Children born with Pfeiffer, Apert, Cruzon syndrome or nonsyndromic craniosynostosis often suffer from partial syndactyly, shorter bones, craniosynostosis and dental problems. Some individuals suffer from problems involving the nervous system (e.g. anosmia or deafness) but on average the IQ of such children is normal.

1.5. Aims Of The Project

The purpose of this study is to investigate the role of Fgfr1 in Fgf8 morphogen gradient formation and to readdress the question of Fgfr specificity in zebrafish. More specifically the questions I am hoping to address are:

What is the function of Fgfr1 in the early zebrafish development?

How would decoupling of Fgfr endocytosis and signaling processes influence Fgf8 morphogen gradient formation?

How does Fgf8 signaling depend on receptor endocytosis?

What are the phenotypes of Fgfrs 1-4 knockdown/mutations in zebrafish?

What role do other Fgfrs than Fgfr1 play in Fgf8 signaling?

2. Materials and Methods

2.1. Materials

2.1.1. Chemicals

All chemical used in this study were purchased at Sigma, Fluka, Merck and Invitrogen, unless stated otherwise.

2.1.2. Equipment

Dissection microscope	Olympus SZX16
Stereomicroscope	Olympus MVX10 with DP71 digital camera
Compound microscope	Zeiss Imager.Z1 and Olympus BX61
Confocal microscope	Leica TCS-SP5, upright with 40x and 63x dipping lens
Pneumatic Picopump	WPI PV820
Micromanipulator	Narishige M-152
Needle puller	Sutter Flaming/Brown P87
Needle grinder	Bachofer GmbH 462
Magnet holders	Kanetec MB-B and Narishige
Pipette holder	WPI
Needles (transplantation)	WPI TW100F-3 (injection), TW100-3
Tungsten wire	Fine Science Tools
Dissection Forceps	Fine Science Tools

2.1.3. Kits

DNA Miniprep an Midiprep Kits	Qiagen and Fermentas
Gel extraction/PCR purification Kit	Qiagen, Fermentas, Macherey-Nagel
mMessage RNA synthesis Kit	Ambion
DIG Labeling Kit	Roche
TOPO Cloning Kit	Invitrogen
Advantage Polymerase Kit	Clontech
Platinum Pfx Polymerase Kit	Invitrogen
SMART RACE cDNA Amplification Kit	Clontech
QuickChange Site Directed Mutagenesis Kit	Stratagene
First Strand SuperScript Kit	Invitrogen
Brilliant SYBR Green QPCR	

Master Mix	Qiagen
T4 Ligase Kit	Promega
Vectastain Elite ABC Kit	Vector Laboratories, USA
ECL Chemiluminescence Kit and Films	GE Healthcare/Amersham

2.1.4. Buffers

E3 Embryos medium:

5mM NaCl

0.17mM KCl

0.33 mM $CaCl_2$

0.33 mM $MgSO_4$

10^{-5}% methylene blue

E2 transplantation medium:

15 mM NaCl

0.5 mM KCl

1 mM $CaCl_2$* $2H_2O$

1 mM $MgSO_4$ * $7H_2O$

0.15 mM KH_2PO_4

0.05 mM Na_2HPO_4 * 2 H_2O

0,7 mM $NaHCO_3$

PBS:

1.7 mM KH_2PO_4

5.2 mM Na_2HPO_4

150 mM NaCl

PBST:

PBS, 0.1% Tween-20

Ringer Buffer:

110 mM NaCl

3.5 mM KCl

2.7 mM CaCl

2.5 mM $NaHCO_3$

Danieau Medium:

58 mM NaCl

0.7 mM KCl

0.4 mM $MgSO_4$ * $7H_20$

0.6 mM $Ca(NO_3)_2$
5 mM HEPES (pH 7.2)

2x SDS Loading Buffer:
50 mM Tris HCl (pH 6.8)
2% SDS
0.1% bromophenol
10% glycerol
280 mM β-mercaptoethanol

1x TAE Buffer:
40 mM Tris-acetate
1 mM EDTA

PAGE Running Buffer:
25 mM Tris HCl (pH 6.8)
240 mM glycine (electrophoresis grade) pH 8.3
0.1 % SDS

10 x Blotting Buffer (1 l):
30,8 g Tris base
144.1 g glycine
20 ml SDS 10%
10% methanol was added to1x buffer

IP Solubilization Buffer:
50 mM HEPES (pH 7.5)
150 mM NaCl
10% glycerol
1% triton X-100
1 mM EDTA
1 mM EGTA
10 mM NaF
30 mM β-glycerol phosphate
0.2 mM Na_3VO_4
Freshly added Proteinase Inhibitor Cocktail

HNTG Buffer:
20 mM HEPES (pH 7.5)
150 mM NaCl

0.1% Triton X-100
10% glycerol

PFA 4%:
4% paraformaldehyde in 100 mM phosphate buffer pH 7.4, stored in aliquots at -20°C

20x SSC Buffer:
175.3 g NaCl
88.2 g sodium citrate (* $2H_2O$)
800 ml H2O
1 M citric acid up to pH 6.0
fill up to 1 l, autoclave

MABT:
100 mM Maleic acid
150 mM NaCl
adjusted to pH 7.5 with solid NaOH, filtered through 0.2 μm filter
0.1% Tween-20

DIG Block:
2% Blocking reagent (Boehringer) in MABT

Hyb^- Buffer:
50% formamide
5x SSC (pH 6.0)
0.1% Tween-20

Hyb^+ Buffer:
Hyb^-
0.5 mg/ml torula (yeast) RNA
50 μg/ml heparin

Embryo Genotyping (Digestion) Buffer:
50 mM KCl
10 mM Tris HCl pH 8.3
2 mM $MgCl_2$
0.1 mg/ml gelatin
0.45% NP40
0.45% Tween20

Finclip Lysis Buffer:

100 mM Tris HCl pH 8.3

200 mM NaCl

0.2% SDS

5 mM EDTA

Proteinase K 100 μg/ml

DNA Extraction Buffer:

10 mM Tris HCl pH 8.2

10 mM EDTA

200 mM NaCl

0.5% SDS

200 μg/ml Proteinase K

2.1.5. Antibodies and Detection Systems

Anti-DIG-AP FAB fragments, Boehringer

Anti-Fluorescein-AP FAB fragments, Boehringer

Fast Red Tablets, Sigma

DAB, Sigma

Anti-myc, Santa Cruz Biotechnology

Anti-GFP, Santa Cruz Biotechnology

Anti-HA High Affinity, Roche

Anti-ubiquitin, Sigma

Anti-DrFGFR1a, Eurogentec (produced in this study)

2.1.6. Enzymes

Restrictive enzymes were purchased from Fermentas and New England Biolabs. Polymerases and Reverse Transcriptases were obtained from Invitrogen, Fermentas, Clontech and Ambion, unless stated otherwise.

2.1.7. Plasmids and constructs

Several DNA constructs were used for generation of in situ hybridization probes and injection mRNA. In general, constructs used for probes were based on pBluescript II SK vector (Stratagene), pCRII vector (Invitrogen) and other, while constructs used for mRNA for injection were based on pCS2+ vector (provided by D. Turner, Washington). However, some constructs were used for both ISH and RNA (as pointed out in the table).

Plasmid insert	Vector Backbone	Source	Sense/Antisense RNA (digest/Pol)
Cellubrevin-GFP	pCS2+	CP Heisenberg Lab	Sense: NotI/SP6
Dlx2a		Monte Westerfield	Antisense: BamHI/T7
Fgf24	pBSK-SK-	Druce Draper	Antisense: NotI/T7
Fgf8	PCS2+	Didier Stainier	Antisense: XhoI/T7
FGFR1a	pCS2+	(Scholpp et al. 2004)	Sense: NotI/SP6 Antisense: BamHI/T7
FGFR1a	pZL1		Antisense: HindIII/T7
FGFR1a-GFP	pCS2+	This study	Sense: BssHII/SP6
FGFR1a-myc	pCS2+myc	This study	Sense: NotI/SP6
FGFR1a-RFP	pCS2+	This study	Sense: NotI/SP6
FGFR1a^{W667}mRFP	pCS2+	This study	Sense: NotI/SP6
FGFR1a^{Y753F}	pCS2+	This study	Sense: NotI/SP6
FGFR1a^{Y753STOP}	pCS2+	This study	Sense: NotI/SP6
FGFR1b	pCRII-TOPO	This study	Antisense: KpnI/T7
FGFR1b incl. 5'UTR	pCRII-TOPO	This study	Antisense: KpnI/T7
FGFR2	pBSK-SK	Bernard Thisse	Antisense: XhoI/T3
FGFR2^{L545STOP}	pCS2+	This study	Sense: NotI/SP6
FGFR3	pSPORT	Inna Sleptova-Friedrich	Antisense: KpnI/SP6
FGFR4	pBSKII-SK	Bernard Thisse	Antisense: HincII/T7
Flag-Ubiquitin4KR	pcDNA3.1	Yosef Yarden Lab	Sense: Bst1107I/T7
GFP-GPI	pCS2+	P. Keller	Sense: NotI/SP6
Grb2	pCR2+	This study	Sense: NotI/SP6
HA-ubiquitin	pcDNA3.1	Yosef Yarden Lab	Sense: Bst1107I/T7
HsCaveolin-GFP	pCS2+		Sense: NotI/SP6
HsRab9-CFP	pCS2+	Leah Herrgen	Sense: NotI/SP6
Krox 20	pBSK-SK	Trevor Jowett	Antisense: PstI/T3
MyoD	pBS-SK	Eric S. Weinberg	Antisense: EcoRV/T7
Pea3	pBS-SK	Herbert Steinbeisser	Antisense: NotI/T7
Rab11-Cherry	pCS2+	Matthias Nowak	Sense: NotI/SP6
Rab5c-YFP	pCS2+	Steffen Scholpp	Sense: NotI/SP6
Rab7-CFP	pCS2+		Sense: NotI/SP6
RFP-GPI	pCS2+	Arndt Siekmann	Sense: NotI/SP6
SecretedGFP	pCS2+	Isato	Sense: NotI/SP6
Sprouty 2	pBS-SK	Christine & Bernard Thisse	Antisense: BamHI/T7
Sprouty 4	pBS-SK	Bernard Thisse	Antisense: NotI/T7
Tbx5	pCRII-TOPO	Rebecca E.Bielang	Antisense: SpeI/T7
XFD	pSP64T	Amaya	Sense: EcoRI/SP6
5'UTR-EGFP-FGFR1a	pCS2+	Rachel Yu/Maria Kolanczyk	Sense: NotI/SP6
dnFGFR4-mRFP	pCS2+	Rachel Yu	Sense: NotI/SP6
Fgf8-EGFP	pCS2+	Rachel Yu	Sense: NotI/SP6
Ntl	pBS-SK	Stefan Schulte-Merker	Antisense: XhoI/T7
Pax2a	pGEM3	Terje Johannsen	Antisense: BamHi/T7
Fgf8-mRFP	pCS2+	Rachel Yu	Sense: NotI/SP6

2.1.8. Fish lines

Tilling fish lines were obtained as a result of a ZF-Models screen and found in Hubrecht TILLING Fish Library in cooperation of Dresden (Germany) and Utrecht (The Netherlands) TILLING Labs. Founders were outcrossed into various wildtype backgrounds at least 3 times before phenotypic analysis.

Acerebellar (ace) mutant carrying a loss of function allele (ti282a) in Fgf8 (Reifers et al., Development, 1998) was obtained through intercrossing heterozygous carriers.

Spiegel danio (spd) was sent as homozygous adult carriers from Prof. Christiane Nusslein-Volhardt Lab and subsequently used for FGFR1a^{W671STOP} complementation test.

2.2. Methods

2.2.1. Zebrafish raising and maintenance

Zebrafish were mated, harvested and raised as described in (Westerfield 2000). Wildtype embryos used in this study belonged to TL, AB, WIK, Tü or Gol strains.

2.2.2. Embryo Preparation prior to injection

Parent fish were setup on the afternoon prior to mating in setup tanks and laid eggs within 20 minutes from the start of the day/being setup in one net. The eggs were harvested shortly after spawning. Control embryos were kept in E3 medium at 28.5°C and staged according to morphological criteria described by (Kimmel et al. 1995). Embryos for injection were dechorionated mechanically by forceps or chemically by pronase treatment prior to injection. During pronase dechorionation embryos were kept in 1mg/ml enzyme for a couple of minutes until first embryos popped out of the chorions. At this point embryos were extensively washed in a large Petri dish coated with 1% agarose in E3 medium. Dechorionated embryos were always kept in the E3 or E2 medium and transferred to Perti dishes coated with 1% agarose in E3 medium.

2.2.3. Needle preparation

Needles for injection and transplantation were pulled with the use of two different sets of parameters resulting in optimal needle tip length and thickness. Injection needles, containing a filament, were filled with a small amount of reagent and the tip was broken with dissection forceps. Injection needles were disposed of after use. Needles for transplantation, without filament, were broken at standardized diameters of the opening adjusted to the cell sizes at desired stages of developmnent. The needle opening was sanded on a needle grinder resulting in a blunt opening. Transplantation needles were stored and used many times.

2.2.4. RNA injections

The injection volume of a drop was measured prior to injection in heavy mineral oil deposited on a dipping slide. The volume was calculated from the diameter of the drop at 40x magnification, at the moment when the drop is round and close to the surface. In general a drop of 5 divisions on an ocular scale at magnification 40x was calculated as 1 nl. Injected volume was kept between 1-2 nl per embryo and never exceeded 4 nl of an RNA solution at 50-200 ng/nl in H_2O with 0.2% Phenol Red. For some experiments mini-ruby was added as lineage tracer. RNA was stored in aliquots at - 80ºC.

Dechorionated embryos were transferred with a fire-polished glass Pasteur pipette into a dish coated with 1% agarose with wells of single embryo width (formed by a custom made mold). Aligned embryos were then injected at one cell stage into the cell at the entry of the cytoplasmic streaming from the yolk.

2.2.5. Morpholino preparation and injections

Morpholino stocks were prepared as advised by Genetools protocols. The concentration of stocks was measured on Nanodrop, using 0.1N HCl as medium and the custom nucleic acid setup with Constant = 30 and absorption wavelength λ = 265. Master stocks of morpholino at 1 mM concentration were diluted 1: 5 or 2: 5 and in Danieau medium with 0,02 mg/ml Fast Green dye. Working stocks of MO were stored at 4ºC. The drop size was measured as above and the volume was similarly restricted to 1-4 nl/egg. Embryos were injected at 1-2 cell stage as above, into the cytoplasmic streaming. Shortly after the first cell divisions started, unfertilized eggs were sorted out and the remaining injected embryos were counted in further statistics.

2.2.6. Cell transplantation

Petri dishes for transplantation were prepared with a special mould, which printed very small one-embryo sized wells in the agarose. Embryos were transferred into these wells and oriented with the animal pole up. The manual transplantation setup consisted of a syringe fastened to the bench, connected with a narrow insulated tube to the needle holder, which in turn was attached to a micromanipulator. The pressure in the needle was controlled manually by pulling and pushing the syringe piston gently. The cells were transplanted by careful manual suction of single cells out of the donor embryo and injection of these cells into the animal pole of the host embryo, just below the epiblast.

2.2.7. Protein bead implantation

Acrylic beads of 10 μm diameter were prepared by incubation overnight in recombinant zebrafish Fgf8-Cy5/PBS solution. The protein concentration used in this study was 150 pg/ml, of which approximately 50% were labeled. The protein stability was tested before and showed that beads show high rate of protein degradation already after 5 days in 4ºC. Therefore, each experiment was performed on beads up to 3 days after preparation.

Beads soaked in Fgf8-Cy5 were implanted into the host embryos between sphere and 30% epiboly. In order to access the bead by confocal microscopy, beads were implanted shallowly under the epiblast, using a Tungsten wire. Embryos for this experiment were placed in transplantation Petri dishes with single embryo agarose wells and oriented such that animal pole was facing upwards. The time course experiments were conducted in 28ºC in the incubator or on a preheated microscope stage.

2.2.8. Whole mount in situ hybridization

Embryos were fixed in 4% PFA overnight at a desired stage of development. After fixation embryos were washed well in PBST and transferred in 100% methanol and into -20ºC for at least 2h for dehydration and freeze cracking. Embryos could be stored this way for months. Subsequently, embryos were rehydrated in 50% MetOH/PBST and PBST and digested in 10 μg/ml Proteinase K/PBST solution. Duration of the digest was adjusted according to the developmental stage of the embryos and the strength of the given enzyme stock. Digestion was stopped by washing the embryos in 2% glycine/PBST and subsequent fixing in PFA (20 min). After fixing, samples were washed in PBST again and transferred for prehybridization into Hyb^+ for 2-6 hours. From prehybridization until blocking step embryos were always incubated in 68ºC oven on a rocking platform. Hybridization was started by replacing Hyb^+ on the samples with DIG or Fluorescein labeled probes diluted in Hyb^+ overnight.

Washing of embryos after hybridization was achieved by progressive transfer of embryos into Hyb^- (5 min), 25% Hyb^- in 2x SSCT (3x 10 min), 2xSSCT (5 min) and 0.2 SSCT (2x 30 min). After that embryos were transferred into 50% MABT/0.2SSCT in the room temperature and changed after 5 min into MABT.

Samples were then transferred into 2% DIG block solution for 1h blocking incubation. Subsequently the antibody incubation (2h at RT) was started where the antibody was diluted 1:4000 in 2% DIG Block buffer.

The embryos were then washed 4x 15 min in MABT and transferred into a 24-well plate. After washing the color reaction was initiated by replacing MABT with BM Purple reagent. The reaction was developed in the dark overnight in 4ºC or for 2-5h in room temperature until sufficient staining intensity was reached. The color reaction was stopped by a few PBST washes and post-fixation in PFA. Subsequently samples were washed 3 times in PBS. For imaging embryos were cleared and stored in 70% glycerol.

For detection of the Fluorescein probe, embryos were incubated 3x 15 min in 0.1MGlycine/HCl (0.1% Tween20, pH 2.2), washed in PBST and transferred again into MABT. After a 45 min blocking in 2%DIG Block/MABT at room temperature embryos were transferred into fresh anti-fluorescein-AP antibody at 4ºC overnight (dilution 1:1000).

Subsequently samples were washed in PBST and preincubated with 0.1M Tris/HCl (pH 8.2). After preincubation the color reaction was initiated by putting dissolved Fast Red

Tablet solution on the samples. The reaction was developed in the dark until desired intensity. The reaction was then stopped by quick PBST wash and PFA post-fixing.

2.2.9. Biotin detection

To detect the transplanted mini-ruby labeled donor cells in a host embryo, Vectastain Elite ABC kit was used. First, 16 μl of each solution A (streptavidin) and solution B (biotin-peroxidase) were diluted in 1ml PBST and incubated for 30 minutes. After in situ hybridization, embryos were washed with PBST and then incubated in the previously prepared AB solution for 45 minutes at room temperature. Then, they were washed 5 minutes, 10 minutes and 15 minutes with PBST and stained using DAB tablets (Sigma), according to manufacturer's instructions. The reaction was stopped by several washes in PBST.

2.2.10. Agarose Gel Electrophoresis

Agarose gels were prepared in TAE Buffer and boiled in a microwave for melting. DNA fragments differing by more that 200 bp were resolved on 1% gels, whereas genotyping samples characterized by 20-50 bp size differences were resolved on 2% gels. Gels before setting were mixed with 5% ethidium bromide. Electrophoresis was run in a TAE filled chamber at a constant voltage of 80-120 V, depending on the chamber and gel size (10-20V/1cm gel length). After the gel was satisfyingly resolved (as judged by the loading dye band separation) the bands were photographed in a UV chamber with an attached camera. Alternatively, bands were cut out of the gel with a scalpel under a low-UV illumination.

2.2.11. Cloning

Cloning steps were designed using Vector NTI software (Invitrogen). Cloning of genes or gene fragments from cDNA was done by RT-PCR and subsequent TOPO cloning and TOP10 E.Coli transformation, according to manufacturer's protocol. DNA fragments, which were cloned in specific sequence into one vector, were clone by restrictive digest and ligation between chosen restriction sites.

In order to combine sequences into a fusion protein construct, a neutral and flexible linker was used, which was encoded as an overhang into the gene-specific primer. In most cases the sequence used for linker (up to 6 aa long) encoded Gly-Ser-Gly-Ser tandem repeat, which was shown by David Drechsel (Protein Expression Facility MPI-CBG Dresden) to cause least steric tension. In order to propagate cloned DNA, chemically competent E.Coli bacteria XL2 Blue were used for transformation and culture.

Colonies after cloning were checked for presence of an insert either by colony PCR (where instead of purified template a whole bacterial colony was added to the reaction) or by miniprep, restriction digest and agarose gel electrophoresis. Positive clones were then sent to sequencing for verification.

2.2.12. RNA isolation

RNA isolation from fish embryos was achieved using Trizol Reagent (Invitrogen). Embryos were homogenized in Trizol by multiple squeezing through a 0.7 mm needle into the 10 ml syringe. Homogenized embryos were then treated according to the Trizol RNA extraction protocol.

2.2.13. Synthesis of DIG labeled probes for in situ hybridization

DIG labeled antisense riboprobes were synthesized from DNA plasmids containing cDNA of the gene of interest. The plasmid DNA was first linearized with the appropriate restriction enzyme and then used as a template for RNA synthesis, using a DIG labeling kit (Roche Diagnostics, Germany). After synthesis, the DIG labeled RNA was precipitated by incubation with LiCl, overnight at -20°C. The RNA was then pelleted by a 30-minute centrifugation at 13000 rpm at 4°C, washed with 70% ethanol and re-suspended in 100 μl of RNase-free water. This solution was further diluted to 500 μl with hybridization solution. Routinely, a dilution of 1:100 of this stock was used for in situ hybridization protocols.

2.2.14. PCR

PCR reactions were performed on Eppendorf thermocycler according to standard protocols advised by the producer of the polymerase. Genotyping reactions were all performed with use of Taq Polymerase using a standard program: 25 cycles, 57ºC annealing temperature and 72ºC elongation. All PCR reactions for cloning were performed using Platinum Pfx Polymerase or Advantage Polymerase, which guaranteed higher fidelity of the amplification. Annealing temperatures used were for the most cases used according to the Wallace rule, calculated by the prediction software: Tm = 2°C * (A+T) + 4°C * (G+C).

The elongation time was calculated roughly to be 1min/kb, e.g. 2,5 kb Fgfr1a gene was amplified using 3 min. elongation time.

In order to achieve increased product specificity and yield, nested PCR with an internal primer pair was used. Nested primers for genotyping contained overhangs for forward and reverse M13 primer in case the product was to be sequenced. Nested primers for cloning often contained overhangs with restriction sites for further specific subcloning into the vector.

2.2.15. Site Directed Mutagenesis

Site directed mutagenesis primers for introducing Y753F change in Fgfr1a construct were designed as 45 nt long forward and reverse oligonucleotides, complementary to each other and to the template, except the change site. The reaction was setup according the instruction provided by the manufacturer (Stratagene). Bacteria used for transformation of the quickchange product were provided in the kit (Supercompetent XL1 Blue E.Coli).

2.2.16. RACE PCR

RNA for RACE PCR was isolated from one-day-old embryos. The first strand DNA was synthesized according to the protocol (Clontech). Gene specific primers were designed according to Manual guidelines: long (~30 nt), Tm<70ºC. Two gene specific primers were designed for each gene and the nested primer did not overlap with the first primer.

DNA was then amplified according to the provided protocol using Advantage Polymerase (Clontech).

2.2.17. Quantitative Real Time PCR

Primers for q-PCR were designed such that the product was about 200 bp for both, Fgfr1a and the internal control, 18S. The specificity of primers was validated first on regular RT-PCR and the conditions were optimized for best and most specific yield.

The RNA for q-PCR was isolated as described above from embryos staged precisely in order to compare wildtype and mutant embryos. 20 embryos per each sample were pooled together.

The reactions were setup as advised in Brilliant SYBR Green QPCR manual, where each Fgfr1 and each internal control 18S were prepared in triplicate. The reactions were run on realtime PCR instrument Stratagene MX4000 with SYBR Green and Reference Dye measurements after each cycle (total of 30 cycles).

The measurements were collected and exported to Excel sheet for further calculations. The relative amounts of transcripts were calculated using $2^{-\Delta\Delta CT}$ method described in detail by (Livak and Schmittgen 2001). Standard deviations and significance were calculated using Excel statistics tools.

2.2.18. RNA for injection

Injection plasmid construct was first linearized so that the linear sequence ended behind the polyA signal sequence, downstream of the gene of interest. Efficiency of linearization was checked on an agarose gel electrophoresis and the linear DNA was purified using a Gel Extraction Kit. Subsequently, DNA was used in an in vitro RNA synthesis reaction using suitable mMessage kit (containing SP6, T7 or T3 Polymerase). DNA was digested at the end of reaction with DnaseI. The RNA was then precipitated in $LiCl_2$ and subsequently dissolved in ddH_2O. The RNA concentration was determined in a Nanodrop. Most RNA stocks were diluted to a working concentration of 200pg/nl, split into small aliquots and stored in -80ºC.

2.2.19. Imaging subcellular structures

Living embryos were mounted in moulds of agarose-coated transplantation dishes, containing E3 media. The embryos were oriented with the side of interest facing up. Confocal images were acquired on upright Leica SP5 confocal microscope with HCX APO L UVI 40x/0,8 WATER (dipping) or HCX APO L UVI 63x/0,9 WATER (dipping) objectives. For co-

localization studies of multiple laser line combinations, images were acquired by line-by-line sequential, bidirectional scanning, using a suitable combination of laser excitation lines (458, 476, 488, 496, 514, 561, 633). For example for GFP/RFP acquisition 488 and 561 laser lines were used, whereas mRFP/Cy5 acquisition required the use of 561 and 633 laser lines. The pinhole was adjusted to 1 Airy for all and the images were acquired at 1048x1048 resolution.

In order to collect as much data as possible on subcellular structures, the focus was set on first 3 most superficial cell layers in the embryo. The data was stored and processed in a database using LAS AF 1.8.2 software. Composites were assembled using Adobe Photoshop and Adobe Illustrator.

2.2.20. Cartilage alcian blue staining

Larvae were fixed in 4% PFA overnight. The larvae were then washed in PBS and incubated twice overnight first in 50% EtOH, then 100% EtOH in order to dehydrate. Dehydrated larvae were stained for cartilage and calcified tissue in alcian blue solution containing: 70% EtOH, 30% Acetic acid and 20 mg Alcian Blue. After about 24h the larvae were neutralized in saturated sodium borate for several hours. Subsequently the samples were bleached in 15% of 3% H_2O_2 and 85% KOH. After bleaching the larvae were washed in PBS and preserved in 70% Glycerol.

2.2.21. Whole mount alizarin red skeletal staining

2.2.21.1. Staining all internal skeleton

Adult fish (at least 3 months old) were sucrificed on ice in MESAB overdose and fixed in 4% PFA for 2 days. Fixed fish were rinsed in water and incubated in 100% isopropanol overnight in room temperature to partially remove fat. Later fish were transferred into bleach (80% KOH, 20% of 3% H_2O_2) at 37ºC for several hours in order to remove the color pattern. After bleaching fish were washed in 1% KOH and the scales were removed with a needle. Subsequently the tissue was rendered transparent by prolonged trypsin digestion in a solution containing: 35% saturated sodium borate, 65% ddH_2O and 1% trypsin (Sigma, powder). After the tissue reached about 60% transparency the specimens were stained with alizarin red (0.1g alizarin red in 1% KOH) for 24h. After that the skeletons were destained in KOH for 2 days, with occasional buffer change, until the tissue was clear and the bones were dark red. The specimens were then preserved and photographed in 70% glycerol.

2.2.21.2. Staining scales

Staining scales was performed similarly as staining internal skeleton but without scale removal and trypsynization. Scales were also well visible without bleaching.

2.2.22. Genotyping Mutant fish

Embryos and young larvae were first lysed in Embryo Lysis Buffer in 55ºC for several hours until the tissue disappeared. Lysates were then used directly as template source. Adult fish were fin-clipped under anesthesia (6 ml of 0.4% MESAB in 1% Na_2HPO_4 * $2H_2O$ per 100 ml E3). Fin-clips were lysed in Tissue Lysis Buffer in 55ºC until the tissue decomposed. Subsequently the DNA was isolated by isopropanol precipitation and resuspended in 100 µl H_2O.

Genotyping was always performed in two rounds of PCR reactions with outer and inner (nested) primer pairs, amplifying on average 400-600 bp genomic DNA fragments. The same primers were used earlier in TILLING screen for sequencing amplicons of interest.

PCR products were then either directly sequenced or analyzed using Derived Cleaved Amplified Polymorphic Sequences method (dCAPS – see list of websites), using restriction digest. The table below lists all enzymes that were used to distinguish mutations in TILLING mutant lines. PCR products were digested overnight and resolved on 2% agarose gels. The band size shifts were then registered and analyzed.

Mutation	Enzyme used in dCAPS	Gel bands prediction
Fgfr1^{W671STOP}	MboI	WT higher band of 269 bp gets cleaved in mutant and results in a smaller band of 244 bp
Fgfr1^{F679F}	MboII	WT (290 + 202 bp) cleavage site is lost in mutant resulting in a higher band of 492 bp
Fgfr1^{Y326STOP}	MseI	WT higher band of 206 bp gets cleaved in mutant and results in a smaller band of 165 bp
Fgfr2^{L545STOP}	BfmI (SfeI)	WT higher band of 183 bp gets cleaved in mutant and results in a smaller band of 140 bp
Fgfr4^{R36STOP}	PagI (BspHI)	WT higher band of 600 bp gets cleaved in mutant and results in 2 smaller bands of 433 and 166 bp
Fgfr4^{Y43STOP}	EcoRV	WT (413 + 152 + 34 bp) cleavage site is lost in mutant resulting in a higher band of 447 bp

2.2.23. Western Blot

2.2.23.1. Sample preparation

Embryos for Western Blot were pooled at a desired stage and deyolked using ½ Ringer Buffer. Embryos were homogenized by pipetting up and down in yellow tip (200 µl). After a brief incubation the embryos were spinned in a tabletop mini-centrifuge and the supernatant was discarded. The cell pellet was then lysed in 2x SDS Loading Buffer and boiled in 95ºC for 5 min. The sample was ready to use or stored in -20ºC for weeks.

2.2.23.2. PAGE

Polyacrylamid gels were prepared as described in (Sambrook and Russell 2001) and cast in Biorad chambers. Smaller proteins were resolved on 12% developing gels, whereas

Immunoprecipitation gels were of 6,5% due to high molecular complexes. The electrophoresis was run at constant 40 mA.

2.2.23.3. Transfer and detection

Transfer of proteins on Immobilion-P transfer membrane (Millipore) was performed in a semi-dry setup (Biorad) at 90 mA per gel for 2 hours. After transfer membranes were stained shortly in Ponceau Solution in order to see the resolution and abundance of the protein bands. Subsequently, the membrane was washed in PBST and transferred into the blocking buffer (3% milk in PBST) for an hour. The primary antibody incubation was usually allowed overnight at 4ºC (antibody in blocking buffer). The antibody was then washed off by 3x 10 min milk/PBST washes and the secondary HRP-antibody was applied for 30 min. The second antibody was washed off with PBST (3 x 10 min). The exposure was done in a photographic cassette using ECL Reagent Kit and detectec in a Kodak Film developer machine. Film exposure varied from 30 sec to 20 min.

2.2.24. Immunoprecipitation of FGFR from embryos

2.2.24.1. Sample preparation

Embryos for immunoprecipitation were dechorionated and harvested at shield stage. In order to pull down sufficient amout of protein 100 embryos were taken per sample. Embryos were place on ice in 1 ml solubilization buffer per sample. The lysate was vortexed from time to time. After 20 minutes incubation the lysate was centrifuged for 20 mins at 4ºC, 13000 rpm. The supernatant was then collected into a fresh tube and the protein concentration measured.

2.2.24.2. Immunoprecipitation

25 μl of 50% slurry of GammaBind G Sepharose (Amersham) was use per sample. Initially the necessary amount of sepharose was washed twice with solubilization buffer. The beads were then resuspended in approximately 300 μl solubilization buffer with addition of 10 μg IP antibody (anti-myc or anti-Fgfr1a). The antibodies were allowed to couple with the beads for 1h at 4ºC with mild agitation. Coupled beads were subsequently washed 3 times with solubilization buffer and resuspended in 200 μl final volume. This volume was then aliquoted in equal amounts into the tubes containing the embryo lysate samples.

The immunoprecipitatation was then allowed at 4ºC with gentle rotation for 1h. After IP, the beads were washed 3 times in HNTG. The beads were then centrifuged and the excess of buffer was removed. This sample was then boiled in 2x SDS Loading Buffer and taken as a ready-to-go Western Blot sample. The western Blot was developed either using anti-ubiquitin or anti-HA antibodies, depending on the sample.

2.2.25. DEAB retinoic acid inhibition

In order to inhibit retinoic acid production in developing embryos I used 4-(Diethylamino)-benzaldehyde, DEAB, which blocks activity of RA producing Aldh enzymes. In order to block RA signaling during gastrulation embryos were dechorionated and placed in agarose coated dishes with E3 and 10 mM DEAB or DMSO as control. The dishes were preincubated in the inhibitor/control solution for a couple of hours in order to equilibrate the agarose. The incubation period used was between 30% and TB, when the medium and dishes were exchanged. Subsequently, the embryos were fixed at desired stage and treated in experimental and control groups.

2.2.26. Overview of the TILLING approach

Ligand-receptor specificity can be approached by a direct comparison of phenotypes evoked by single ligand and receptor loss-of-function. Knowledge of Fgf8 loss-of-function phenotypes in zebrafish provides information about functions of the ligand, which can be then compared to the receptor mutant phenotypes.

In order to produce receptor mutant fish, we have screened the Dresden and Hubrecht TILLING Libraries for two regions in each receptor gene. The amplicons, that is fragments of genes chosen for lesion detection in the TILLING library, were designed using two predictions tools, CODDLE and LIMSTILL (see table of websites in Chapter 6). Both prediction softwares help locating amplicons in coding regions of the gene as well as compute probabilities of obtaining non-sense mutations. The table below summarizes information about screened regions.

The numbers of exons do not agree with the latest release of zebrafish genome assembly (Zv7), because all predictions were made on Zv4 and Zv5, when many genes were wrongly annotated.

Amplicons used for screening ENU TILLING library

Gene	Exons covered	Predicted STOP chance	Screened area (bp)	Non-sense mutations	Mis-sense mutations
Fgfr1a	7	8,95%	427	1	2
	18,19	6,65%	431	1	3
Fgfr2	2	6,39%	139	-	1
	7	6,98%	434	1	-
Fgfr3	2	6,39%	576	-	7
	7	6,84%	402	-	1
Fgfr4	2,3	7,80%	678	2	2
	13,14	7%	702	-	4

Screened amplicons were located either in the very early positions in the gene (for producing early nonsense mutants) or within the tyrosine kinase domain (for producing dominant negative mutants). TILLING Facility in MPI-CBG Dresden screened 12288 fish in Hubrecht and Dresden Tilling libraries. Among 25 of detected missense and nonsense mutations we found six that were likely to result in a dysfunctional protein, which I described in this work. We have screened the library for all Fgfr genes found in zebrafish until 2005 (i.e. not Fgfr1b), however, we did not find any nonsense or interesting missense (e.g. in conserved sites) mutations in Fgfr3.

3. Results

Based on extensive studies of Fgf mutants and their expression patterns there is some understanding of their functions in early development (Ornitz and Itoh 2001). There is still, however, little known about the function of Fgfrs and their specificity for ligands in vivo. In the following I present the generation of fgfr loss-of-functions situations by mutagenesis and morpholino knockdown. I also describe my approach to study endocytosis of Fgfr1 in vivo in overexpression experiments.

3.1. Expression of *fgf8a*, *fgf3* and *fgf24*

In order to address ligand-receptor specificity I should briefly describe the expression of three members of the Fgf ligand family, which were previously shown to play a role in early development (Figure 3.1). These are fgf8a, fgf3 and fgf24, which act redundantly or cooperatively in zebrafish dorsal-ventral (D-V) patterning, specification of mesoderm, positioning of MHB, left-right asymmetry and patterning of the eye, ear, heart and many other (Reifers et al. 1998; Picker et al. 1999; Reifers et al. 2000; Phillips et al. 2001; Draper et al. 2003; Picker and Brand 2005).

Fgf8a is initialized after midblastula transition in the dorsal marginal zone. Later and throughout gastrulation it becomes expressed in the margin (Fig 3.1 A). As epiboly progresses, the expression becomes stronger on the dorsal and weaker on the ventral side. At about 70% epiboly an additional domain of expression comes up in presumptive hindbrain area. At the beginning of somitogenesis, fgf8a starts being expressed also in the telencephalon, the hindbrain domain is restricted to prospective rhombomeres 2 and 4, whereas posterior expression labels newly arising somites, floor plate, lateral neural plate and presomitic mesoderm. Fgf8a is also faintly expressed in the heart primordium. Beyond 8 somites the hindbrain expression is restricted to MHB only and from about 20 somites Fgf8a is also present in the retina. In one-day embryos fgf8a is expressed in the MHB, optic stalks, telencephalon, otic vesicle, dorsal somites and caudal fin fold.

Similarly, fgf3 and fgf24 are both expressed in the margin during gastrulation (Fig 3.1 B, C). Fgf3 is expressed from midgastrula in presumptive rhombomere 4, whereas fgf24 is expressed in anterior axial mesoderm. Later in development expression of the two fgfs diverges.

During somitogenesis fgf3, which belongs to the Fgf8a synexpression group, is also expressed in the telencephalon, hindbrain and tailbud. Its expression gets later restricted to rhombomere 4 and MHB. Later during somitogenesis, fgf3 is also weakly expressed in posterior somites and strongly in neural crest cells. The expression comes up also in otic vesicles and some areas of the telencephalon.

Expression of fgf24 during somitogenesis is restricted to otic and olfactory placodes, polster and tailbud. At later stages (18 s) fgf24 is also expressed in pharyngeal arches, pectoral fin primordium and lenses.

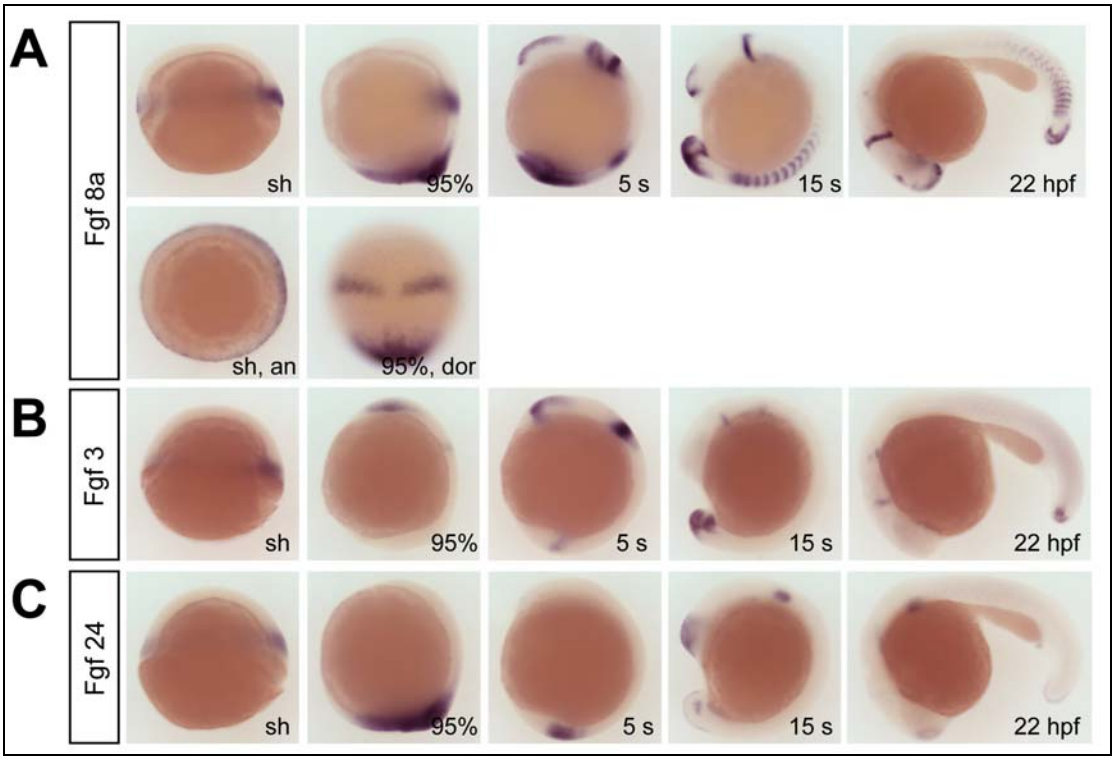

Figure 3.1 Expression patterns of *fgf8a, fgf3* and *fgf24*
Fgf8a (A) is expressed in the margin during gastrulation. At midsomitogenesis a domain at the future hindbrain comes up. During segmentation, *fgf8a* is also seen in the telencephalon, somites, the presomitic mesoderm and the fin fold. *Fgf3* (B) is expressed in the margin during gastrulation. Later it is also present in the forebrain, in the MHB and the tailbud. From late somitogenesis *fgf3* can be additionally detected in the otic vesicles, the fin fold and the neural crest. *Fgf24* (C) is expressed in the margin during gastrulation. During segmentation it is present in the tailbud, olfactory buds and otic vesicles. Late in segmentation it can be also detected in the pectoral fins and in the fin fold.

3.2. Functional analysis of Fgfr1

3.2.1. Expression of Fgfr1

Both Fgfr1a and b are maternally provided and are ubiquitously expressed until midgastrulation (Fig. 3.2 A and 3.3 A). At this stage the ventral expression starts disappearing. Fgfr1b is also downregulated in dorsal midline and dorsal margin. From tailbud until mid-somitogenesis the ubiquitous dorsal expression of Fgfr1a becomes restricted to the forebrain, the MHB, somites and presomitic mesoderm (Fig. 3.2 B and 3.3 B). It is also found at low levels in the hindbrain.

During later somitogenesis (20 somites – 24 hpf) Fgfr1a transcript can be found in pharyngeal arches, the MHB, several domains of the telencephalon and the diencephalon, including the optic stalk and the olfactory placode (Fig. 3.2 C,D). Fgfr1a is expressed in the

lateral line primordium. In the tail expression persists in the posterior somites and tailbud, which gets restricted to the tailbud by 24 hpf.

In comparison, Fgfr1b is expressed in broader domains of diencephalon, midbrain, cerebellum and ventral hindbrain (Fig. 3.3 C, D). The telencephalon is completely devoid of Fgfr1b, which instead is expressed in the retina. There is a weak expression in the neural crest and inner cell layer of otic vesicles, whereas the expression in the trunk and somites seems to stay diffuse at low levels. Posterior somites and presomitic mesoderm express Fgfr1b strongly until after 24 hpf.

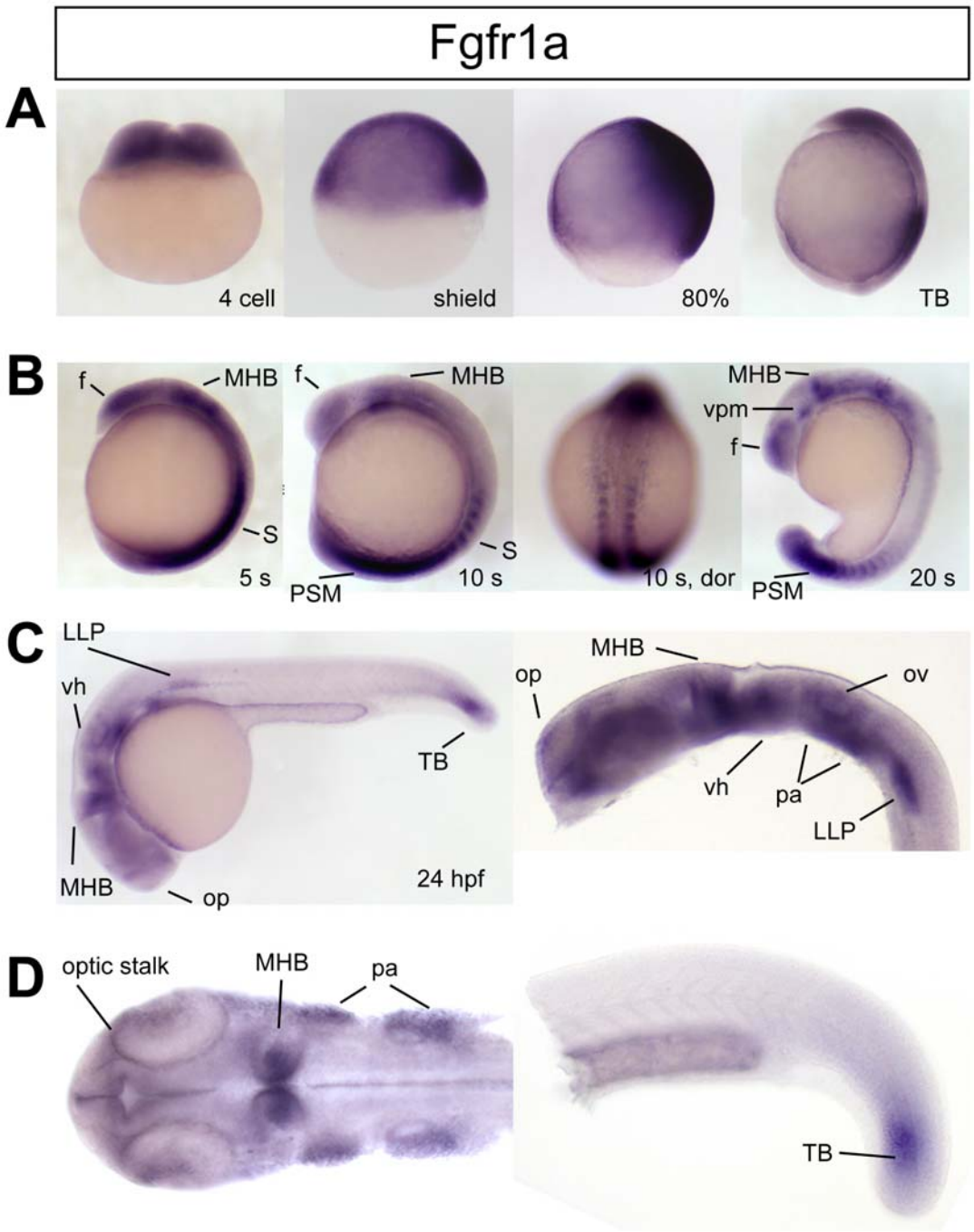

Figure 3.2 Expression pattern of Fgfr1a
Fgfr1a is maternally provided and expressed ubiquitously throughout blastula and early gastrulation stages. Late in gastrulation it is downregulated on the ventral side and still strongly expressed dorsally

(panel A). Later the expression becomes restricted to brain and presomitic mesoderm (panel B). At 24hpf Fgfr1a is restricted to olfactory placode and optic stalks, diencephalon, midbrain-hindbrain boundary, ventral hindbrain, otic vesicles, lateral line primordium, few posterior somites and tailbud. At 24 hpf, expression in somites and telencephalon have disappeared but persists in the lens and epiphysis (panels C, D). Abbreviations: f – forebrain, LLP – lateral line primordium, MHB – midbrain-hindbrain boundary, op – olfactory placode, ov – otic vesicle, pa – pharyngeal arches, PSM – presomitic mesoderm, TB – tailbud, vh – ventral hindbrain, vm – ventral posterior midbrain.

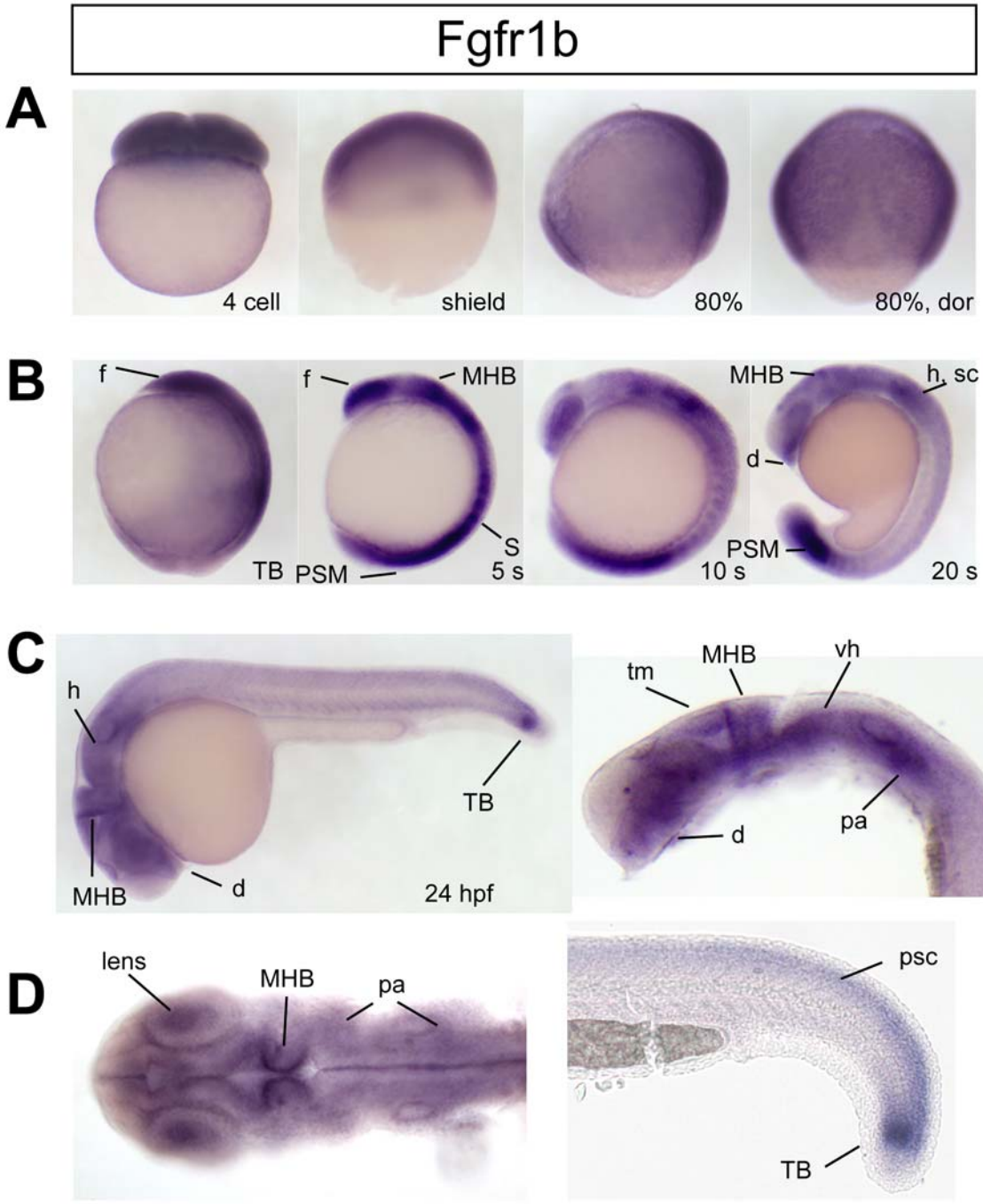

Figure 3.3 Expression pattern of Fgfr1b
Expression of Fgfr1b is almost identical to Fgfr1a at early stages, with some small differences: during late gastrulation Fgfr1b in downregulated at dorsal midline and dorsal margin (panel A). Later, during somitogenesis it appears to be more ubiquitous than Fgfr1a. Fgfr1b transcript is not found in telencephalon but is quite abundant in the eye vesicles. At 24 hpf, it is quite strongly expressed throughout neural tube, expect telencephalon and dorsal hindbrain. It is weakly expressed in the spinal cord, lenses and otic vesicles. Abbreviations: d - diencephalon, f – forebrain, h – hindbrain, MHB – midbrain-hindbrain boundary, pa – pharyngeal arches, psc – posterior spinal cord, PSM – presomitic mesoderm, s – somites, sc –anterior spinal cord, TB – tailbud, tm – tectum of midbrain, vh – ventral

hindbrain.

3.2.2. Analysis of Fgfr1 loss-of-function

3.2.2.1. Fgfr1a mutant zebrafish

Three independent mutations in Fgfr1a were isolated in the TILLING screen for Fgfr mutants (summarized in Figure 3.4, the TILLING approach is described in the Materials and Methods). The early stop mutation is located in exon 8, which is incorporated exclusively into Fgfr1a IIIb isoform. Presumably, this mutation results in IIIb isoform loss-of-function (allowing only a small portion of the extracellular domain to be produced). Much like in FGFR1IIIb -/- mutant mice there are no embryonic or adult defects detectable in homozygous Fgfr1a^{Y328STOP} -/- fish.

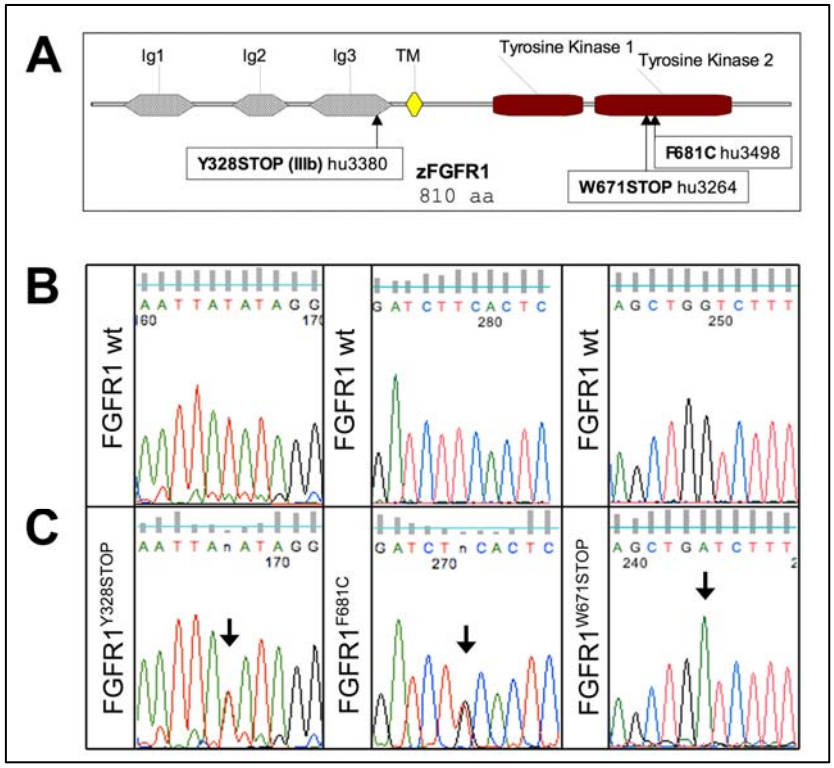

Figure 3.4 Summary of Fgfr1a TILLING mutants
Three mutations were found in Fgfr1a gene (A). Fgfr1^{Y328STOP} is located on exon 8, which means it affectes Fgfr1 IIIb isoform. Fgfr1a^{W671STOP} results in partial disruption of tyrosine kinase domain. Fgfr1^{F681C} is a substitution in a conservative residue of tyrosine kinase. The genetic context and the nature of mutations is summarized in a panel of chromatogram traces (B).

We also found a missense mutation - Fgfr1a^{W681C} where a highly conserved phenylalanine 679 in the tyrosine kinase domain is changed to a cystein. This mutation also did not cause any developmental or adult phenotypes when brought to homozygosity. However, another Fgfr1a mutant, a late W671 nonsense mutation in the second kinase domain resulted in a near loss-of-function situation and it will be described in detail in further sections of this work.

3.2.2.2. Maternal zygotic Fgfr1^{W671STOP} shows a strong reduction of Fgfr1a message RNA

Homozygous Fgfr1^{W671STOP} mutant fish were viable and fertile. I did not observe any abnormal phenotypes during early embryonic development. Based on protein domain and crystal structure of FGFR1a one can try to predict functionality of the mutant Fgfr1a^{W671STOP} protein. This truncated form lacks some of its functional tyrosines that have been shown to play a role in protein endocytosis, PLCγ signaling, activation and regulation (i.e. Y718, Y753) (Sorokin et al. 1994) (Cross et al. 2002). Fgfr1a^{W671STOP} retains, however, its juxtamembrane domain, its activation tyrosines Y640 and Y641, and its predicted ATP-binding pocket (InterPro prediction). Nevertheless, the protein is much shorter and may have lost some of the integrity of the remaining domain.

First, I have examined both the endogenous expression of the mutant protein in vivo and the functional characteristics of the mutant protein in overexpression experiments (Figure 3.5). I mated homozygous mutant fish and analyzed expression of Fgfr1a in maternal zygotic (mz) Fgfr1^{W671STOP} embryos by in situ hybridization (Fig 3.5 A).

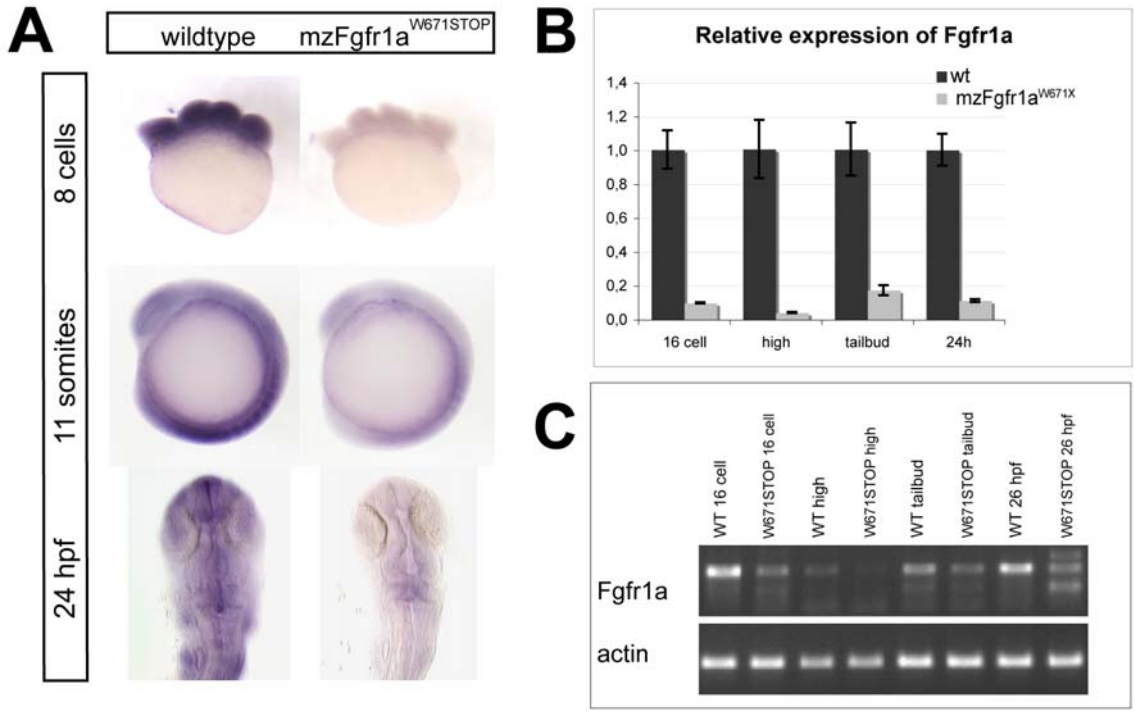

Figure 3.5 Expression of *fgfr1a* is reduced in mzFgfr1a^{W671STOP} embryos
In situ hybridization (A), Q-PCR (B) and RT-PCR analysis (C) unambiguously show that Fgfr1a expression is greatly reduced in mzFgfr1a^{W71STOP} homozygotes. Fgfr1a transcript shows over 90% reduction also at very early stages of development such as 16 cells (normalized against 18S levels as an internal control).

MzFgfr1^{W671STOP} mutant embryos exhibit strongly reduced levels of the Fgfr1a transcript compared to wildtype control. In order to verify this result quantitative real time PCR and RT-PCR were done on the RNA from embryos at four selected early development time-

points (Fig 3.5 B and C). Both experiments indicate downregulation of fgfr1a transcript in mutant embryos. Relative quantitative analysis estimated mutant fgfr1a transcript levels as 10% of the wildtype norm.

3.2.2.3. Fgfr1^{W671STOP} uptake and the signaling capacity are reduced

To test the functionality of the mutant protein I have cloned Fgfr1a^{W671}-mRFP construct. Upon overexpression the fusion protein is capable of inhibiting Fgf signaling in gastrulating embryos (Fig. 3.6 A) but to a lesser degree than the overexpression of dominant negative FGFR1 – XFD (Fig. 3.6 B). In order to test the ability of mutant Fgfr1a to endocytose Fgf8 I performed a transplantation assay (Figure 3.6 C). I implanted receptor-overexpressing cells into Fgf8-GFP overexpressing host embryos (the nature of control Fgfr1a-RFP fusion protein is described later in section 1.2.3.1). When observed 30 min post transplantation, Fgfr1a^{W671}-mRFP expressing cells exhibit less uptake of Fgf8-GFP compared to Fgfr1a-RFP cells (Fig 3.6 D).

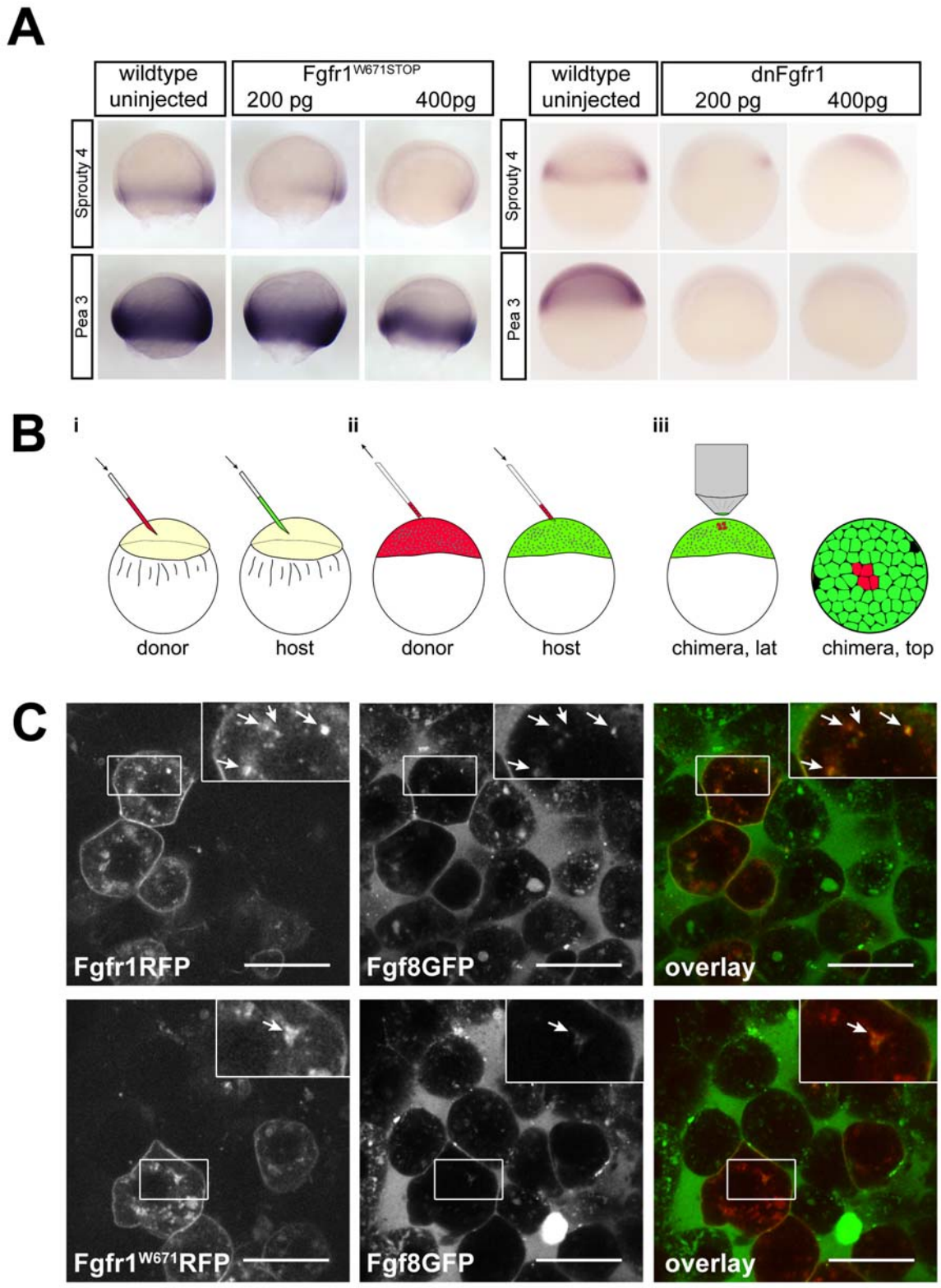

Figure 3.6 Fgfr1a^{W671STOP} inhibits Fgf signaling and Fgf8 endocytosis upon overexpression
Mutant protein Fgfr1^{W671STOP}, upon overexpression strongly blocks Fgf signaling (A), similar but less strongly than dominant negative Fgfr1 (dnFgfr1) (B). Fgfr1^{W671STOP} is not internalized as well as wildtype receptor (D). Confocal image shows receptor-overexpressing cells in Fgf8GFP host embryos 30 minutes post transplantation. Scale bar 25 μm. The scheme of experiment is presented on panel C.

3.2.2.4. Late phenotypes in mutant fish – the role of genetic background

Despite my expectations based on earlier studies in mouse (Yamaguchi et al. 1994) and zebrafish (Scholpp et al. 2004) I did not find any serious developmental defects in mzFgfr1^{W671STOP}. During gastrulation there is a slight delay in development, which is later overcome and no other abnormal phenotype was detected. The survival of homozygous fish from heterozygous incrosses was below expected Mendelian 25% (see table below).

Date	Cross	Mutant	dCAPs	No. finclips	WT	Heterozygotes	Homozygotes
11.01.08	incross hets (AB)	Fgfr1^{W671STOP}	MboI	45	15 (33,3%)	23 (51,1%)	7 (15,5%)
07.07.08	incross hets (Tu)	Fgfr1^{W671STOP}	MboI	17	7 (41,2%)	8 (47%)	2 (11,7%)

Table 6 Genotyping statistics for TILLING line Fgfr1^{W671STOP}

Simultaneously to our reverse genetic approach, the group of Christiane Nüsslein-Volhardt found a mutant in a forward genetic screen for adult skeletal phenotypes, which was subsequently mapped to the region of Fgfr1a on LG8. This mutant was found to have mispatterned and bigger scales in a very similar fashion to a strain of carp called Mirror carp (Cyprinus carpio morpha noblis). The Tübingen Fgfr1a mutant line was called analogously in German: Spiegel danio (spd), which represents Fgfr1a allele t3R705H. The genetic variance characterizing scale-less carp can be also linked to mutations in its Fgfr1 gene, which is duplicated in carp (Nicolas Rohner, personal communication). Therefore, we decided to test allelic complementation for two Fgfr1a alleles t3R705H (spd) and hu3264 (Fgfr1a^{W671STOP}). We intercrossed mzFgfr1a^{W671STOP} and homozygous spd fish and raised their progeny to adulthood (Fig. 3.7). We found numerous transheterozygotes with scale patterning defects supporting the association of mutations in Fgfr1a and dermal skeleton development.

The penetrance of this phenotype is, however, background dependent, where Tübingen (Tü) background shows maximum scale loss and Tupfel long fin (TL) background shows no phenotype. In the intercross of spd fish in Tü background and mzFgfr1a^{W671STOP} in TL we found individuals showing a wide spectrum of scale loss severity. Mutant fish in the Tü background appeared in general more fragile and only a few homozygous Fgfr1a^{W671STOP} individuals survived beyond 2 weeks of age (see Table 1).

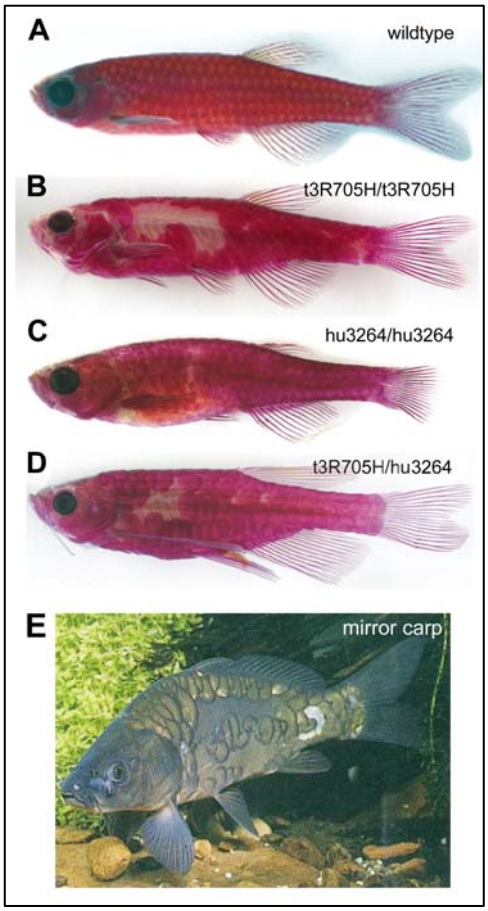

Figure 3.7 Late phenotypes in homozygous Fgfr1^{W671STOP}
Wildtype fish show a regular array of small scales of similar size (A). Spiegel danio homozygotes carrying t3H705R alleles show reduction in number, increase in size and irregular pattern of scales (B). Similarly, homozygous Tilling mutant of allele hu3264 show abnormal scale patterning and additionally fin growth defect (C). Transheterozygotes of both Fgfr1 mutant alleles show similar phenotypes (D). The penetrance of the phenotype varies in strength, probably due to the presence of a strain specific silencer gene. Photography by Nicolas Rohner. Spiegel danio, allele t3H705R, strikingly resembles scale phenotype of a mirror carp (E).

3.2.2.5. Fgfr1a morpholino knock-down

Because both Fgfr1a^{W671STOP} and Fgfr1a^{R705H} (spd) might have some residual activity, I decided to examine the early role of the gene through morpholino knockdown. I have used 3 independent translation blocking morpholinos, two of which were described earlier in the literature (Scholpp et al. 2004) (Thummel et al. 2006) (Fig. 3.8 A). In all morpholinos, no transcriptional changes were detected using pax2a, pea3, sprouty4, erm or fgf8 probes at 28 hpf (some shown in Fig 3.8 B). Testing their blocking potential on fusion protein constructs showed that they could effectively inhibit Fgfr1a-GFP production during gastrulation (Fig. 3.8 C). All of these morpholinos did affect the rate of development and caused some cell death in the area of MHB fold in over 90% percent of injected embryos at one day post fertilization (Fig. 3.8 D).

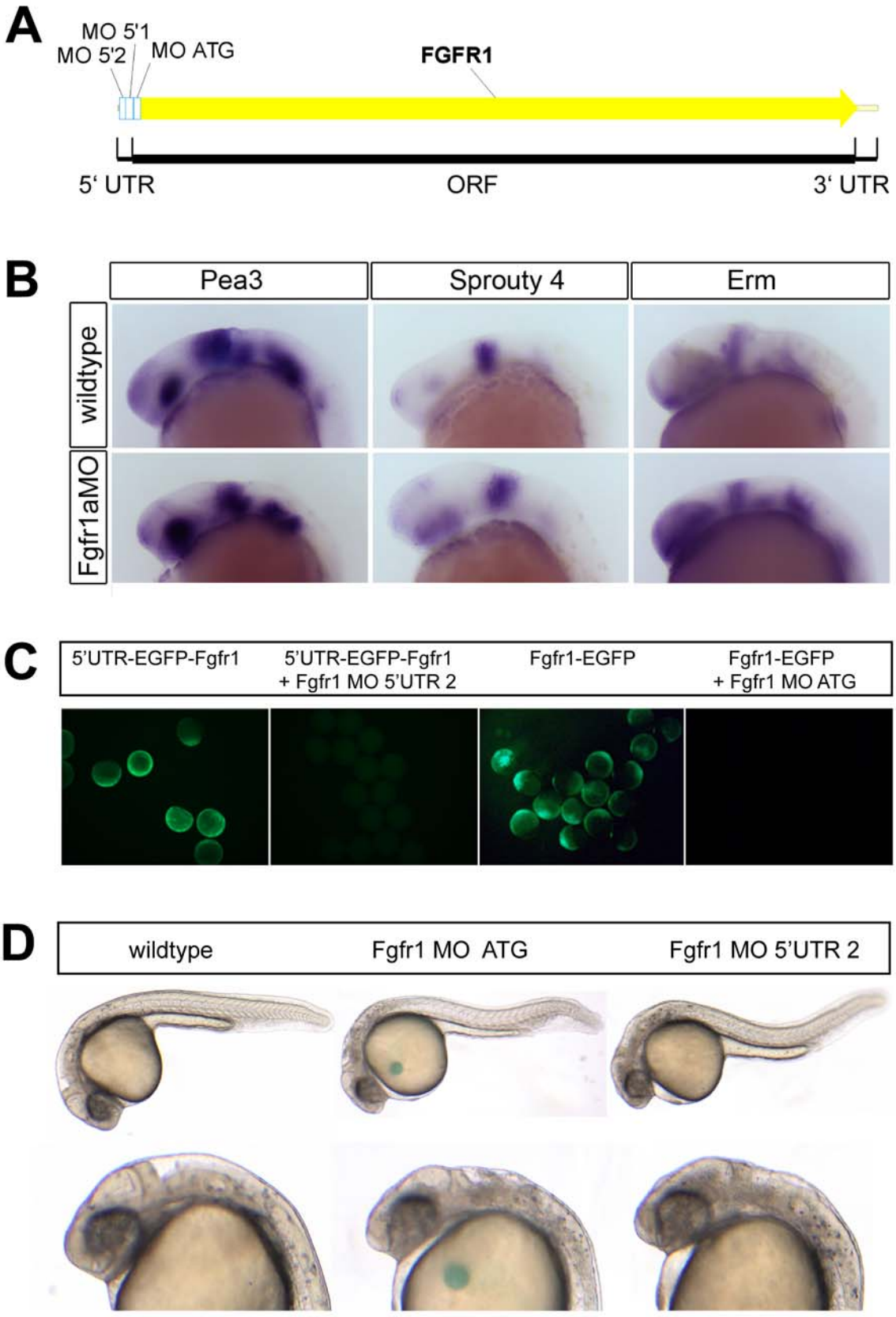

Figure 3.8 Fgfr1a morpholino design and analysis of phenotypes

Three translation blocking morpholinos were used in this study (A). Two were known published ATG and 5'UTR blockers. Neither of morpholinos affects MHB marker gene expression (B). Both published morpholinos blocked Fgfr1-EGFP fusion protein synthesis (C). Both morpholinos showed similar morphological phenotype, scattered cell death in the region of the brain, MHB reduction and condensed

somites (D). For morpholino sequence information see Appendix 5.5.

3.2.2.6. Novel Fgfr1 – Fgfr1b

The unexpected lack of phenotype upon Fgfr1 loss of function as compared to the severe phenotypes observed in mouse, Xenopus and Medaka could be explained by the compensatory activity of Fgfr1 gene found in the new assembly of zebrafish genome (Zv7) on LG10 in location 34,518,886-34,590,597 (Nicolas Rohner, personal communication). On protein level the second Fgfr1 shows 82% identity at core to the already described one, and only the very N- and C-terminus are significantly divergent (see Appendix 5.1 for protein alignment). Thus, in the following these two genes will be regarded as paralogous Fgfr1a and Fgfr1b. I have cloned the full-length cDNA of Fgfr1b and analyzed its expression as already shown in the expression pattern section of this chapter. I could show that Fgfr1b is expressed during early development and that Fgfr1a and b are expressed in a strikingly similar pattern, which supports the notion that they have redundant functions.

3.2.2.7. Morpholino knock-down of Fgfr1b

The morpholino for splice blocking of Fgfr1b was designed and kindly provided by Nicolas Rohner. The effectiveness of this morpholino was tested on RT-PCR amplification of the fragment encoding both flanking exons (Fig. 3.9 A). 0.4 mM morpholino dose leads to full retention of the intron, which in turn introduces a premature stop codon in the transcript. Nevertheless, when injected into the wildtype eggs, it did not cause any obvious phenotypes at early stages of development, except for some tail growth defects in selected few individuals (Fig. 3.9 B).

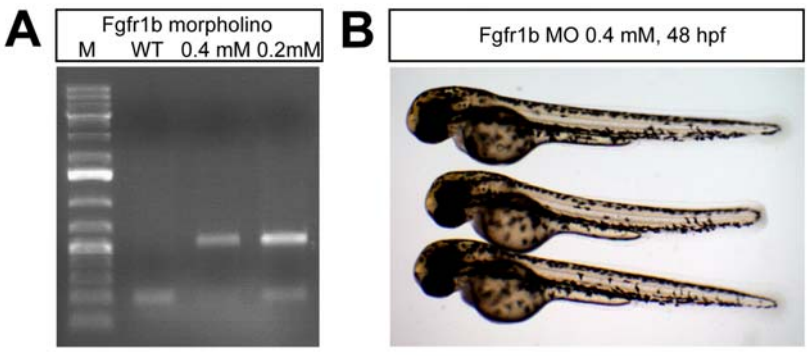

Figure 3.9 Fgfr1b morpholino design and analysis of phenotypes
Splice blocking morpholino targeting splice donor site between Exon 1 and intron 1, works and leads to full intron retention at 0.4 mM concentration (A). The phenotype is very mild, leading to subtle tail growth defects (B). For morpholino sequence information see Appendix 5.5.

3.2.2.8. Fgfr1a and Fgfr1b are involved in posterior mesoderm development

In order to test for possible redundancy of the two variants of fgfr1 genes, I decided to interfere with the expression of both fgfr1 genes simultaneously. To this end I have injected fgfr1b morpholino into the maternal zygotic Fgfr1a^{W671STOP} mutant embryos. Interestingly, double knockdown embryos developed progressively reduced tails and trunk. The phenotypes could be divided into 3 classes of severity, shown on Figure 3.10. Further investigation by in situ hybridization revealed that mzFgfr1a^{W671STOP}/fgfr1b MO morphants indeed lose mesoderm tissue (myoD, Fig 3.10 B). While neither mzFgfr1a^{W671STOP} nor Fgfr1b morphants alone show such phenotype. The brain segmentation and the MHB seems not disturbed (krox20, pax2a) upon Fgfr1 a and b loss of function (Fig. 3.10 B). This phenotype suggests redundancy between Fgfr1a and b during early mesoderm development. Moreover, observed phenotype may reflect only partial Fgfr1a and b loss of function, because splice-blocking fgfr1b morpholino does not target maternally provided RNA and I cannot rule out residual activity of the Fgfr1a^{W671STOP} protein.

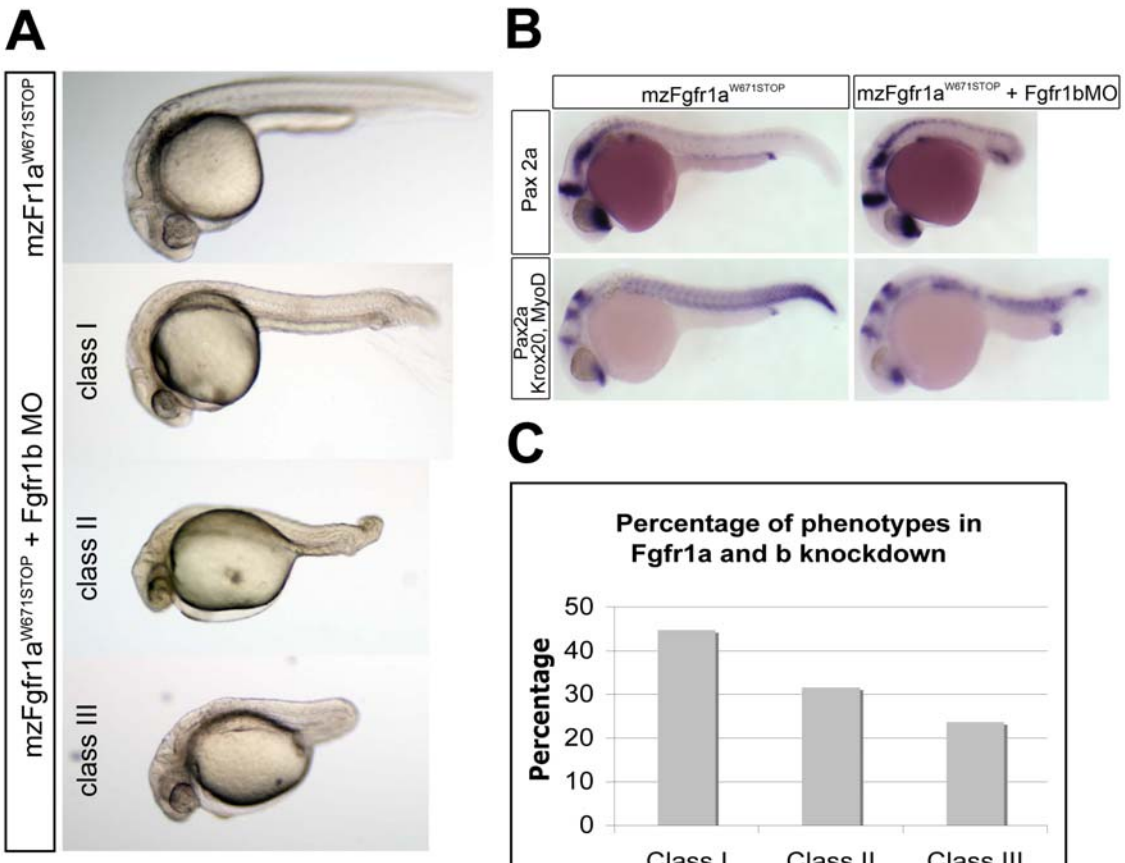

D

Mutant	Class III	Class II	Class I	Total
mzFgfr1a^{W671STOP} + Fgfr1b MO	9	12	17	38
mzFgfr1a^{W671STOP}	0	0	0	18

Figure 3.10 Fgfr1a and Fgfr1b double loss of function analysis
MzFgfr1^{W671STOP} mutant embryos injected with *fgfr*1b morpholino show three classes of phenotypes, which display progressive loss of posterior structures, grouped into three classes of severity (A). *MyoD* expression shows relative loss of mesodermal precursors in the tail. Other markers such as *pax2a* and *krox20* do not differ in morphants (B). The experiment was performed several times and quantified once (C, D).

3.2.3. Trafficking of Fgfr1a

3.2.3.1. Cloning and testing Fgfr1a-GFP/RFP fusion proteins

Elucidating the function of the receptor in Fgf8 signaling and endocytosis involves imaging the subcellular localization and trafficking of the receptor complex. In order to enable observations of Fgfr in vivo, I cloned several fusion protein constructs of Fgfr1a with mRFP or EGFP (Fig. 3.11).

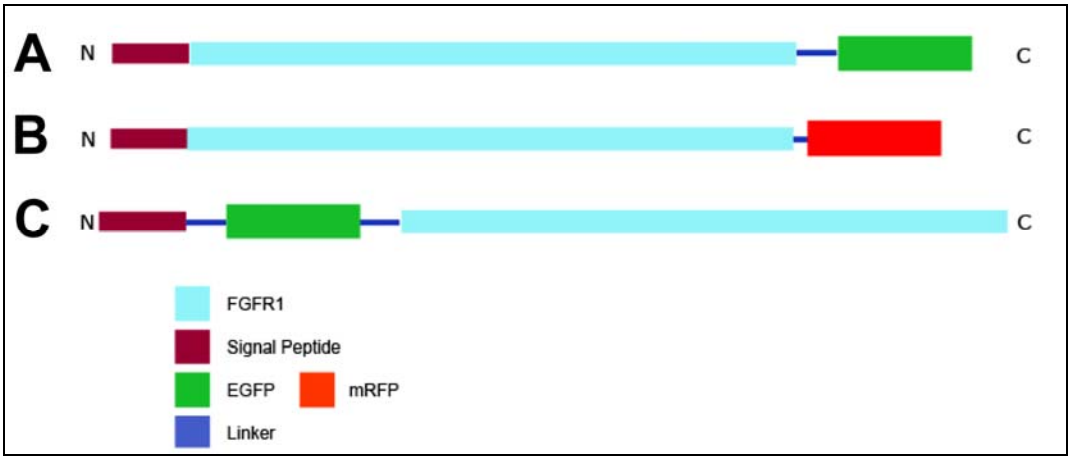

Figure 3.11 Fgfr1a fusion protein constructs
Schematic representation of the Fgfr1a-eGFP (A), Fgfr1a-mRFP (B), and eGFP-Fgfr1a fusion protein constructs. Signal peptide predicted with SignalP online tool (see the list of website).

For cloning of Fgfr1a-EGFP C-terminal fusion protein I used both vector and linker (20 amino acids), which were reported to result in a functional EGFR-GFP fusion protein (Wouters and Bastiaens 1999). As EGFR share many structural similarities with Fgfr, I assumed both EGFP fusions could have similar properties (Fig. 3.11 A). Fgfr1a-RFP was cloned in a similar fashion, just with a very short 2 amino acid linker (Fig. 3.11 B).

The N-terminal fusion was obtained by subcloning EGFP fragment between a predicted 22 amino acid long signal peptide and the rest of the Fgfr1a sequence, separated by a 6 amino acid linker on each side (Fig. 3.11 C).

All fusion protein constructs resulted in production of fluorescent proteins upon injection of in vitro synthesized mRNA into one-cell stage embryos (experimental setup for all colocalization experiments is depicted on Figure 3.12). All fusion proteins localized to the plasma membrane and many vesicular structures of varying morphology as indicated by the

overlap with membrane markers, such as GPF-GPI and mRFP-GPI (green fusion proteins shown in Fig. 3.13).

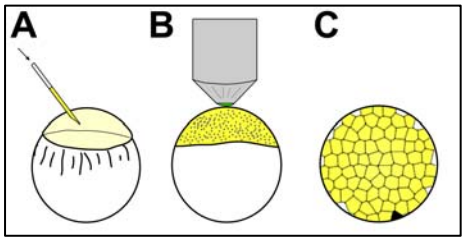

Figure 3.12 Scheme of colocalization experiments setup
Colocalization experiments start with injection of two mRNAs into one-cell-stage embryos, coding for both Fgfr1-FP and a marker (A). At late blastula stages (sphere) embryos are imaged at the animal pole (B). For the optimal resolution, embryos are imaged at the level of first few cells deep (C).

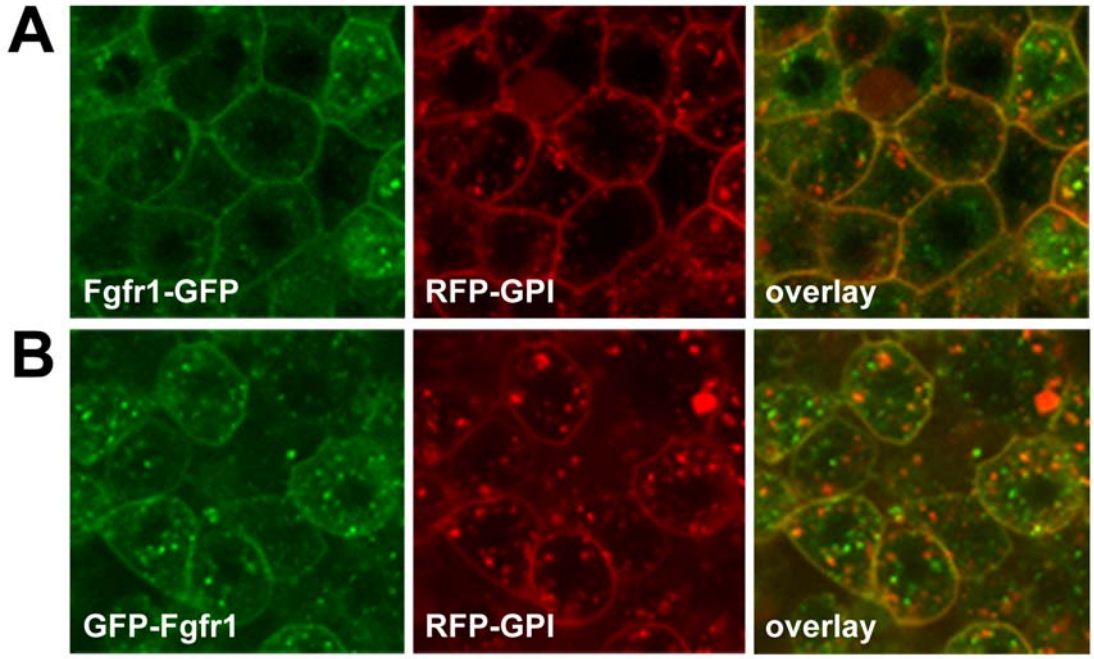

Figure 3.13 Fgfr1-RFP and GFP-Fgfr1 localize into membranous structures
Both n-terminal EGFP-Fgfr1 fusion protein (A) and a c-terminal fusion Fgfr1-EGFP (B) largely overlap with the membrane marker RFP-GPI. Much of the protein is present in the plasma membrane. Majority, however, appears in numerous vesicles inside the cells and a dispersed cytoplasmic staining. Fgfr1-RFP displays identical localization (not shown here).

I next tested the biological activity of the fusion protein by overexpression and detection of Fgf target gene expression. Overexpression of the wildtype fgfr1a even at high levels (400 pg) does not cause any phenotype. Fgf target gene expression and the progression of gastrulation remain the same. I tested, therefore, whether the Fgfr1a fusion constructs behave similarly upon overexpression (Fig. 3.14). At lower injection doses (100 pg) Fgfr1a-mRFP does not cause any phenotype. However, when the injection dose was increased up to 200-400 pg, Fgfr1a-RFP and other fusions cause ectopic induction of Fgf target genes (Fig. 3.14).

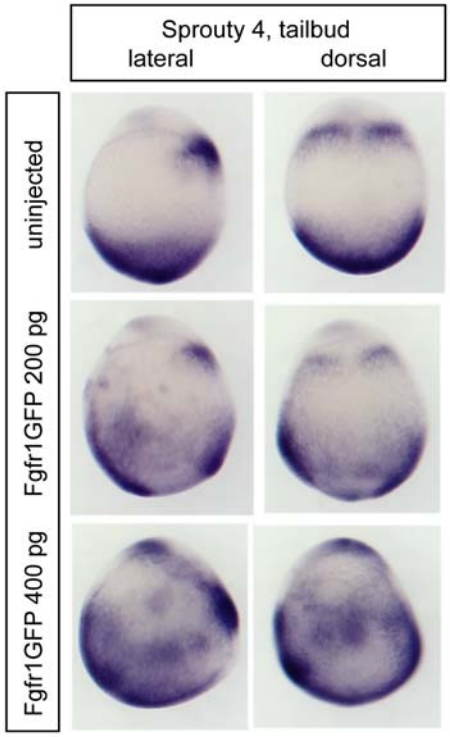

Figure 3.14 Ectopic activation of Sprouty 4 upon Fgfr1GFP overexpression
Overexpression of Fgfr1-FP proteins results in a dose dependant ectopic activation of Fgf target genes, such as Sprouty 4 during gastrulation.

3.2.3.2. Fgf8 is taken up by Fgfr1a overexpressing cells

To test whether Fgf8 endocytosis can be mediated by Fgfr1a I performed a transplantation assay in zebrafish embryos at blastula stages (Fig 3.15). The host embryo was injected at one cell stage with Fgf8-GFP RNA. The donor embryo was overexpressing Fgfr1a-RFP. At sphere stage single cells were transplanted into the host embryos and the uptake of Fgf8-GFP into Fgfr1a-RFP expressing cells was measured. As a control for receptor mediated uptake, secreted-GFP, which should be Fgfr1a independent, was used. Fgfr1a-RFP cells were readily taking up Fgf8-GFP and both markers were found in overlapping punctae inside cells (Fig 3.15 A). In comparison, little secreted-GFP uptake was observed (Fig 3.15 B).

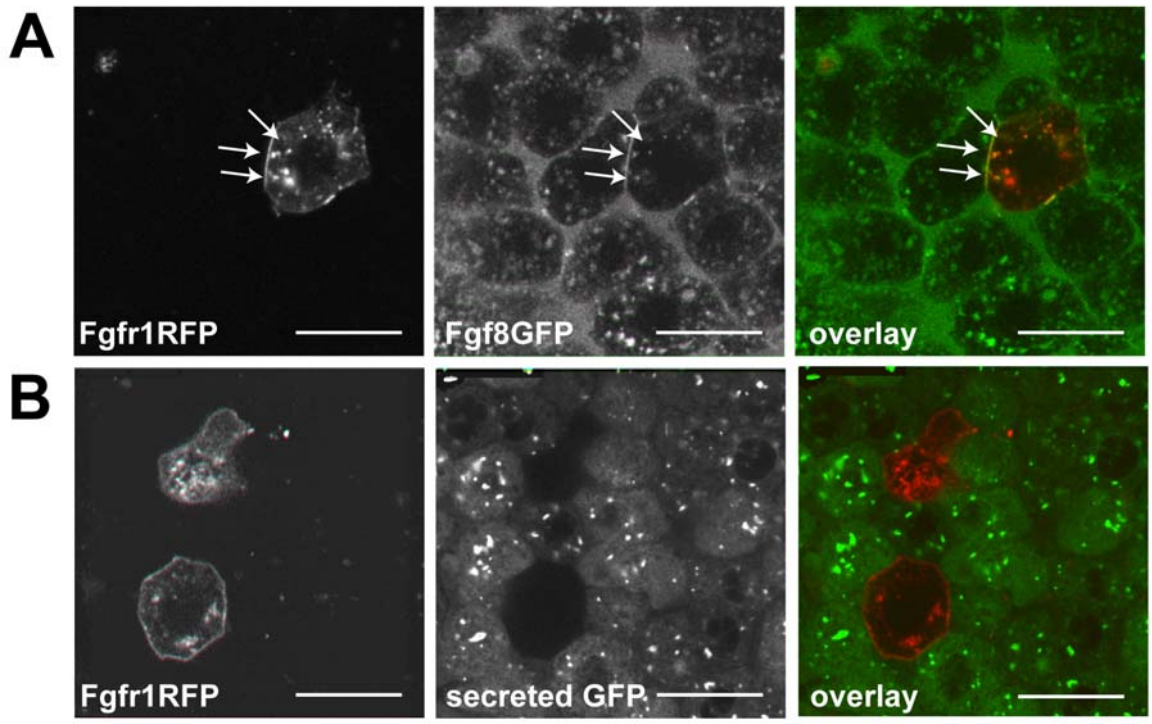

Figure 3.15 Fgf8 is endocytosed in association with Fgfr1
Cells overexpressing Fgfr1-RFP, when transplanted into Fgf8-GFP expressing host embryo, readily uptake the ligand from the extracellular matrix. Punctae of Fgf8 inside transplanted cells overlap with Fgfr1 positive endosomes (B). Control transplantation into a host embryo expressing secreted GFP does not show such uptake or colocalization (C). Scale bars 25 µm.

3.2.3.3. Fgfr1a shows partially overlapping subcellular distribution with endosomal markers

I took advantage of a possibility of imaging zebrafish embryos during gastrulation period, at about sphere stage. In each experiment, I coinjected RNA for an endosome marker (100-200 pg) and Fgfr1a-RFP (200 pg) or Fgfr1a-GFP (200 pg) and imaged embryos at late blastula at the animal pole using confocal microscopy. Although Fgf8 is expressed only at the margin Fgf1 is already expressed ubiquitously. Because at late blastula Fgf target genes are expressed almost ubiquitously I interpreted measured embryos as representative of a steady and low signaling state of the Fgfrs (Figure 3.16).

Fgfr1a partially colocalizes with Rab5c and Cellubrevin, both of which label small, early endosomes in clathrin dependent endocytosis. About 30-40% of intercellular receptor punctae colocalize with either of the two markers (Figure 3.16 A,E). Cellubrevin labels also part of the fast recycling endosomes (McMahon et al. 1993). A low level of overlap with caveolin marker (Figure 3.16 C) shows that Fgfr1a can be endocytosed through both CDE and NCE.

Fgfr1a was also found to largely overlap with Rab7 (Figure 3.16 B) – a marker of late endosomes suggesting progression of the cargo towards lysosomal degradation. These

endosomes were also morphologically distinct, bigger and often located at the periphery of the nucleus.

Marker	% overlap	P-value	Morphology
Rab5	39,7%	0,0002	small periferal endosomes
Rab7	38,3%	1,9E-05	large perinuclear endosomes
Caveolin	20,1%	0,0009	subcortex membrane invaginations
Rab11	1,4%	0,2	small periferal endosomes
Cellubrevin	29,9%	2E-06	small periferal endosomes

Table 7. Estimation of average overlap of Fgfr1a-RFP and endocytic markers
The values in the table are an approximation derived from manual counting all Fgfr1a-RFP and co-localized punctae in cells, n=7. Morphology of endosomes based on size and subcellular localization. P-value calculated in a two-tailed paired t-test. The p-value of Rab11 suggests that the amount of observed overlap is statistically insignificant.

In attempt to estimate the extent of receptor recycling at a steady state Rab11-GFP was used together with Fgfr1a-RFP (Fig 3.16 D). Unfortunately, the nature of recycling endosomes, being very small and extremely close to the cell membrane, made it difficult to truthfully judge the extent of colocalization. The amount of observed overlap with the Rab11 punctae deeper in the cell is statistically insignificant, however the population at the cell cortex was not optically resolvable from the membrane in vivo. In order to more precisely assess the amount of recycling, one would need to create a recycling assay on dissociated zebrafish cells.

Figure 3.16 Fgfr1a is present in many types of endocytic vesicles
Fgfr1a can be found overlapping with early endosomes (Rab5, Cellubrevin in A and E) of clathrin dependent endocytosis. It is to a lesser degree found also in caveolae (C), mostly close to the membrane. Fgfr1aRFP is also largely overlapping with Rab7 positive late endosomes (B). In contrast, there is almost no overlap with Rab11 recyccling endosomes (D). Scale bar 25 µm.

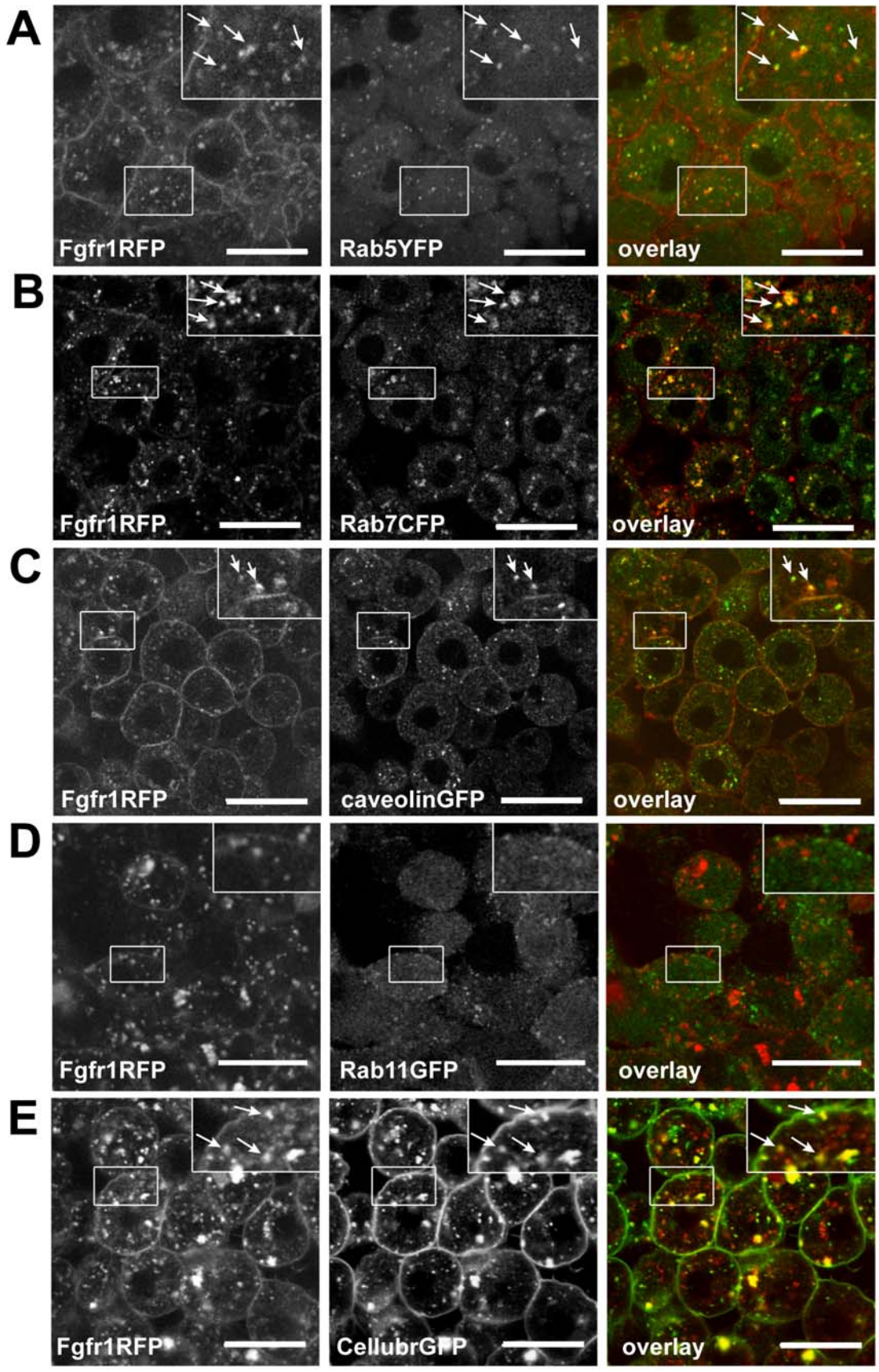
A
Fgfr1RFP
Rab5YFP
overlay
B
Fgfr1RFP
Rab7CFP
overlay
C
Fgfr1RFP
caveolinGFP
overlay
D
Fgfr1RFP
Rab11GFP
overlay
E
Fgfr1RFP
CellubrGFP
overlay

3.2.3.4. Fgfr1a Antibody

None of the commercially available FGFR1 antibodies works for detection of zebrafish Fgfr1a. In order to visualize endogenous expression of the Fgfr1a protein I decided to produce custom-made peptide antibody against fish protein (using the service of Eurogentec). The peptides were designed in the areas of greatest polymorphism between all Fgfr receptors (see Appendix 5.2 for Fgfr1-4 protein alignment), and with the greatest antigenicity prediction (see websites list for the URL of the used prediction algorithm). The N-terminal peptide antibody (LQSQGRAIQDEAPAE) should recognize the protein on the extracellular side and the C-terminal peptide antibody should detect cytoplasmic end of Fgfr1a (CKFPPHPNRGVAFKKR).

Four isolated purified anti-sera were tested and only one of them resulted in the detection of bands of predicted Fgfr1a size (100 kDa) on a Western Blot. The specificity of this antibody is confirmed by the detection of the over expressed fusion protein as well as endogenous truncated protein in Fgfr1a^{W671X} mutant embryos (Figure 3.17). However, the antibody may detect also other Fgfrs, because in Fgfr2^{L545STOP} (mutant fish strain described later) samples it detected smaller protein products. Despite many trials in various conditions I did not get a reliable signal on whole mount staining. Overall, the antibody could be used only in biochemical experiments from embryos extracts and was not used in colocalization experiments due to low affinity to fixed tissue.

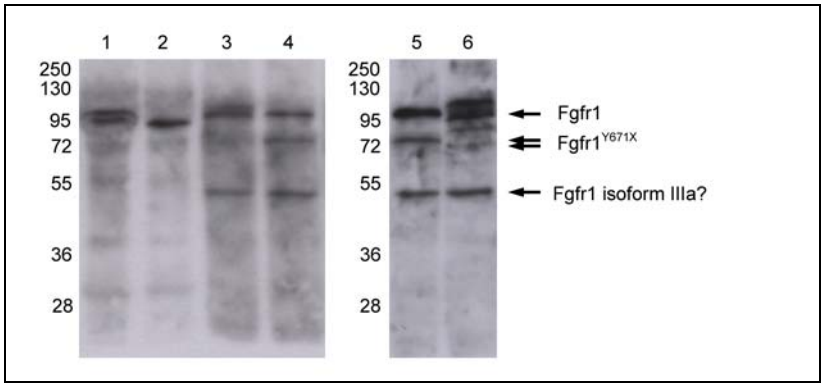

Figure 3.17 Fgfr1 antibody
Two Western Blots on whole embryo lysates show detection of Fgfr1 at about 110 kDa and presumably other Fgfrs. The lanes 1-5 represent: 1 – wildtype, dome stage, 2 – wildtype dome stage, 3 - wildtype 24 hpf, 4 - huFgfr1^{W671STOP} 24 hpf, 5 – huFgfr1^{W671STOP} 24 hpf, 6 – huFgfr2^{L545STOP} 24 hpf. At 24 hpf, a shorter Fgfr1 isoform is produced, which is probably analogous to human Fgfr1IIIa secreted isoform. The predicted sizes of Fgfr1^{W671STOP} and Fgfr2^{L545STOP} are of 75 kDa and 60 kDa, respectively. The new Fgfr1 antibody recognizes Fgfr1 and additional bands in Fgfr2 mutant, suggestive possible incomplete specificity.

3.2.3.5. Fgfr is ubiquitylated in vivo in gastrulating zebrafish embryos

Ubiquitylation is a progressively well understood type of posttranslational protein modification, which allows directing the substrate to degradation, regulating its trafficking in the cell or its activation (Haglund and Dikic 2005). The extent of receptor ubiquitylation may have an effect on the speed of Fgfr endocytosis and degradation.

In order to examine the extent of Fgfr ubiquitylation in vivo I performed immunoprecipitation. Two hundred embryos per sample were either lysed at sphere stage and used for pull-down with Fgfr1a antibody (described above) or dissociated and treated with a pulse of high concentration recombinant Fgf8 (100 ng/µl) prior to lysis and pull-down. Subsequently, Ubiquitin moieties were detected on a Western Blot with resolved Fgfr1a IP samples. I could detect high molecular complexes of Fgfr1a-Ub, which intensified upon additional Fgf8 pulse (Fig. 3.18 A). Similar pattern of band was obtained, when Fgfr1a-myc and HA-ubiquitin constructs were injected into tested embryos, Myc antibody used for pull-down and HA antibody for Ub detection on a Western Blot.

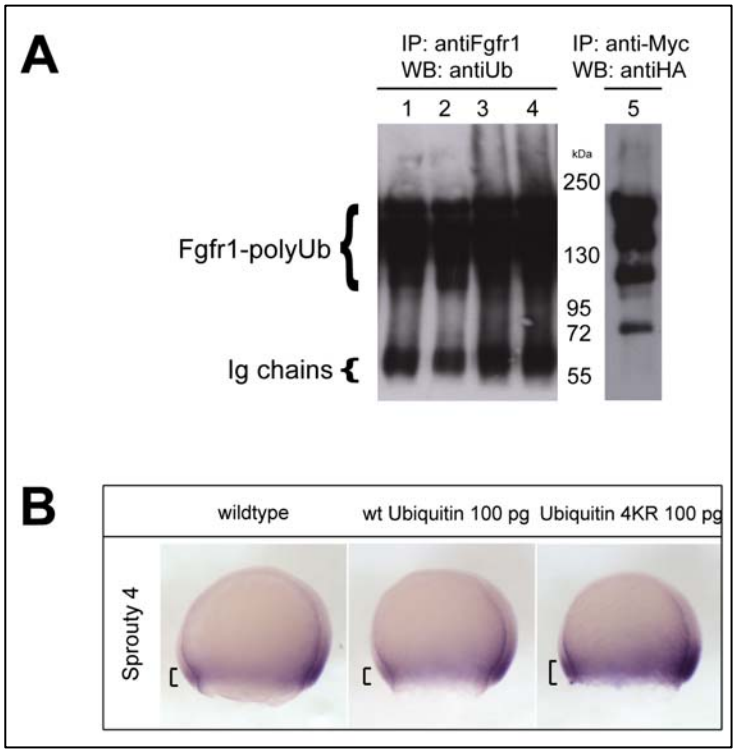

Figure 3.18 Fgfr1 is ubiquitylated in vivo in gastrulating embryos
Immunoprecipitation on extracts from embryos at shield stage (A). Lanes 1 and 2 represent pull-down of Fgfr1 from dissociated embryos with newly produced antibody and detection of Ubiquitin (Ub) on Western blot. For lanes 3 and 4, cells were incubated in 100 ng/ml recombinant Fgf8 for 30 mins. Higher molecular weight chains of ubiquitin are detected. Lane 5 represents a pull down from embryos expressing Fgfr1-myc and HA tagged Ubiquitin. Immunoprecipitation was performed with use of α-myc antibody, Western Blot detection was carried out using α-HA antibody. Panel B shows in situ hybridization with Sprouty 4 probe to assess the influence of ubiquitin and ubiquitin 4KR overexpression in gastrulating embryos. An insignificant upregulation of Sprouty 4 was detected only upon Ub4KR overexpression.

Knowing that ubiquitylation modifies Fgfrs in vivo, I tested the requirement of this modification for correct Fgf8 signaling in the early embryos. Overexpression of wildtype Ubiquitin does not affect the range of target gene induction. Ub-4KR is a mutant form of Ubiquitin, which blocks formation of the polyUb chains because it lacks lysines required for chain attachment of other moieties. I used mRNA coding for Ub4KR to examine the relation between ubiquitylation and Fgf8 signaling (Fig. 3.18 B). Overexpression of the mutant

Ubiquitin, Ub-4KR, results in a slight upregulation of Sprouty 4 induction, which should be quantifiable with qPCR analysis.

3.2.3.6. Cloning of endocytosis deficient Fgfr1a mutant versions

Assessing the role of receptor endocytosis in its signaling function requires decoupling of the two processes. In order to inhibit receptor endocytosis but retain signaling ability I cloned two mutant Fgfr1a constructs, which were studied in tissue culture and fulfilled these criteria in vitro (Sorokin et al. 1994) (Fig. 3.19). Both, truncation of the carboxyterminal domain by 58 amino acids as wells a sole point substitution Y766F in human protein (in fish Y753) resulted in 90% inhibition of Fgfr1 uptake but not signaling via MAPK pathway.

Because Y753 (mouse Y766) is directly interacting with PLCγ, this pathway is not active in the context of mutant receptor. It is still unclear what is the in vivo function of the PLCγ signaling in Fgf signaling during embryonic development. The structural nature of the mutant Fgfr1 overexpression constructs cloned for use in zebrafish embryos is depicted on Fig. 3.19 A.

3.2.3.7. Expression of Fgfr1a Y753 mutants in embryos reduces Fgf8 endocytosis

In order to investigate whether mutant Fgfr1a causes similar reduction of endocytosis as in tissue culture, I injected Fgfr1a mutant RNA together with a membrane marker into the host embryo and implanted an Fgf8Cy5-soaked bead into the animal pole at sphere stage. In a time-course experiment, the punctae inside and outside of the cells were counted and compared after normalization. For statistical analysis I have counted punctae within whole frames, meaning all cells close and far from the source. Punctae overlapping with the membrane marker on a border of cells were considered “outside of cells”, whereas punctae observed within cell boundaries, were counted as “inside cells”.

The uptake of Fgf8 is reduced noticeably but not dramatically in both mutants, however, it recovers and reaches almost normal levels at a steady state (after about 2h) (Fig 3.19 B). Due to differences between embryos and brightness of the beads the standard error of the mean is relatively high, making the observed differences significant only at a level of 90%. The variance can be also caused by small differences in the protein overexpression in the host embryos. Both mutants display decreased endocytosis rate, however, the rate of trafficking and more detailed analysis of receptor degradation remains to be investigated.

Figure 3.19 Overexpression of mutant Fgfr1 inhibits Fgf8 endocytosis
Two mutant versions of Fgfr1 were cloned in order to decouple endocytosis and signaling of Fgfr1 (A). Tyrosine Y753 was either replaced by phenylalanine or removed along with the c-terminal tail (bold font). Fgf8Cy5 coated beads were implanted at sphere stage into the animal pole of embryos overexpressing membrane marker and Fgfr1 versions (B). Panels C and D show representative pictures of the Fgf8Cy5 uptake experiments. Fgf8 released from the bead diffuses and is endocytosed by the cells outlined by the membrane marker RFP-GPI. The cells expressing wildtype receptor rapidly uptake

Fgf8. Cells overexpressing mutant Fgfr1 endocytose Fgf8 with a delay. Scale bar 20 µm. The time course experiments of Fgf8 uptake are quantified on panel E, error bars = SEM.

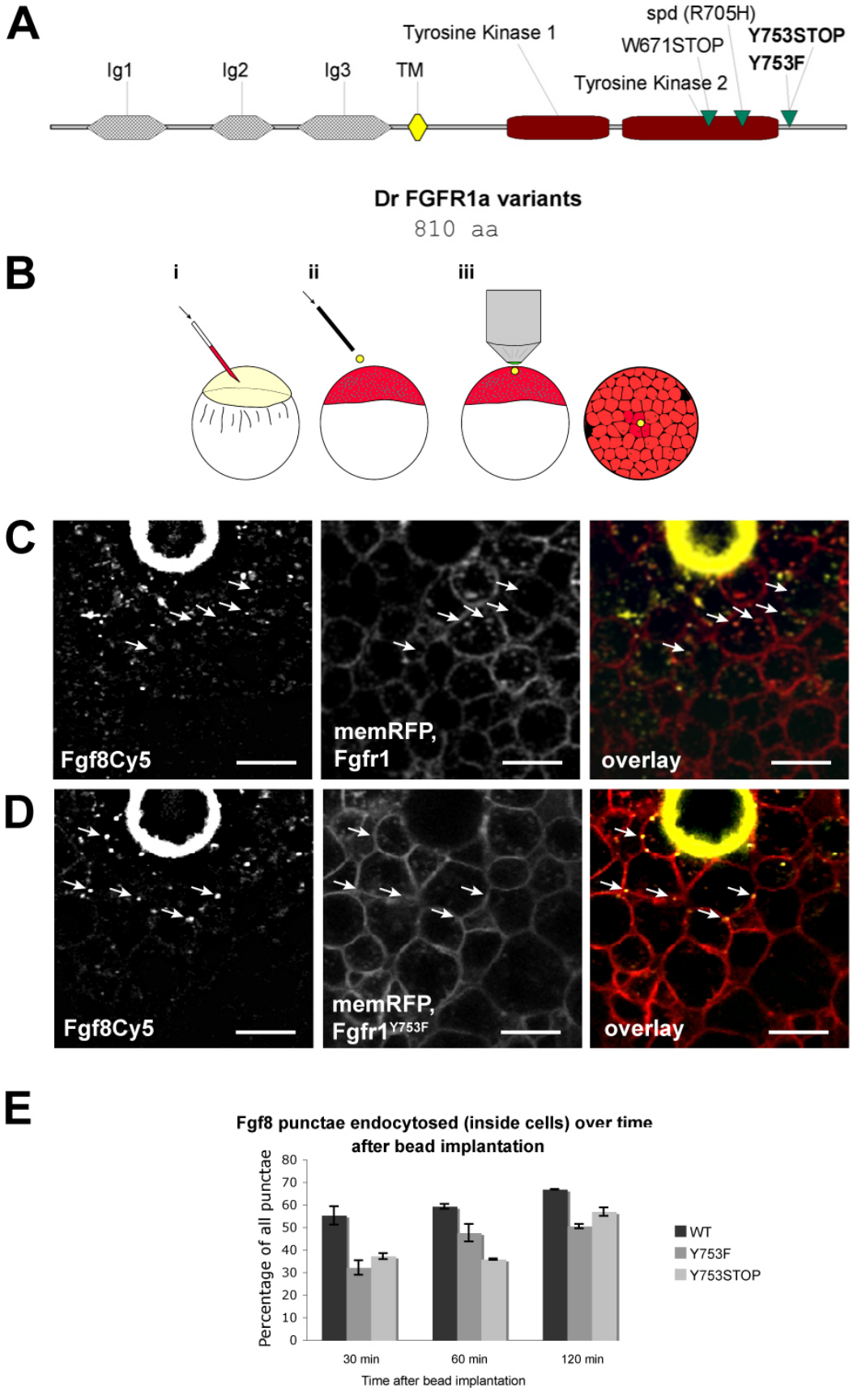

3.2.3.8. Endocytosis deficient Fgfr1a cause expansion of Fgf target gene expression

The restrictive clearance model assumes that inhibition of the receptor-dependent endocytosis should allow further diffusion of Fgf8 and effectively an expansion of target gene induction. To study the effect of mutant Fgfr1a overexpression on the Fgf target gene expression I injected 200 pg mRNA of each mutant construct and developed an in situ hybridization for target genes at 80% epiboly. Indeed, both Fgfr1^{Y753STOP} and Fgfr1^{Y753F} cause an expansion of sprouty 4 and pea3, however, to drastically different levels. Where Fgfr1^{Y753STOP} causes only a slight upregulation, Fgfr1^{Y753F} results in complete ectopic activation of sprouty4 and pea3 (Figure 3.20 A). Such differences are not reflected by the ligand uptake assay.

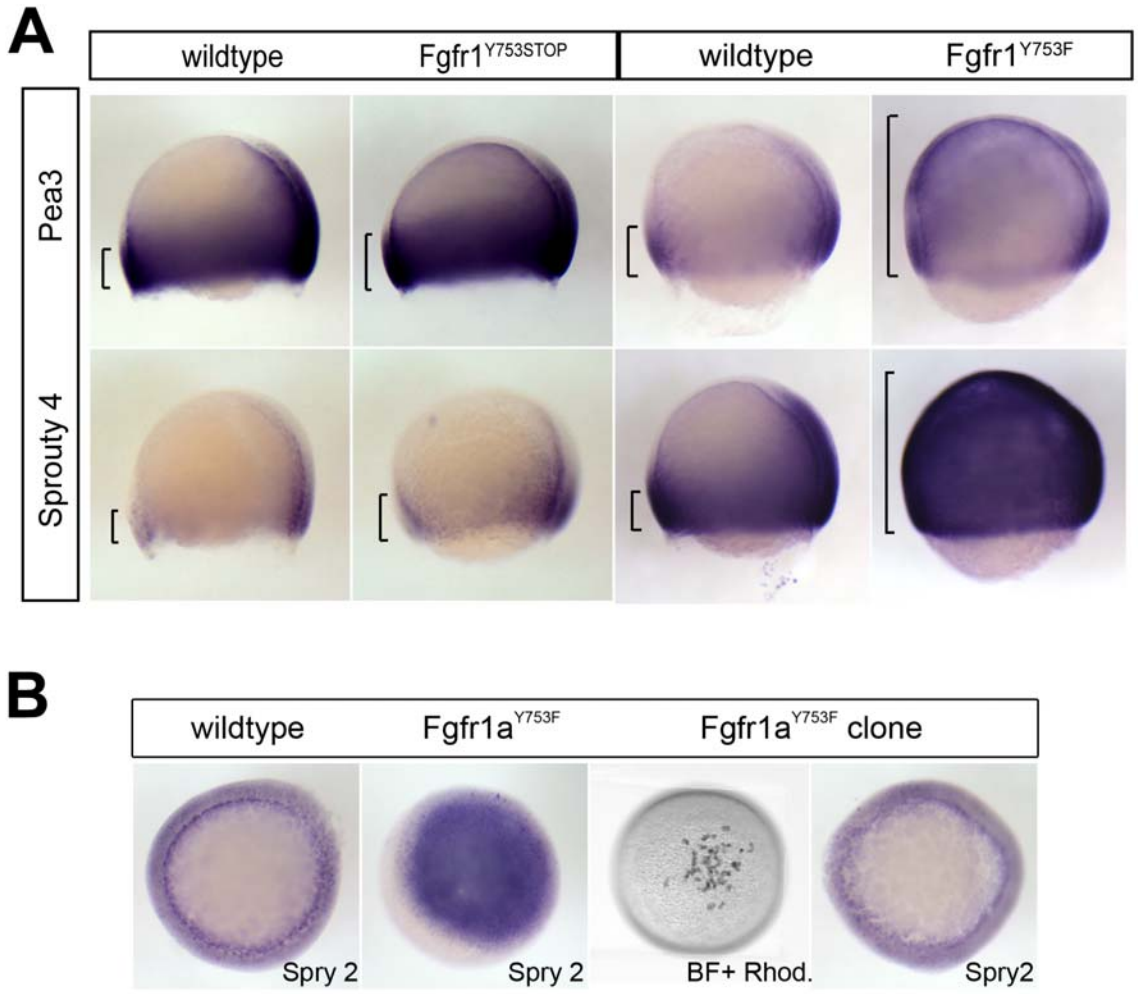

Figure 3.20 Mutant Fgfr1 causes Fgf target gene expansion
Overexpression of mutant Fgfr1 versions causes expansion of both short and long-range Fgf target genes (A). Fgfr1^{Y753STOP} causes a very small change (in order of 2-3 cell diameters). Fgfr1^{Y753F} causes a dramatic expansion of both *sprouty 4* and *pea 3*. Transplantation of cells expressing Fgfr1^{Y753F} into the animal pole of wildtype embryos shows that there is no Fgf target activation in the clone (n = 24 clones of about 20-30 cells each), hence activation is dependent on the neighboring cells (i.e. is not cell autonomous, probably ligand-dependent) (B).

In order to understand the mechanism of Fgfr1^{Y753F} mediated activation of Fgf signaling I tested ligand-dependency of Fgfr1^{Y753F}. Cells expressing mutant receptor were transplanted into the wildtype embryo into the ventral side of the animal pole, where endogenous Fgf8 does not reach. My results indicate, that the cells in the clone (n = 24 clones) do not express Fgf target gene sprouty 2, which points to the ligand dependent mechanism of receptor hyperactivation (Fig. 3.20 B).

3.3. Analysis of Fgfr2

3.3.1. Expression of Fgfr2

The transcript of Fgfr2 is first detected at 90% epiboly as a weak domain in the paraxial mesoderm (not shown). At tailbud stage an additional domain can be detected in the forebrain and midbrain. At 5 and 6 somites expression becomes stronger in optic vesicles and midbrain (Fig. 3.21 A). As segmentation progresses more distinct sub domains in mid- and hindbrain specify and the paraxial mesoderm domain extends with increasing number of somites. Posterior part of the body is completely devoid of Fgfr2. The somitic expression of Fgfr2 disappears after 15 ss stage and stays only in the ventral mesenchyme (Fig. 3.21 B). The expression in the eye is now restricted to the developing lens. At 24 hpf, Fgfr2 is strongly expressed in lenses, diencephalon, anterior midbrain and in several segments of the hindbrain, including R1, R4 and R6 (Fig. 3.21 B). Beyond one day during larval stages the transcript can be only detected in the area of the head and pectoral fins.

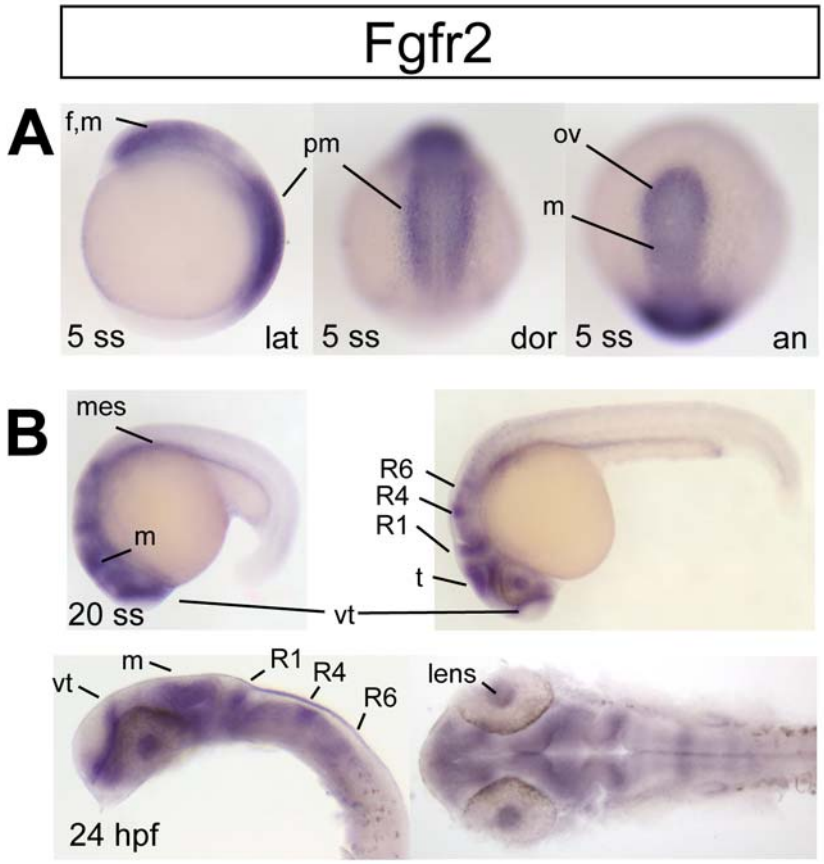

Figure 3.21 Expression pattern of Fgfr2
Fgfr2 transcript is found at the onset of somitogenesis and is expressed in forebrain, midbrain, and paraxial mesoderm. Between 5 and 10 somites stage it is transiently strongly expressed in the optic vesicles (A). Later this expression is reduced to the lens only. Staining in the paraxial mesoderm disappears by 15 ss and persists only in the ventral mesenchyme. During somitogenesis Fgfr2 is expressed also in distinct patches in the hindbrain. By 24 hpf the expression in the hindbrain is restricted to rhombomeres 1,4 and 6 (B). Abbreviations: f – forebrain, h – hindbrain, m – midbrain, mes – ventral mesenchyme, ov – optic vesicle, pm – paraxial mesoderm, R – rhombomeres, t – tectum, vt – ventral telencephalon.

3.3.2. Fgfr2 mutant zebrafish

3.3.2.1. Characterization of the mutant protein

We have isolated one mutation in Fgfr2 in the TILLING screen (Fig. 3.22). The mutation $Fgfr2^{L545STOP}$ is located in the first of split tyrosine kinase domains. The protein product arising from such mutation would lack kinase activation Y650/Y651 residues, the ATP-binding pocket and all downstream regulatory elements.

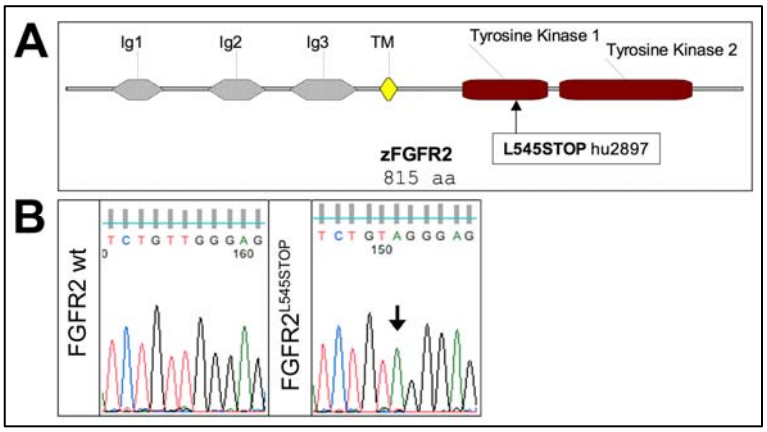

Figure 3.22 Fgfr2 TILLING mutant
Mutation found in Fgfr2 is an early truncation, which should render the receptor dominant negative (A). The genetic context and the nature of mutations is summarized in a panel of chromatogram traces (B).

I tested the expression of endogenous Fgfr2 in mutant larvae and wildtype siblings by in situ hybridization (Figure 3.23 A). I found that Fgfr2 transcript was strongly downregulated. It would be interesting to see a quantitative measurement of this downregulation in a Q-PCR experiment.

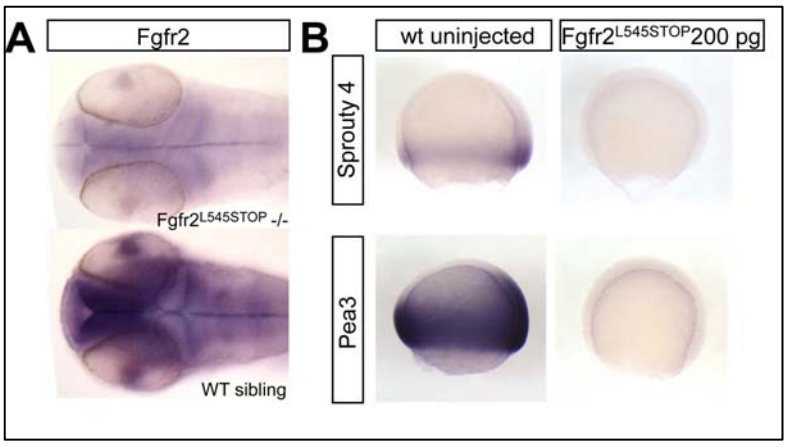

Figure 3.23 Fgfr2^{L545STOP} mutant analysis
Homozygous Fgfr^{2L545STOP} embryos (here 36 hpf) show much weaker Fgfr2 expression, suggestive of RNA non-sense mediated decay (A). Fgfr2 expression construct, Fgfr2^{L545STOP}, acts in a dominant active way, blocking all Fgf target gene expression (B).

Also, overexpression of the cloned mutant construct Fgfr2^{L545STOP} completely blocks Fgf target gene induction, similar to XFD (Figure 3.23). Both experiments suggest a strong Fgfr2 loss-of-function in Fgfr2^{L545STOP} mutant homozygotes.

3.3.2.2. Preliminary analysis reveals a role of Fgfr2 in growth, fertility and adult bone ossification

Surprisingly, homozygous mutant embryos and larvae show no phenotypes that could be expected in connection with Fgfr2 expression pattern. None of the tests concerning development of brain or facial skeleton showed any abnormalities (Figure 3.24). Fgfr2 plays an early and essential role in mouse development. Mouse Fgfr2 knockout embryos die at preimplantation presumably due to failure in development of the placenta (Arman et al. 1998). Even though zebrafish develops ex utero I was expecting early defects also in homozygous

Fgfr2^{L545STOP} zebrafish due to reports on conditional Fgfr2 knockout phenotypes in mouse (Yu et al. 2003).

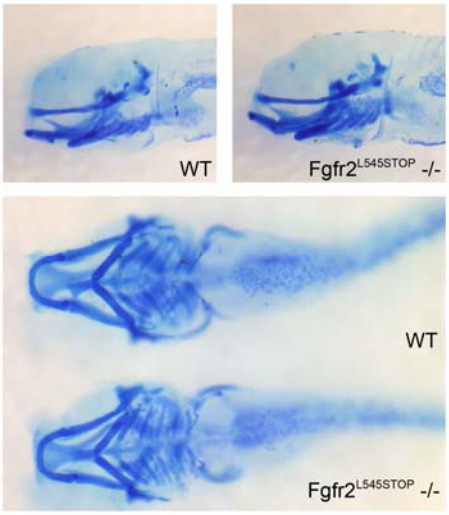

Figure 3.24 Larval pharyngeal region in Fgfr2^{L545STOP}
Larvae of Fgfr2^{L545STOP} +/- incross develop normally, at least in the first week. Some developmental delay is observed but not very significant. Pharyngeal arches and jaws develop normally compared to wildtype siblings.

Nevertheless, the adult homozygous fish (at least two months old) were found significantly smaller then their heterozygous or wildtype siblings (Figure 3.25 A-E). The fish survived well (see genotyping statistics in Table 4) but were on average 27% shorter. The penetrance of this phenotype was close to 100% independent of the genetic background (wt strain), which allowed detecting homozygous mutants based on reduced size. Homozygotes were also unable to mate (lay eggs or fertilize eggs).

Date	Cross	Mutant	dCAPs	No. finclips	WT	Heterozygotes	Homozygotes
04.12.07	incross hets (WIK)	Fgfr2^{L545STOP}	BfmI	45	13 (28,8%)	23 (51,1%)	9 (20%)
04.12.07	incross hets (AB)	Fgfr2^{L545STOP}	BfmI	44	13 (29,5%)	25 (55,5%)	6 (13,3%)

Table 8 Genotyping statistics for TILLING mutant line Fgfr2^{L545STOP}

Live homozygous fish generally had bent or wavy AP body axis with signs of kyphosis, i.e. curvature of the upper (thoracic) spine. Interestingly, the pathological body shape seems to progress with the age of fish (not shown). Therefore, homozygous Fgfr2^{L545STOP} fish were stained in alizarin red for visualizing internal skeleton. Homozygotes display a combination of skeletal phenotypes summarized in Figure 3.25 F-M. The skulls of mutant fish are shorter and the position of cranial sutures is shifted to the posterior side (Fig. 3.25 F,J). Neural spines of mutant fish are shorter and bent backwards, whereas ribs and anterior dorsal radials appear thinner and wavy (Fig. 3.25 H,L). The shape of the spine is slightly bent in the mutant fish and the hypural arches, which connect spine and tail fin, are thicker and disarrayed compared to the wildtype siblings (Fig. 3.25 I,M).

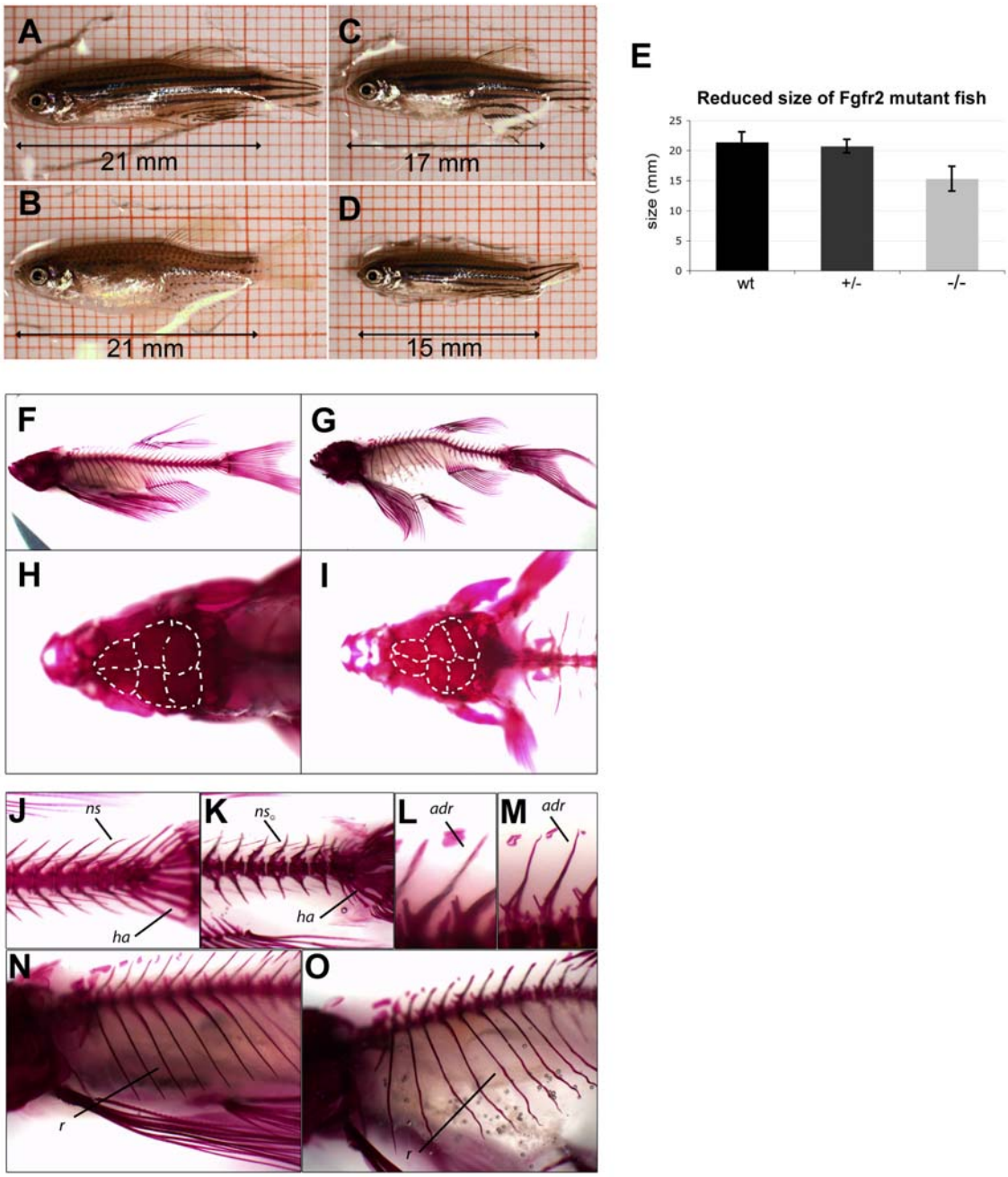

Figure 3.25 Adult phenotypes of Fgfr2^{L545STOP}
Adult fish in Fgfr2^{L545STOP} incrosses vary in size. Wildtype siblings (A) and heterozygotes (B) reach over 2 cm body length, whereas homozygous mutant fish (C, D) are on average 5 mm smaller (27%) (E), n = 34. Alizarin red skeleton staining reveals abnormal ossification in the homozygous mutant fish (G,I,K,M,O) compared to their wildtype siblings (F,H,J,L,N). The mutant fish have kyphosis (G), thin and wavy ribs, *r*, and anterior dorsal radials, *adr* (M,O), thick and curled neural spines, *ns*, and hypural arches, *ha* (K). The skull appears shorter, as if all facial bones where compressed together (I).

3.4. Analysis of Fgfr3

3.4.1. Expression of Fgfr3

Fgfr3 transcript is first detected at tailbud stage in the prospective diencephalon and the anterior hindbrain. During somitogenesis it is found in distinct domains in the diencephalon, anterior hindbrain, anterior spinal cord, axial mesoderm and tailbud (Fig. 3.26). At 24 hpf Fgfr3 gets restricted to diencephalon, strong expression in the R1 and the anterior spinal cord. It is weakly expressed in the dorsal posterior hindbrain. It also persists as a small domain in the tail fin.

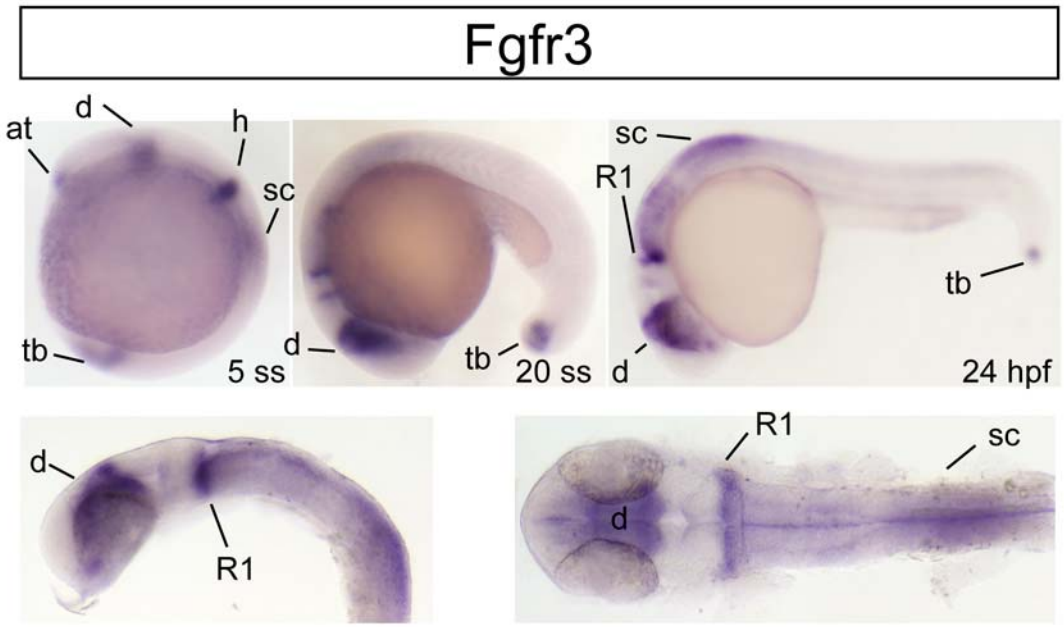

Figure 3.26 Expression pattern of Fgfr3
During somitogenesis (5 ss) several domains form in the anteriormost forebrain, in presumptive diencephalon, anterior hindbrain, anterior spinal cord and tailbud. Expression persists until 24hpf, with some transient axial mesoderm during midsomitogenesis. At 24 hpf Fgfr3 is expressed strongly in diencephalon and rhombomeres one. Expression in the posterior hindbrain is weak, while it is stronger in the anterior spinal cord. Some cells in the tail bud also form a small Fgfr3 domain. Abbreviations: at – anterior telencephalon, d – diencephalon, h – hindbrain, R1 – rhombomere 1, sc – spinal cord, tb – tailbud.

3.4.2. Fgfr3 knockdown

We did not find any non-sense or interesting mis-sense mutations in Fgfr3 gene in the TILLING screen. I have designed two Fgfr3 translation blocking morpholinos, however, neither of them evoked any early developmental defects. It would be necessary to verify the effectiveness of these morpholinos in order to draw any conclusions. It would be greatly interesting to induce Fgfr3 knockdown, because of many functions associated with this gene in higher vertebrates (Colvin et al. 1996; Horton et al. 2007).

3.5. Analysis of Fgfr4

3.5.1. Expression of Fgfr4

Expression of Fgfr4 is first detected as a ubiquitous staining at blastula stages, shortly prior gastrulation. At the onset of gastrulation Fgfr4 transcript can be found everywhere except the marginal zone (Fig. 3.27 A). At about 70% epiboly the uniform staining on the dorsal side starts showing a gap of expression at the level of prospective posterior hindbrain and midline (notochord). At bud stage expression is already restricted to prospective midbrain, anterior hindbrain and the paraxial and lateral mesoderm.

During somitogenesis three domains in the anterior part of the embryo can be distinguished (Fig. 3.27 B). They are equivalent, according to (Thisse et al. 1995), forebrain (diencephalon), anterior dorsal hindbrain (R1-3) and anterior spinal cord with stripes of lateral mesoderm on the sides. Later in somitogenesis, there is also a prominent expression in the posterior part of the somites and the posterior spinal cord and the more caudal and ventral groups of cells in the growing tail. At 24hpf Fgfr4 can be detected in the ventral telencephalon, diencephalon, tectum of the midbrain and the dorsal part of the anterior hindbrain, at the level of R1-3 (Fig. 3.27 C, D). The transcript can be also more faintly detected in the anterior spinal cord in the posterior stripe beginning at the level of R7 (Figure 3.27)

At later stages between 36-48h low levels of Fgfr4 are present also in some progenitors of the heart, ear, lens, pectoral fin and branchial arches (not shown).

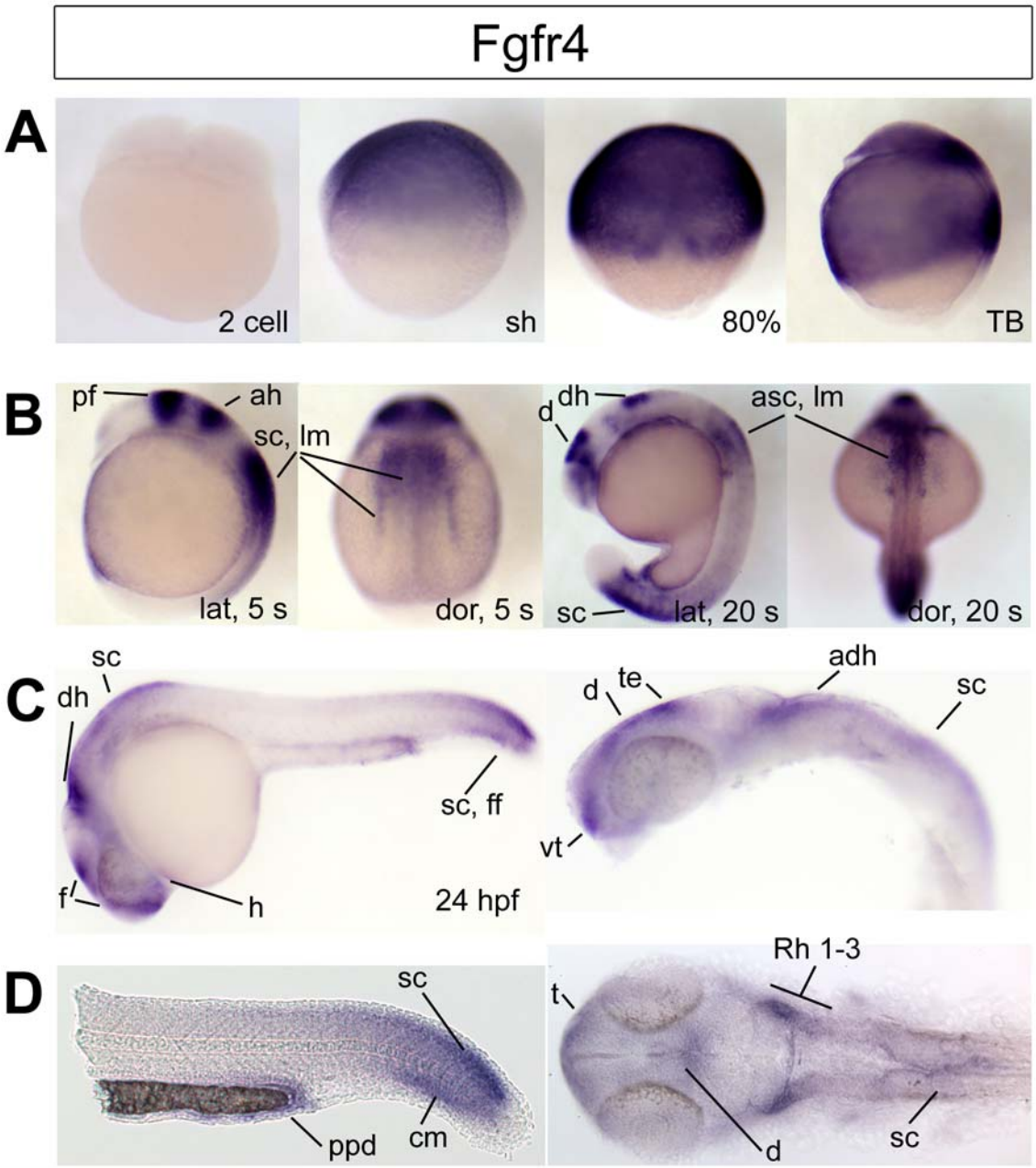

Figure 3.27 Expression pattern of Fgfr4
Fgfr4 transcript is first found at late blastula stages. At gastrulation it is present everywhere except the margin. From midgastrula stages two gaps in the expression appear at the dorsal midline and in the hypoblast at the level of prospective posterior hindbrain (panel A). During early somitogenesis, expression persists in posterior forebrain, anterior hindbrain, anterior spinal cord and lateral mesoderm. Later during somite formation Fgfr4 is also expressed in posterior spinal cord, notocord and most caudal mesoderm. At 24 hpf Fgfr4 transcript can be found in ventral telencephalon, dorsal diencephalon, tectum and first three rhombomeres of the hindbrain. Posteriorly, Fgfr4 is present in the distal tips of the spinal cord, caudal mesoderm and prospective pronephric duct. Abbreviations: ah – anterior hindbrain, asc – anterior spinal cord, cm – caudal mesoderm, d – diencephalon, dh – dorsal hindbrain, f- forebrain, lm – lateral mesoderm, pf – posterior forebrain, ppd - prospective pronephric duct, t – telencephalon, vt – ventral telencephalon.

3.5.2. Fgfr4 mutant zebrafish

3.5.2.1. Fgfr4 TILLING knockout lines

Among most promising mutant lines isolated from the TILLING library, we found two early nonsense mutations in Fgfr4. The genetic nature of both mutations is depicted on the Figure 3.28.

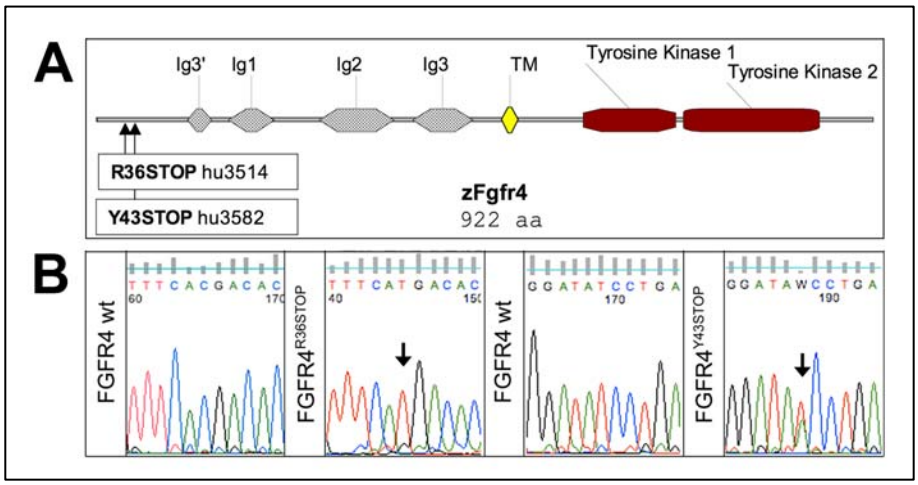

Figure 3.28 Fgfr4 TILLING mutants The two early non-sense mutations in Fgfr4 are expected to induce complete loss-of-function of this gene (A). The genetic context and the nature of mutations is summarized in a panel of chromatogram traces (B).

Due to the very 5' location of the introduced stop codons, both $Fgfr4^{R36STOP}$ and $Fgfr4^{Y46STOP}$ should result in complete Fgfr4 loss-of-function. However, homozygosity of neither of them resulted in any developmental or adult phenotype, which would distinguish them from the wildtype or heterozygous siblings. The recovery of homozygous fish was around expected 25%.

In order to understand whether this lack of phenotype is due to a rescue by alternative transcript or redundancy with other receptors - as observed in mouse (Weinstein et al. 1998)), I decided to perform a 5' RACE PCR to detect possible alternative transcripts. If, upon mutation, fish were able to produce another isoform of the gene, the early stop could be circumvented. Preliminary results show two forms of fgfr4 transcript (including 5' UTR), one of which excluded first 4 exons and contained an in frame ATG codon downstream of the detected mutations (Fig. 3.29). This result has to be, however, confirmed by testing more individuals.

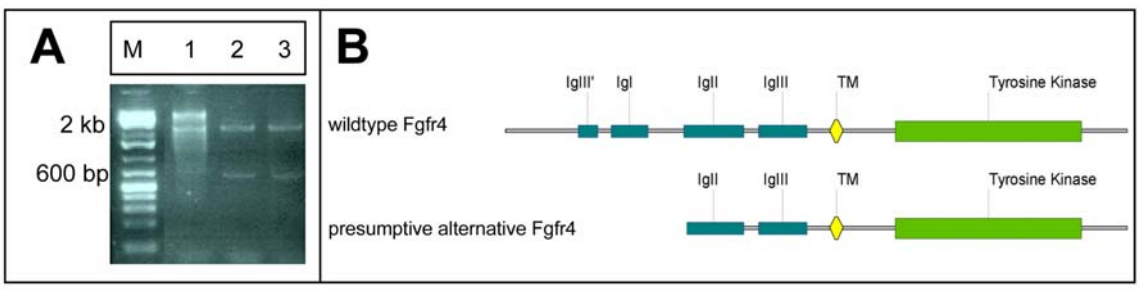

Figure 3.29 Fgfr4Y36STOP and Fgfr4R43STOP alternative transcripts
5' Race PCR (A) of Fgfr4 reveals that wildtype embryos (lane 1) produce only a long version of the transcript (2kB band), whereas Fgfr4^{Y36STOP} and Fgfr4^{R43STOP} (lanes 2 and 3) produce two forms of the transcript, long and short (600 kB), As checked by sequencing, shorter product starts downstream of both mutations, within exon 5, which includes an alternative start codon. Presumptive alternative protein structure is schematized in B.

The presence of other high affinity Fgfrs may explain why Fgfr4 is actually not essential for early development. This hypothesis is, however, questionable in light of experiments with the use of Fgfr4 morpholino knockdown described below.

3.5.2.2. Fgfr4 morpholino knock down

In order to create embryos with Fgfr4 loss-of-function both translation and splice blocking morpholinos were designed and tested (Figure 3.30). Among splice blockers I have isolated one, which led to complete intron retention (see e8-i8/9 in Fig. 3.30 C). Such transcript includes a premature termination codon and the resulting protein stops after the second Ig domain (hence, also after the potential alternative start codon). The early phenotype (24h) is characterized by a slight developmental delay, cell death in the hindbrain and small eyes (Fig. 3.30 D).

Subsequently all translation blockers were tested. The efficiency of MO ATG was assessed based on ability to block translation of injected Fgfr4-RFP, however, it caused developmental arrest (Fig. 3.30 C). MO 5'UTR showed phenotype similar to this of Fgfr4 MO e8, suggesting it being specific for Fgfr4 loss of function.

To see whether the cell death in the hindbrain, which was quite extensive at higher doses of morpholinos, is really due to Fgfr4 loss of function or rather a morpholino toxicity problem, I coinjected Fgfr4 MO and p53 MO (Fig. 3.30 D). This control is widely accepted as one way to detect morpholino toxicity and stress effects, which are triggering p53-dependent pathway to apoptosis (Robu et al. 2007). Coinjections led to a reduction of cell death in the brain, suggesting that it might be Fgfr4 independent (being rather a toxicity effect). Other phenotypes, such as small eyes, messy morphology of the hindbrain and fin growth defect were not rescued, which was confirmed for both 5'UTR and e8 morpholinos.

Figure 3.30 Fgfr4 morpholino design and analysis of phenotypes
Four morpholinos were designed to block donor splice sites in Fgfr4 gene (A). One of them, Fgfr4 MO e8/I8-9 showed complete retention of the intron leading to production of an alternative transcript, encoding a premature stop codon (A, B). Additionally, three translation blocking morpholinos were designed (C) and by phenotype similarity Fgfr4 MO 5'UTR1 was chosen. Both chosen morpholinos (termed e8 and 5'UTR from now on) caused highly similar phenotypes, best characterized at 24 hpf by small eyes and cell death in the hindbrain area. Coinjection of p53 morpholino coinjection reduced cell death greatly (D). Other observed Fgfr4 knock down phenotypes will be described below. For morpholino sequence information see Appendix 5.5.

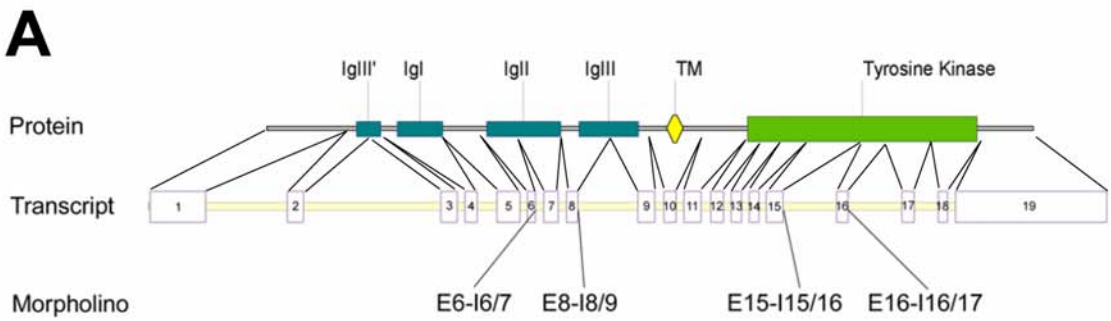
A
IgIII'
IgI
IgII
IgIII
TM
Tyrosine Kinase
Protein
Transcript
Morpholino
E6-I6/7
E8-I8/9
E15-I15/16
E16-I16/17

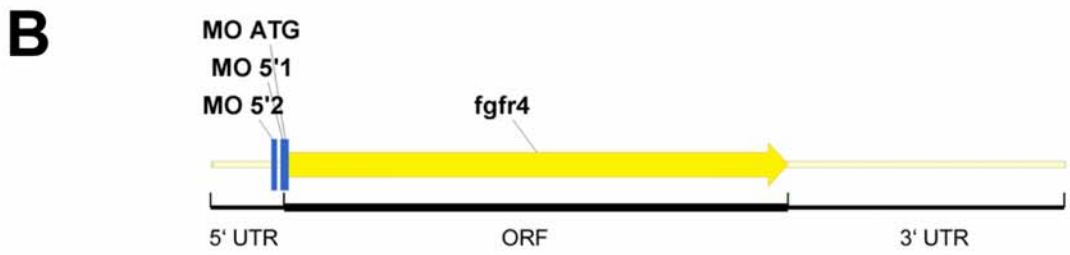
B
MO ATG
MO 5'1
MO 5'2
fgfr4
5' UTR
ORF
3' UTR

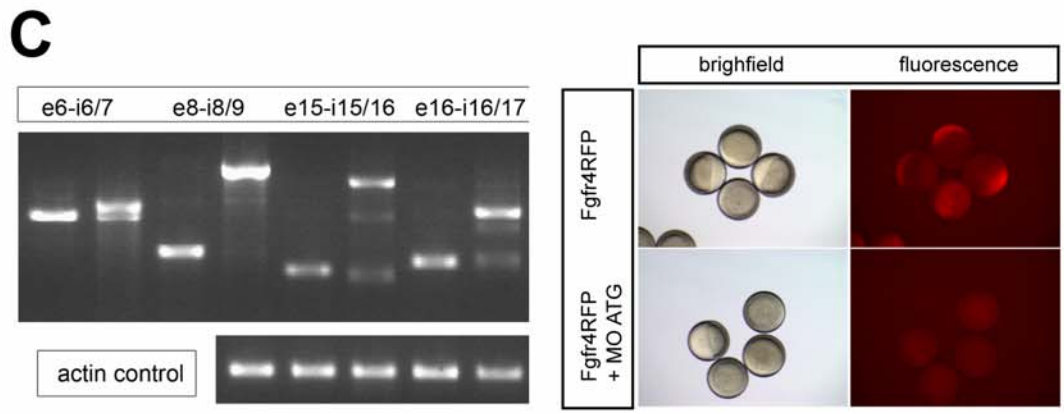
C
e6-i6/7
e8-i8/9
e15-i15/16
e16-i16/17
actin control
brighfield
fluorescence
Fgfr4RFP
Fgfr4RFP + MO ATG

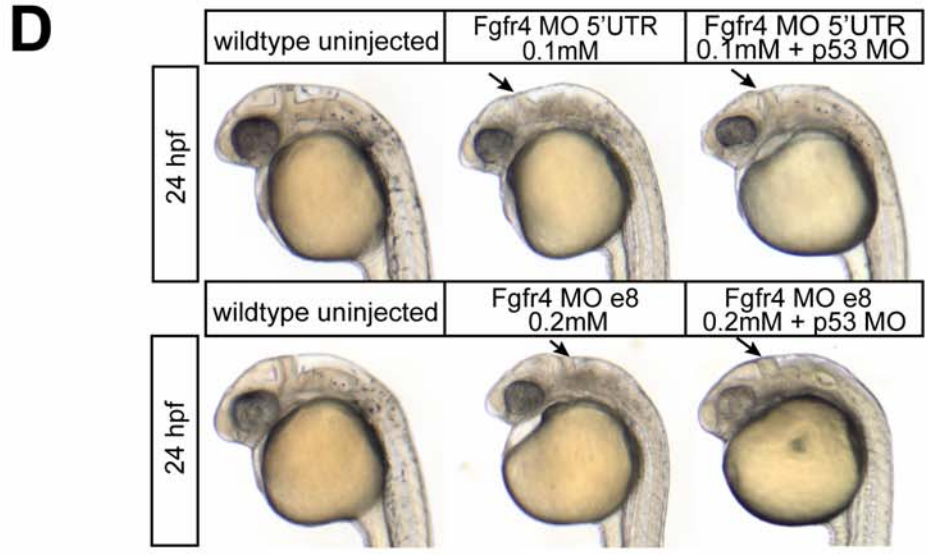
D
wildtype uninjected
Fgfr4 MO 5'UTR 0.1mM
Fgfr4 MO 5'UTR 0.1mM + p53 MO
24 hpf
wildtype uninjected
Fgfr4 MO e8 0.2mM
Fgfr4 MO e8 0.2mM + p53 MO
24 hpf

3.5.2.3. Late phenotypes suggest pleiotropic involvement in organogenesis during early zebrafish development

Young Fgfr4 morphants larvae develop complex phenotypes, which may arise partially as secondary effects of the Fgfr4 loss-of-function (Figure 3.31). Two-day-old larvae exhibit either hindbrain edema or irregular hindbrain morphology suggestive of segmentation defects. Morphant larvae have small eyes and edematous pericardial sac. Later in development the larvae fail to develop pectoral fins (strongly reduced in hypomorphic situation). The body axis is bent and the jaw is bent and displaced.

Morpholino has a limited activity in developing embryos due to dilution of MO in dividing cells, and looking at later stages is almost certainly a very complex situation. For the clarity of analysis, I therefore decided to look at stages of gastrulation and segmentation, because late phenotypes are a combination of secondary effects due to early knockdown and specific late knockdown effects. Inspired by phenotypes during late organogenesis I focused mainly on pectoral fin and myotome development. In the following I will describe only the very early involvement of Fgfr4 in morphogenesis and tissue specification of the pectoral fins.

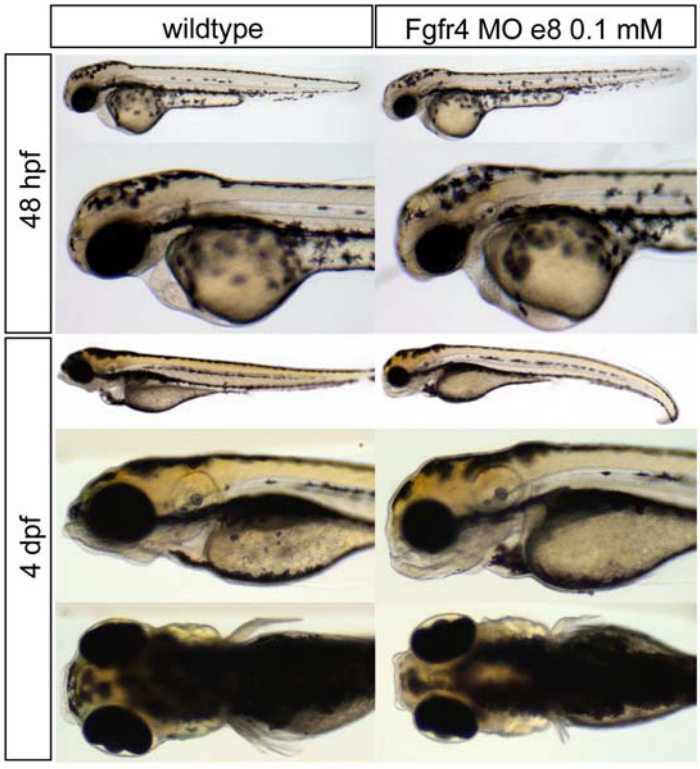

Figure 3.31 Summary of early Fgfr4 loss of function defects
A two-day larva injected with Fgfr morpholino develops hindbrain edema and small eyes. A four-day-old larva shows a variety of defects including jaw development defects, small eyes and deformed or missing pectoral fins. Some individuals develop also bent body axis.

3.5.2.4. Fgfr4 is essential for pectoral fin field specification and fin induction

Fgfr4 is very dynamically expressed during early development (see above). It is distinctly present during gastrulation in presumptive paraxial mesoderm while during early segmentation it is present in lateral mesoderm and somites. Expression of Fgfrs in mesoderm is likely important for the perception of Fgfs and connected fate decisions in the mesoderm and its derivative structures. Thus, Fgfr4 is a very good candidate for an early Fgf signaling marker of structures derived from lateral mesoderm.

I analyzed fin development in Fgfr4 morphants at four stages of development (Fig. 3.32). Firstly, I took 9-somite stage as an onset of the fin field specification (as labeled by the expression of the earliest fin field marker - tbx5). Secondly, at 20-somite stage, I looked again at tbx5 to control for potential delays in fin field specification. I then looked at 30 hpf embryos, when fins start to outgrow and the AER is specified and lastly, at 4 dpf to assess the overall morphology of the fins after Fgfr4 knockdown.

Fgfr4 knockdown leads to a change in the tbx5 domain already at the stages when its expression first comes up i.e. 9 somites. Double ISH experiments with myoD, a marker of somitic muscle precursors, allowed assessing precisely the position of the labeled lateral mesoderm as compared to somite number. At the 9 somites stage the lateral tbx5 expression demarcates presumptive fin (level of somites 1-3) and heart primordium (more anterior). Disruption of Fgfr4 leads to shortening of the tbx5 domain and the expression in the fin field is not recovered over time. Later in development at the time of fin induction AER is not specified (no dlx2a expression) and the fin bud is not formed (Figure 3.28). Consequently, many of the 4-dpf morphant larvae (0.2 mM MO) develop either no fins or reduced fins, which may be due to incomplete Fgfr4 knockdown (higher morpholino injection doses, such as 0.4 mM MO, lead to complete loss of fins).

	Two fins	Reduced fins	One fin	No fins	Total
WT	42	0	0	0	42
Fgfr4 MO e8	3	15	14	13	45

Table 9. The distribution of fin phenotypes in Fgfr4 morphants

Based on morpholino analysis Fgfr4 is likely to act upstream of Tbx5 at gastrulation or early segmentation stages. Fgfr4 expression in the lateral mesoderm at 5-somite stage supports this notion (Fig 3.27). The expression in the fin field persists only until about 20-somites stage (Fig 3.32), where at later stages Fgfr1a and Fgfr2 can be found in outgrowing fins.

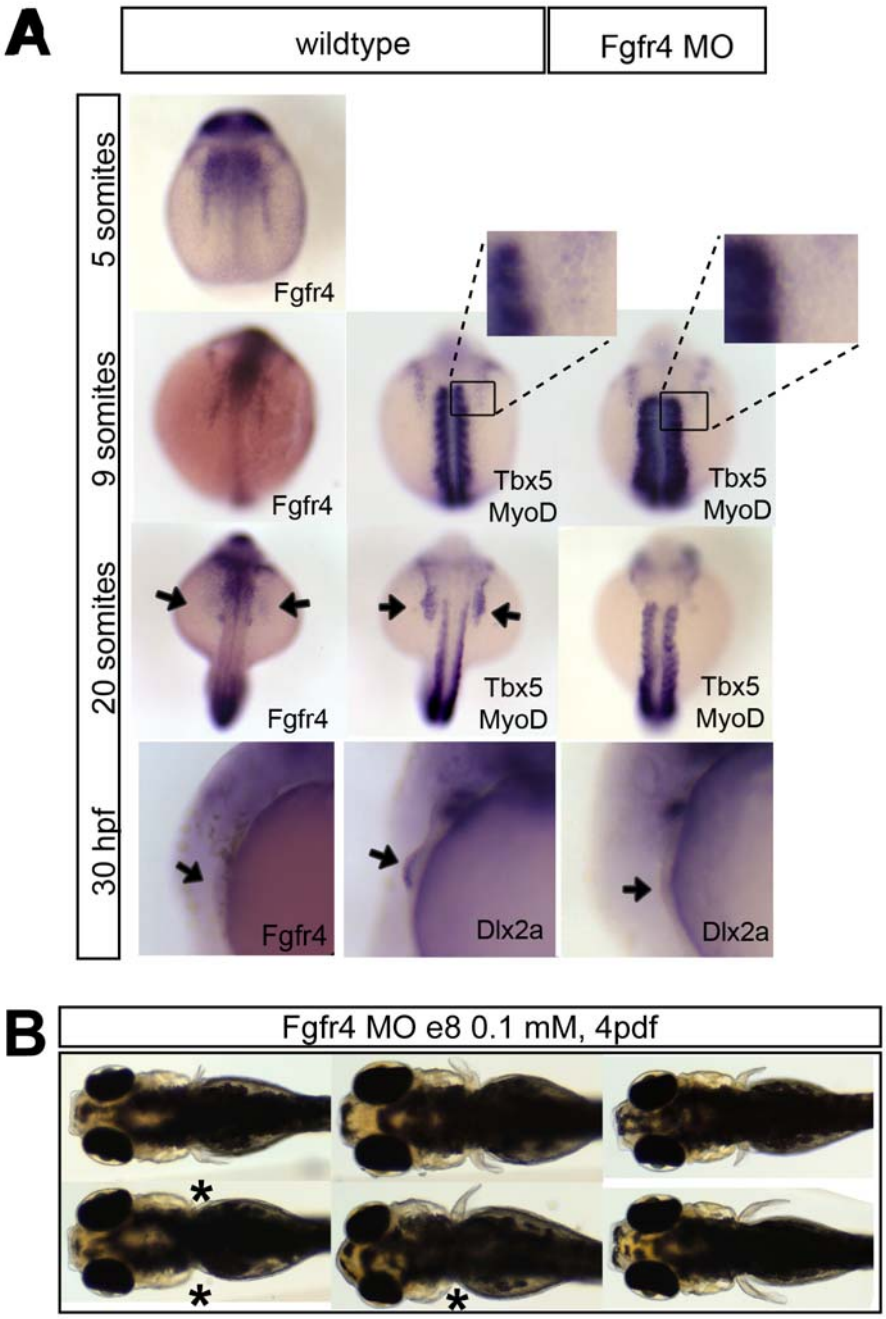

Figure 3.32 Fgfr4 in involved in fin field specification
Fgfr4 knockdown results not only in defects of fin growth but also fin induction (A). *Tbx5* identifies the fin field at around 10 somite stage. At this stage the posterior part of the lateral mesoderm domain (at the level of first 3 somites) seems to be weaker or gone in Fgfr4 morphants. This expression is not recovered later in development and leads to impaired fin induction. The AER does not develop as demonstrated by the *dlx2a* staining at 30 hpf. The expression of Fgfr4 in the lateral mesoderm at essential fin field specification stages complements the evidence of Fgf signaling at these early stages. A pool of embryos injected with Fgfr4 morpholino develop a range of fin reduction, which is probably due to partial mosaicism in efficiency of Fgfr4 knockdown (B).

3.5.2.5. Fgfr4 acts downstream of retinoic acid

In order to determine the position of Fgfr4 in the cascade of genes specifying the fin field, I concentrated on the retinoic acid (RA) – the first morphogen required for fin specification. Inhibition of retinoic acid signaling during gastrulation and segmentation leads to complete loss of fins. Therefore, I examined the expression of Fgfr4 upon RA inhibition using DEAB inhibitor (10^{-5} M) in the timeframe between 30% epiboly and fixation time (TB, 5 or 10 somites).

Surprisingly, preliminary data show a dramatic change in fgfr4 expression, which may be due to different proportions between tissues specialized upon RA signaling. At tailbud stage, the hindbrain domain of fgfr4 is expanded, which is consistent with previous reports concerning hindbrain patterning by RA (Maves and Kimmel 2005). In contrast, the mesodermal domain of fgfr4 expression is significantly shorter, which suggests that RA is required for establishment of the pool of mesoderm (Fig 3.33 A-D). This has to be, however, verified by co-labeling with mesodermal markers.

Consistently, at 5 and 10 ss, upon DEAB treatment, fgfr4 expression in the hindbrain is enlarged and fused with the spinal cord domain. Anterior spinal cord domain is much weaker and lateral mesoderm domains seem to be strongly reduced compared to the wildtype (Fig 3.33 E-H). The staining in the posterior halves of somites (paraxial mesoderm) is also downregulated. Taken together, fgfr4 expression shifts upon DEAB inhibitor treatment suggest that it acts downstream of retinoic acid in the fin field specification.

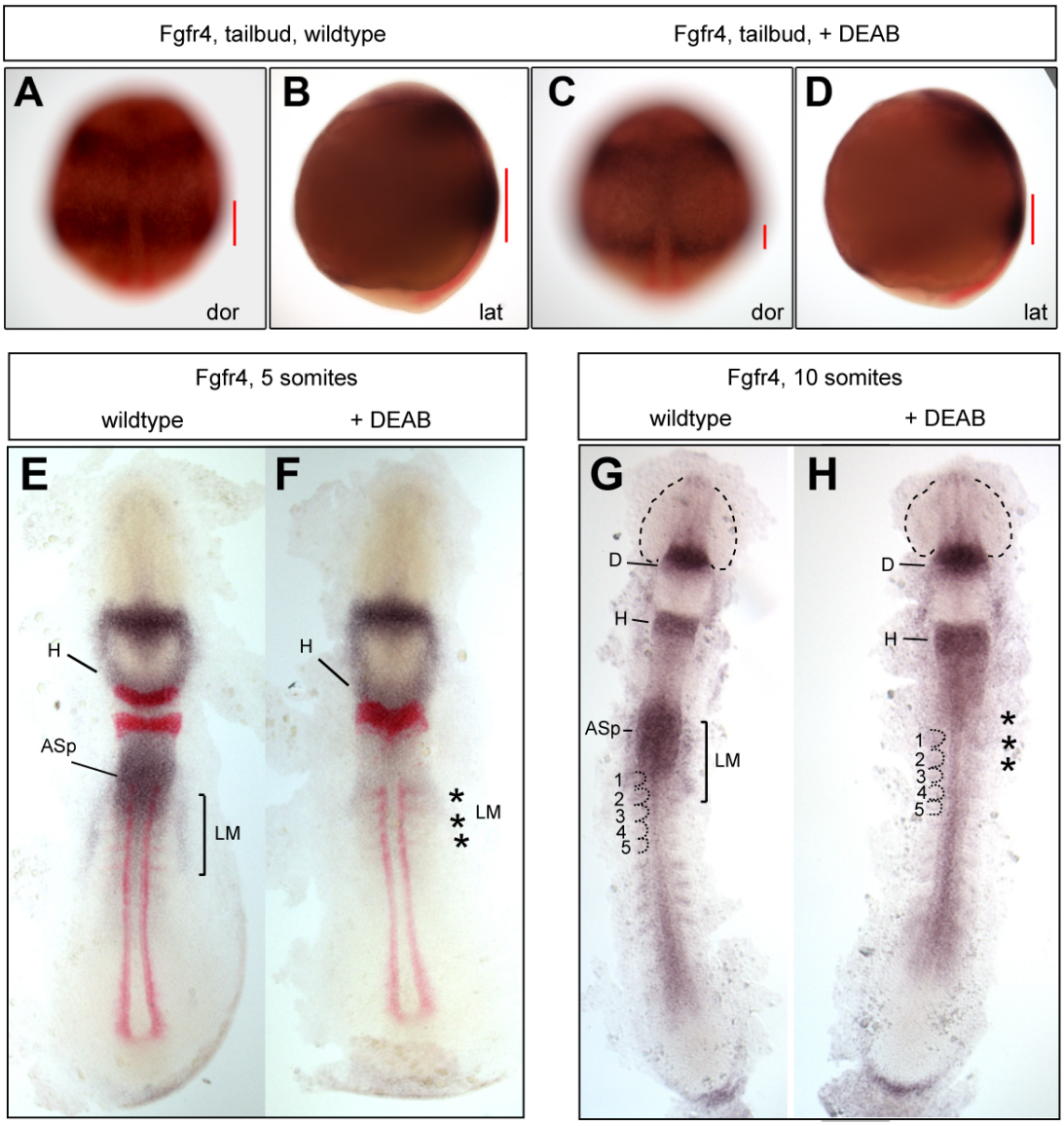

Figure 3.33 Fgfr4 acts downstream of retinoic acid
Embryos treated with DEAB inhibitor between 30% epiboly and tailbud show shifts in Fgfr4 expression. At tailbud mesoderm domain appears much reduced, whereas hindbrain domain expands (A-D). At 5 and 10 somites hindbrain domain fuses with the spinal cord domain, whereas the lateral mesoderm expression cannot be seen any longer. Also the staining in the posterior part of the somites appears downregulated in DEAB treated embryos (E-H). Abbreviations: Asp – anterior spinal cord, D – diencephalon, H – hindbrain, LM – lateral mesoderm, numbers stand for first 5 somites, asterisks demarcate the level where lateral mesoderm domain is missing. Fluorescein probes (in red) demarcate adaxial mesoderm (myoD) and rhombomeres 3 and 5 of the hindbrain (krox20).

4. Discussion

4.1. Fgfr1a mutant lines

In mouse, the role of FGFR1 has been extensively studied in multiple conditional knockout approaches. FGFR1 loss-of-function leads to abnormal gastrulation and embryonic lethality due to mesoderm and midline defects (Deng et al. 1994; Yamaguchi et al. 1994). Through conditional knockout techniques FGFR1 was shown to play role in mesoderm migration, somitogenesis, limb growth, neural crest migration, skeletal development and neuronal differentiation at the midbrain-hindbrain boundary (MHB) (Ciruna et al. 1997; Partanen et al. 1998; Trokovic et al. 2003; Trokovic et al. 2005; Jukkola et al. 2006).

In contrast, medaka headfish mutant, encoding a dysfunctional Fgfr1a^{W181C}, Fgfr1 loss-of-function did not reveal its role at the MHB, but it did lead to loss of all posterior body structures, suggestive of its involvement in the early Fgf signaling during development and formation of the paraxial mesoderm (Yokoi et al. 2007; Shimada et al. 2008).

In order to isolate Fgfr loss-of-function mutants in zebrafish I have participated in the TILLING screen. At first we designed TILLING amplicons based on the previous zebrafish genome assemblies, Zv4 and Zv5, in order to target specific exons in receptor genes. Both of used genome assemblies contained incomplete and erroneous annotation of many genes. Despite my efforts I did not find any Fgfr duplicates in these versions of the zebrafish genome. After closer analysis of the new genome assembly Zv7 (released in July 2007) and other genomes, it became apparent that many teleosts have two FGFR1 genes, including zebrafish, medaka, stickleback and pufferfish, which is consistent with the teleost genome duplication hypothesis (Nicolas Rohner, Thomas Becker, personal communication). In carp, two Fgfr1a related genes were found, which is consistent with carp-specific genome duplication by hybridization (allotetraploidy) (David et al. 2003).

The screen for zebrafish TILLING mutants has yielded in some non-sense and mis-sense mutations that occurred to have little or no value for functional studies. Among three disruptive mutations found in Fgfr1a I did not find expected severe phenotypes, which we could later explain by the complementary function of Fgfr1b.

4.1.1. Fgfr1a^{Y328STOP} and Fgfr1a^{F681C}

Fgfr1-3 have been shown to produce various isoforms, reported for both human and zebrafish genes (Partanen et al. 1998; Scholpp et al. 2004; Eswarakumar et al. 2005). These isoforms result from alternative splicing of mRNA by incorporation of alternative exons 7, 8 or 9, which encode the IgIII domain versions IIIa, IIIb and IIIc, respectively. The early Fgfr1a^{Y328STOP} mutation, which by prediction should result in a complete Fgfr1IIIb loss-of-function, did not reveal any phenotype, suggesting that Fgfr1aIIIb is not produced or

dispensable. However, in order to draw conclusions, one would have to analyze this mutant on the protein level and show that isoform IIIb is indeed, not produced. On the other hand, Partanen and others argue that IIIb and IIIc isoform act redundantly in development, where isoform IIIc dominates over IIIb. Consistently, knockout mice carrying a disrupted version of FGFR1IIIb develop normally (except for a slight tail growth defect) (Partanen et al. 1998). In addition to the possible redundancy between splice versions, in fish the second Fgfr1 may compensate for the loss of Fgfr1IIIb (see section 4.3).

Among the isolated mis-sense mutations we found a mutant carrying the F681C substitution. It was chosen for closer investigation because of high conservation of F681 residue in the kinase domain II (see appendix 5.1). So far, there have been no reports suggesting its functional significance. Although the molecular consequences of the mutation are not clear, they could be addressed in the tissue culture assays such a kinase activity assay and receptor internalization assay. In the context of zebrafish development, the F681C mutation appears to be unimportant.

4.1.2. Fgfr1^{W761STOP} mutant is likely a loss-of-function allele

The potential of dominant negative Fgfr proteins in embryological studies has been initiated in the study of Fgf signaling in Xenopus embryos (Amaya et al. 1991). It has been shown that overexpression of dnFGFR1 (XFD), obtained by removing the tyrosine kinase domains of the cytoplasmic receptor tail, has a potential to block Fgf signaling, which leads to gastrulation defects and loss of mesoderm formation. The ability to block Fgf signaling is explained by the heterodimerization of XFD with wildtype receptors, thereby disabling their activation. In order to study receptor function in Fgf8 signaling I was interested in obtaining mutant fish with dominant negative or endocytosis deficient Fgfr1, which is the prime candidate for an early Fgf8 receptor.

From my observations, the Fgfr1a^{W671STOP} TILLING mutants carried a functionally disrupted version of Fgfr1a. The truncation of the protein does not render Fgfr1a dominant negative, but it does affect its endogenous expression levels, endocytosis and signaling (see below). There are two possible explanations for Fgfr1a transcript downregulation, one being a regulation of the hypomorphic receptor expression as an element of a feedback loop, the other being a spontaneous mRNA degradation by non-sense mediated decay. The latter is often observed in early stop mutations, as a way to prevent the production of deleterious dysfunctional proteins (Alberts 2002). In case of Fgfr1a^{W671STOP} mRNA decay is a more probable explanation as an autoregulatory loop before the onset of zygotic transcription (8 or 16 cell stages) is rather unlikely.

Cloning of a mutant Fgfr1a^{W671STOP} expression construct allowed me to assess the molecular nature of the truncated protein. Based on overexpression experiments I concluded that Fgfr1a^{W671STOP} is a hypomorph, which is endocytosed slower and has a potential to inhibit

Fgf signaling upon overexpression. It would be interesting to clarify, whether the receptor is activated properly. Altered activation could result in altering the threshold of sensitivity to Fgf8, thereby shortening the range of signaling (lower Fgf8 concentrations are not able to activate the receptor anymore, see section 4.8).

Due to a combination of the non-sense mediated decay and signaling defects I regarded mzFgfr1a^{W671STOP} as partial loss-of-function mutants. However, I did not find any serious developmental defects, which was inconsistent with the reports about strong phenotypes in mouse or medaka Fgfr1 mutants (Ciruna et al. 1997; Shimada et al. 2008).

The allelic complementation of Fgfr1a^{W671STOP} and Fgfr1a^{R705H} (the spiegel danio mutant Fgfr1 allele) supported the notion that the truncation of Fgfr1a causes its partial loss-of-function. However, the molecular nature of the R705H is not clear and needs further investigation. Because adult individuals of both mutants show similar scale mispatterning phenotypes we expect Fgfr1a^{R705H} to act also as a hypomorph, although the lethality of homozygous Fgfr1a^{W671STOP} suggests stronger loss-of-function.

Interestingly, the degree of scale loss is dependent on the genetic background. Tupfel long-fin fish do not exhibit any defects, whereas Tübingen fish show a variable loss of scales. We hypothesize that there is perhaps a genetic silencer in the TL fish, which rescues the scale development in Fgfr1a mutants. Similar variability of the phenotype, which is dependent on the unknown modifier gene, was observed in carp fish carrying Fgfr1 mutations, which supports the idea of a rescue locus, present only in some strains (Nicolas Rohner, personal communication). The direct comparison of the two species, carp and zebrafish, demonstrates how the analysis of polymorphisms in genes, may provide an interesting insight into the pathways involved in morphological changes in evolution, such as importance of Fgf signaling for the patterning of the dermal skeleton.

4.2. Fgfr1a and Fgfr1b morpholinos

In order to complement my observations of Fgfr1a loss-of-function mutant I tested several morpholinos. Consistent with the mutant analysis, morpholino injected embryos showed only slight brain cell death phenotype but no other obvious defects. This result is only partially consistent with the phenotype published for Fgfr1a morpholino knockdown, which indicated the role of Fgfr1a in the maintenance of midbrain-hindbrain boundary (Scholpp et al. 2004; Trokovic et al. 2005). Morphant embryos at stages I have looked at (until 36 hpf) did not reflect a requirement for Fgfr1a in sustaining MHB marker gene expression.

Similarly, in Fgfr1b morphants the gross morphology of embryos remained like wildtype. A few individuals showed slight tail growth reduction, but not to a significant level. The expression patterns of both genes are almost completely overlapping, which suggests their redundant function in early development.

Morpholino knockdown may not always phenocopy the mutant phenotype for a variety of reasons. The blocking efficiency of morpholino may be lower than that of a mutation. Additionally, some phenotypes observed in morpholino-injected animals may be non-specific, stress induced off-target effects. Also, morpholino have a limited time of stability and cannot phenocopy late onset phenotypes.

4.3. Fgfr1 duplication and redundant function during zebrafish development

During evolution due to gene duplication one of two paralogous genes may lose its function (Hashiguchi and Nishida 2005), act redundantly (Martin and Kimelman 2008) or specify separate functions to act independently (Jovelin et al. 2007). In zebrafish, both Fgfr1 morpholinos evoke very mild phenotypes, which did not agree with reported functions of Fgfr1 in other vertebrates. I have therefore tested for possible receptor redundancy by injecting Fgfr1b morpholino into the $Fgfr1^{W671STOP}$ mutant. This full Fgfr1 loss-of-function caused progressive loss of posterior structures in most injected embryos. The expression of the markers of various brain parts did not reveal any defects but the mesodermal marker confirmed significant loss of mesoderm. I conclude that paralogous fgfr1 genes cooperate during tail development, which is supported by their similar expression patterns. Only interference with the activity of both fgfr1 genes disrupts mesoderm specification/maintenance, which to a certain extent resembles headfish (medaka) Fgfr1a loss-of-function. Presumably, the two copies of fgfr1 gene in medaka adopted different functions than their respective zebrafish homologs, which would provide us with additional information concerning differences between those species in basic patterning mechanisms during development (Furutani-Seiki and Wittbrodt 2004). However, little is known about the second copy of medaka fgfr1 and it is possible that it lost its activity altogether. This could be addressed by examining its expression pattern and the loss-of-function analysis.

It would be also interesting to investigate the function of the carp fgfr1 genes, which were found as four homologous alleles of the zebrafish fgfr1a (justified by tetraploidy in carp). Mutation in one or two of carp Fgfr1 alleles results in scale defects as well. Whether carp also possesses homologous fgfr1b copies remains for further investigation (Nicolas Rohner, personal communication).

At postembryonic stages, the functions of Fgfr1a and Fgfr1b seem to diverge also in zebrafish, at least in some tissues as evidenced by the scale phenotype in Fgfr1a loss-of-function. In situ hybridization on skin of youngster fish shows that only FGFR1a is expressed in the developing dermal skeleton, whereas Fgfr1b is downregulated (Nicolas Rohner – personal communication). Therefore, the loss of only one of fgfr1 genes is sufficient to disturb scale development.

4.4. Functionality of Fgfr1a-eGFP/mRFP

In an attempt to study Fgfr1 function in vivo I have used several Fgfr1 fusion protein constructs, all of which showed subcellular localization expected for a transmembrane protein, in plasma membrane and intracellular organelles. However, tagging the terminus of the receptor (both C- and N- termini) caused ectopic activation of target genes upon higher mRNA injection levels. It is possible that a tag increases protein stability, hence, leads to a dose dependent hyperactivation of the receptor. The stability could be affected by partial steric blockage of the assembly of the intracellular complex responsible for protein degradation. For example, the ESCRT complex is known to regulate the degradation vs. recycling of tyrosine kinase receptors (Raiborg et al. 2003; Raiborg et al. 2008). The N-terminal fusion may be activated in a ligand independent manner, and it was not used for trafficking studies. As the exact reasons for the autoactivation of the C-terminal fusion is unclear, the levels of overexpression were kept moderate in order to avoid gain-of-function phenotypes.

4.5. Fgfr1 trafficking at a steady state

I showed that Fgfr1 is found in the same endocytic structures as Fgf8 in a transplantation assay. This interaction could be predicted despite previous reports that Fgf8 has a very low mitogenic activity in association with FGFR1IIIc (Zhang et al. 2006). Fgfrs are high affinity receptors, presumably interacting with many ligands, where affinity is a function of ligand availability and concentration. Importantly though, in vivo studies on mouse and medaka suggest pairing of Fgf8 and Fgfr1. Mouse FGFR1 mutant displays similar to FGF8 loss-of-function deformity of the MHB (Jukkola et al. 2006) and Fgfr1 mutant in medaka, hdf, phenocopies the morpholino knockdown of Fgf8 in this species (Yokoi et al. 2007). Additionally, I was interested in the role of receptor dependent endocytosis in Fgf8 signaling, which was postulated to delimit the range of target gene induction. I therefore, decided to concentrate on Fgfr1a trafficking and the regulation of receptor endocytosis in Fgf8 signaling.

In tissue culture experiments performed on HeLa cells, different Fgfrs were shown to take up Fgf1 in clathrin-dependent endocytosis as evidenced by colocalization with EEA1, an early endosome marker. All FGFRs, except for FGFR4, are directed to lysosomal degradation and are recycled only to a minimal extent (Haugsten et al. 2005).

I observed intracellular fate of Fgfr1a in embryos at sphere stage, which I considered representative of low signaling state, due to low and ubiquitous expression of Fgf target genes at this stage. In my observations, consistently with previous tissue culture reports, Fgfr1 is taken up through clathrin dependent endocytosis as evidenced by partial colocalization with Rab5 and Cellubrevin. A low degree of colocalization with Caveolin suggests that both pathways, clathrin dependent endocytosis (CDE) and non-clathrin

endocytosis (NCE), can be involved in receptor internalization. The ratio of both routes of endocytosis may depend on the ligand concentration, which was earlier suggested for EGF receptor downregulation (Sigismund et al. 2005; Sigismund et al. 2008). Our knowledge of EGFR trafficking indicates that CDE and NCE play different roles and are employed differentially in response to low and high levels of EGF. Whether the functions of alternative uptake routes are distinct in regulating Fgfr fate (degradation/endocytosis) remains to be elucidated.

Fgfr1 in zebrafish embryos shows no overlap with Rab11 recycling endosomes. Despite some overlap with Cellubrevin (also labeling rapid-recycling endosome species and exocytic structures (Annaert et al. 1997)) it seems that the level of recycling at steady signaling levels is low, which would be consistent with tissue culture reports (Haugsten et al. 2005). Rab11 perinuclear recycling endosomes should be optically resolvable and none were observed overlapping with Fgfr1 (Ullrich et al. 1996). The notion that Fgfr1 is mainly directed to degradation is also supported by a large degree of colocalization with Rab7-positive late endosomes. However, additional study of recycling in dissociated cell culture would shed more light on this matter as some cell culture studies suggest that many fluid (ligand) and lipid (receptor) phase cargos are constitutively recycled rapidly after early vesicle sorting (Gruenberg and Maxfield 1995). The question of Fgfr1 recycling would, therefore have to be addressed in appropriate tissue culture assays.

Importantly, it appears that tissue culture observations overlap to a certain extent with the situation in zebrafish embryos. Perhaps, this can serve as an argument that the trafficking behavior of Fgfr in response to stimulation can be extrapolated from tissue culture to the situation in the living organism. However, I have not observed any nuclear translocation of the Fgfr1a, which was reported in some tissue culture studies (Myers et al. 2003; Reilly et al. 2004; Bryant et al. 2005). It is possible, that nuclear translocation takes place in more specialized cell types and that in undifferentiated embryonic cells this mode of signaling is not employed.

It would be greatly interesting to analyze pathways of Fgfr1a trafficking in context of Fgf8 signaling at high ligand concentrations, which would provide additional information as to how Fgf8 is delimited. Cells close to the Fgf8 source may play a restrictive role, by uptake and direct degradation of receptors and Fgf8. They can, on the other hand, play a permissive role, where at high concentrations Fgf8 is rapidly recycled, hence, allowed to spread further in the tissue.

4.6. Importance of ubiquitylation for Fgf signaling

I observed that Fgfr1a is ubiquitylated in vivo and that fgf8 signaling increases the state of receptor ubiquitylation. Overexpression of Ub4KR, a poly-chain deficient ubiquitin mutant, leads to slight upregulation of sprouty 4 induction. This provides indirectly some

evidence that polyubiquitylation may regulate Fgf signaling. During this study a publication was released by Haugsten et al. 2008, showing that Fgfr1 ubiquitylation is dispensable for its internalization. Similar to EGFR though, lack of ubiquitylation changes FGFR1 trafficking inside the cells, where it is sorted to recycling rather than degradation, because of lack of degradative polyubiquitylation signals for the sorting machinery. K63 (endocytosis) or K48 (degradation) are the best-studied polyUb chains. Without them the protein is theoretically more prone to being recycled and not downregulated. Therefore, Ub4KR may change the Fgfr trafficking rather than its endocytosis. It would be interesting to look in more detail at the dynamics of the Fgfr downregulation in a ubiquitylation deficient state and to assess the role of Fgfr1 ubiquitylation in the establishment of the Fgf signaling range.

In search for components of the ubiquitylation pathway, which would suggest its involvement in Fgf8 organizer activity I looked also at the expression patterns of ubiquitin, ubiquitin-ligase, Cbl, and the ubiquitylation dependent adaptor protein Grb2. All those factors are involved in ubiquitylation of tyrosine kinase receptors, therefore could be expressed in restricted fashion during the patterning of the embryo, however, they are expressed ubiquitously. I concluded that the ubiquitylation machinery is probably constitutively present in all cells and the regulation of Fgfr state is dependent on other cellular components.

4.7. A role of Y753 and c-terminus in Fgfr1 trafficking

The carboxyterminal domain of Fgfr1 is known to include one of tyrosines targeted to autophosphorylation. Y766 (Y753 in fish) on Fgfr1 has been shown to directly bind phospholipase C-γ (PLCγ) enabling signaling through this pathway (Mohammadi et al. 1991). Activated PLCγ can hydrolyse phosphatydyloinositol-4,5-diphosphate (PIP2) to inositol-1,4,5-triphosphate (IP3) and diacylglycerol (DAG). IP3 induces Ca^{2+} release from intracellular stores, whereas DAG activates protein kinase C (PKC). In turn activated PKCδ is able to phosphorylate and stimulate Raf therefore leading to activation of the MAP kinase pathway in a Ras-independent manner (Ueda et al. 1996; Thisse and Thisse 2005). However, no significance was shown for Fgf-induced activation of PLCγ in vitro (Eswarakumar et al. 2005) and in vivo in zebrafish (Lawson et al. 2003; Ma et al. 2007). In mouse, the $FGFR1^{Y766F}$ mutation reveals the role of this tyrosine in the dorsoventral patterning (Partanen et al. 1998). Also uncovered was the importance of Y766 and the entire C-terminal domain for endocytosis (Sorokin et al. 1994; Sorensen et al. 2006). I have cloned mutant constructs of Fgfr1a, $Fgfr1a^{Y753F}$ and $Fgfr1a^{Y753STOP}$, to directly address the question of receptor dependence of Fgf8 “restrictive clearance”.

Observations of Fgf8Cy5 uptake into cells expressing wildtype or mutant receptors confirmed earlier reports about the importance of Y766 (Y753 in fish) in receptor internalization. However, I also found that in embryos Fgf8 is taken up by cells expressing mutated receptors, which may be due to heterodimerization with the wildtype receptors still

present in the cells. The extent of Fgf8 endocytosis was slightly lower for both Fgfr1a^{Y753STOP} and Fgfr1a^{Y753F} expressing embryos, compared to the control embryos expressing wildtype Fgfr1a. Small differences in endocytosis were not reflected by the expansion of the target gene induction, which was drastic for Fgfr1^{Y753F} mutant. I have confirmed that this hyperactivation is dependent on ligand induction in a transplantation assay, where Fgfr1a^{Y753F} overexpressing cells placed in wildtype embryos do not show ectopic target gene expression. Because, reduced endocytosis seems to be insufficient to produce observed drastic target gene expansion (as both mutants show similar uptake reduction), I assume there must be another mechanism of target gene activation with overlapping effects, i.e. the rate of receptor degradation or the duration of signaling. In this context, Fgfr1 endocytosis would not be alone responsible for Fgf8 signaling range.

Overall, the current evidence suggests that Y753 and the C-terminal domain of last 58 amino acids are important for Fgfr endocytosis and signaling, despite conflicting reports from tissue culture assays showing that it induces MAPK signaling to a similar extent as the wildtype receptor (Sorokin et al. 1994). In vivo, small differences in the rate of trafficking or protein degradation may have dramatic effects. Therefore, it would be interesting to quantify mutant receptor trafficking in colocalization assays. The biological relevance of these observations has to be, however, interpreted carefully, because protein overexpression assay address the mechanism of receptor function rather than its specificity and activation control in vivo at endogenous levels.

4.8. The role of Fgfr1 in Fgf8 morphogen gradient formation

Based on my observation of Fgfr specificity in the early development of zebrafish, it is unlikely that Fgfr1a alone mediates Fgf8 signaling during early development. Most probably, Fgfr1b is equally involved, as well as Fgfr4, all of which are strongly expressed during gastrulation. Nevertheless, the study of Fgfr1a function and endocytosis provides some information, which may be relevant for all these receptors. In the wildtype situation, Fgf8 is thought to induce different target genes at different thresholds of Fgf concentration (Fig. 4.1 A). The tyrosine 753 and the C-terminal domain of Fgfr1a are important for endocytosis, which has functional relevance for the range of Fgf8 spreading and target gene induction. Given that the rate of receptor activation is unchanged, inhibition of the ligand endocytosis may lead to the expansion of Fgf8 spreading and the target gene expression (Fig. 4.1 C). Importantly, the rate of Fgfr1a activation is likely to determine the threshold of sensitivity to Fgf8, hence target gene induction. As illustrated by overexpression of the hypomorphic Fgfr1a^{W671STOP}, the change of the threshold of Fgf8 mediated receptor activation, may lead to the shortening of the Fgf8 signaling range (Fig 4.1 B). Alternatively, an overexpression of Fgfr may lead to an increased uptake of the ligand, which could also affect the range of signaling.

In the embryo, Fgf signaling is strongly autoregulated by feedback loops of receptor and ligand expression. Therefore, it is likely, that receptor overexpression would either decrease endogenous receptor production or increase ligand expression. Either way, the overexpression of wildtype Fgfr1 has no effect on target gene induction. In order to understand the mechanism of Fgf8 signaling it will be still necessary to address some basic questions in Fgf8 morphogen signaling:

1. what is the threshold of Fgf8 concentration for activation of each target gene,

2. how does the cellular response differ between high and low Fgf8 concentrations and finally,

3. are there any actively regulated elements in the Fgfr downregulation machinery or is the ligand-dependent endocytosis a constitutive property of the early embryonic cells.

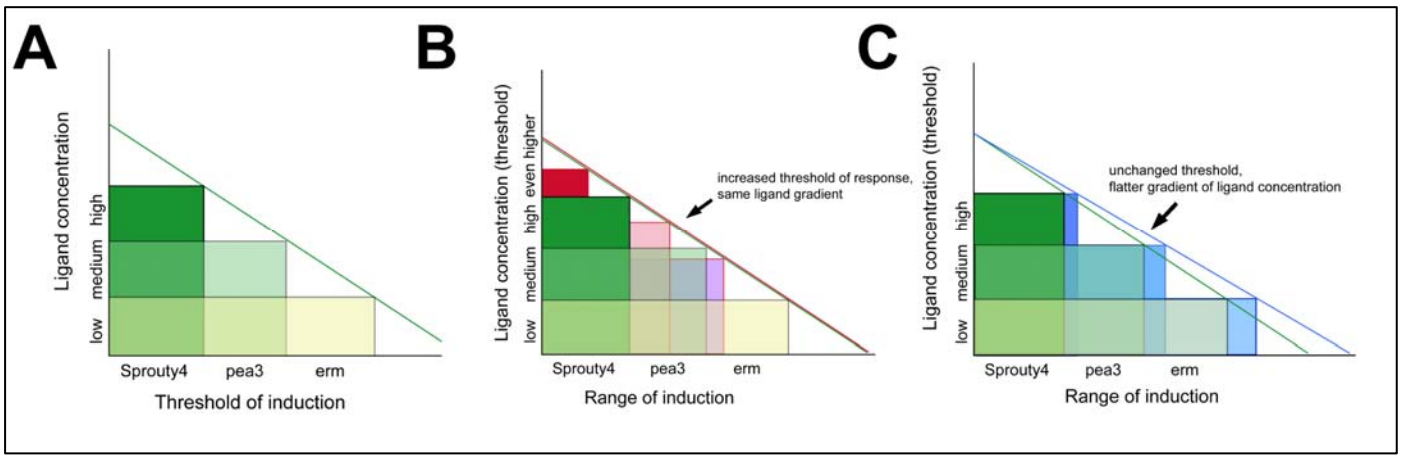

Figure 4.1 Theoretical model of Fgf8 range of signaling

4.9. The essential role of Fgfr2 in zebrafish

The conditional knockout of Fgfr2 in mesenchyme and chondrogenic cells (under Dermo1/Twist2 promoter) in mouse resulted in complex skeletal phenotypes suggesting the role of Fgfr2 in osteoblast function and skeletal growth (Yu et al. 2003). Homozygous mutant mice are dwarfish and are characterized by reduced bone length and bone density. Fgfr2 was shown to be dispensable for osteoblast differentiation, but required for osteoblast proliferation. Teleost osteogenesis differs from mammalian, however, similar to the mammalian situation, in zebrafish the major mode of building cellular and acellular bones is by periosteal osteogenesis, which depends on the activity of osteoblasts (Moss 1961; Moss 1963).

The Fgfr2 mutant isolated from the TILLING screen is characterized by a late nonsense mutation L545STOP. This leads, according to my results, to the likely non-sense mediated decay of Fgfr2 mRNA as well as protein loss-of-function, rendering it dominant negative. The protein that is produced in very small amounts and has a dominant negative character but is unlikely to act in a dominant manner during embryo development. Being both

restricted by a specific expression pattern and present in uncompetitive amounts Fgfr2^{L545STOP} is unlikely to preserve its function. Therefore, I assumed Fgfr2^{L545STOP} homozygotes are strong loss-of-function mutants. However, in order to provide more reliable evidence that Fgfr2 is the only locus affected in Fgfr2^{L545STOP} fish, it would be necessary to generate another mutant allele in Fgfr2 or a rescue construct. Nevertheless, the reduced body size and fragility of the mutant bones, especially ribs, are consistent with the phenotypes observed in mice with conditional Fgfr2 knockout in bones. Differences in some bone growth (neural spines and hypurals appear thicker than wildtype) may result from various modes of osteogenesis, such as fibroblastic metaplasia, employed to build these bones. It would be very interesting to investigate closer the growth of the mutant fish as well as molecular and cellular causes of the bone growth defects observed.

The reasons for differences in body size of the mutant fish are most difficult to study, as there are many environmental and physical factors that may cause a slower growth rate, such as inability to compete for food with the wildtype siblings or the deformity of the jaws. A limited control over these factors is the main problem in research of adult individuals. Mice Fgfr2IIIb -/- embryos are also smaller at birth, which excludes such factors as inability to feed due to malfunction of the jaws. It would be interesting, therefore, to determine the environment-independent causes for a slower growth.

Similarly, it would be challenging to determine the basis of infertility in the mutant fish. Sterility may originate either from behavioral or physical problem and is left for further elucidation. Interestingly, this phenotype could be explained by two reports in which FGFR2 was described to play a crucial role in Sertoli cell differentiation during male sex determination (Schmahl et al. 2004) as well as germ cell migration and survival in mice (Takeuchi et al. 2005). It would be fascinating to closer investigate, whether such essential processes as germ cell migration and Sertoli-like cell differentiation are to some extent conserved between zebrafish and higher vertebrates (Kurita and Sakai 2004).

Surprisingly, the overall phenotype in homozygous Fgfr2^{L545STOP} zebrafish is rather mild compared to the severe FGFR2 or FGFRIIIb knockout in mouse (Arman et al. 1998; De Moerlooze et al. 2000). FGFR2 knockout mice die at preimplantation due to defects in development of the placenta. Disruption of the important FGFR2IIIb isoform leads to multiple defects at birth including a complete agenesis of lungs and limbs, dwarfism, various skeletal abnormalities and skin defects. What is surprising is that mutant zebrafish develop normal limbs (fins), as opposed to the Fgfr2ΔIII knockout mice (Xu et al. 1998). This could be explained by different functions of both Fgfr2 and Fgfr4 during early development of zebrafish as compared to mice. As I observed, Fgfr4 seems to play an important role in the induction of fin field in zebrafish, which has not been reported for other vertebrates. Provided that the phenotypes observed in zebrafish indeed reflect Fgfr2 loss-of-function, one could conclude that FGFR2 adopted mammal specific function and in teleosts, such as zebrafish, and it is rescued by redundant functions of other Fgfrs. One cannot exclude a possibility though, that

Fgfr2^{L545STOP} causes an incomplete loss-of-function, hence, some preservation of its functions in specific organogenesis events.

4.10. Fgfr4 in zebrafish development

FGFR4 has been shown to play a crucial role in limb muscle differentiation in chick (Marics et al. 2002). The role of FGFR4 in chick limb was shown to be dependent on FGF8 signaling from the somites and necessary for differentiation of all muscle types during limb growth. This and other functions of chick FGFR4 (FREK) was previously suggested based on the expression and structure analysis of the protein (Halevy et al. 1994; Marcelle et al. 1994). Interestingly, FGFR4 in chick is strongly expressed in three mesoderm-derived structures: kidney, cartilage and striated muscle.

In mouse, despite FGFR4 expression in endoderm and mesoderm-derived structures (muscle, lung, kidney, pancreas and other), the disruption of FGFR4 did not cause any apparent defects. Its redundant function with FGFR3 in lung development was shown by double FGFR3/FGFR4 knockout (Weinstein et al. 1998). Although FGFR4 occurred to be dispensable for mouse development, some evidence was provided for a unique function of FGFR4 in promoting myogenic differentiation by heterodimerization with FGFR1 (Kwiatkowski et al. 2008).

In zebrafish, Fgfr4 is expressed in a similar fashion to that of the chick or frog, although in fish and frog it is strongly expressed during gastrulation in contrast to mouse and chick. It is, however, structurally different from all FGFR4s of other species as its extracellular domain comprises of four Ig-like domains, instead of two or three. This in consequence suggests its different affinity to Fgf ligands (Thisse et al. 1995). A functional divergence of Fgfr4 between zebrafish and higher vertebrates, such as chick and mouse, is also supported by my and others observations of zebrafish Fgfr4 loss-of-function (see below).

Recently Fgfr4 was associated with the function of Fgf19 in eye and lens development (Tamimi et al. 2006; Nakayama et al. 2008). In human tissue culture experiments FGF19 was shown to bind exclusively to FGFR4 (Xie et al. 1999), however in zebrafish, Fgfr4 has a different extracellular structure and it seems that both Fgfr2 and Fgfr4 may mediate Fgf19 signaling. In zebrafish, both Fgfr2 and Fgfr4 morpholino knockdown was shown to inhibit lens formation, whereas later in development Fgf19 knockdown disrupted development and maintenance of the periocular mesenchyme. This late phenotype was associated with Fgfr4 based on expression pattern analysis, in which Fgfr4 is uniquely expressed in the cornea and the ciliary margin of the larval eye (Tamimi et al. 2006). My observations support these results to a certain extent, as Fgfr4 morphants exhibit strongly reduced in size and sometimes misshapen eyes. Further analysis with use of appropriate markers needs to follow.

Also the mesodermal defects are consistent with the expression pattern, because Fgfr4 morphants display irregular somites, abnormal jaws and lack of pectoral fins. This, however, suggests a much more exclusive role of Fgfr4 in mesodermal derivatives in zebrafish as compared to other vertebrates. Compared to the Fgfr1 loss-of-function Fgfr4 seems to be restricted in its exclusive activity to the intermediate and lateral mesoderm, where it is expressed in a unique fashion. This notion is supported by the observations in medaka, where Fgfr1 was shown to promote axial but not lateral mesoderm (Shimada et al. 2008). It would be greatly interesting to inactivate all early mesoderm Fgfrs, Fgfr1a, Fgfr1b and Fgfr4 in order to assess the extent of their cooperation in the early formation of the mesoderm.

4.11. Pectoral fin development in zebrafish

I found that Fgfr4 knockdown disrupts fin field specification as well as fin induction and growth. This finding is novel and introduces important changes to our understanding of the role of Fgfs in the fin induction process. So far, there was no evidence in zebrafish for such early involvement of Fgf signaling in fin field specification.

Experimental data from chick suggested limb inducing activity of Fgf8 from the somites (Crossley et al. 1996). Also in mouse, Fgf8 was shown to play an inductive role in fin outgrowth (Sun et al. 2002; Mariani et al. 2008). However, earlier activity of Fgf8 could not be addressed with the promoter used for the disruption of the gene (Moon and Capecchi 2000). In zebrafish, Fgf8 expression in the anterior three somites, i.e. the level of fin induction on the lateral sides, is present only at the time of their formation, later the mRNA of Fgf8 gets strongly downregulated, thereby making it an unlikely candidate for an inducer of the lateral plate fate. One cannot exclude the possibility though, that the critical timeframe when Fgf signaling is needed falls between tailbud and early somite formation. Why do Fgf8 mutant, ace, form perfect fins then? It is possible that in zebrafish this process takes more ligands, which are acting redundantly. The Fgf candidate that has been implicated in many processes together with Fgf8a and Fgf3 and is expressed in the somites, is Fgf17b (Cao et al. 2004).

Retinoic acid signaling had been shown to be the earliest factor specifying the prospective fin field (Grandel et al. 2002; Keegan et al. 2005; Marques et al. 2008). In case of hindbrain, somite or heart patterning Fgfs and RA signaling were shown to be signaling in a codependent fashion, suggesting an interplay between these pathways (White et al. 2007; Marques et al. 2008). I observed, that upon RA inhibition, Fgfr4 is expressed in an altered fashion, which is consistent with the observations found in the early embryogenesis of Xenopus (Shiotsugu et al. 2004). This suggests that Fgfr4 acts downstream of RA signaling, although the influence of Fgfr4 knockdown on RA remains to be investigated. In the future experiments it will be interesting to address some open questions such as: what is the nature of the RA and Fgfs interplay in establishing the fin anlage, how is RA involved in lateral

mesoderm specification and what are the Fgf ligands, which specify the fin field via Fgfr4. Is Fgfr4 acting upstream of a late inductive factor, Wnt2b?

I have provided some evidence suggesting that the role of Fgfrs during earliest stages of limb development diverged between zebrafish and mice. In mouse, FGFR2 and FGFR1 have been shown to be involved in induction and outgrowth of the limb, respectively (Xu et al. 1998; Xu et al. 1999). I have found that in zebrafish Fgfr4 instead of Fgfr2 functions in the earliest stages of limb formation, whereas Fgfr1a loss-of-function results in weak fin defects (see Fig. 3.7 in Results). However, because Fgfr2 is also expressed in the lateral plate mesoderm and fin buds, it is still unclear, whether it has a function in limb growth. Surprisingly, Fgfr2^{L545STOP} mutants did not display any fin growth defects. Given the involvement of Fgfr4 in the specification of the fin field, I would like to propose a refined model of the signaling cascade involved in fin formation, which in a temporally simplified manner summarizes known factors in pectoral fin formation (Fig. 4.2).

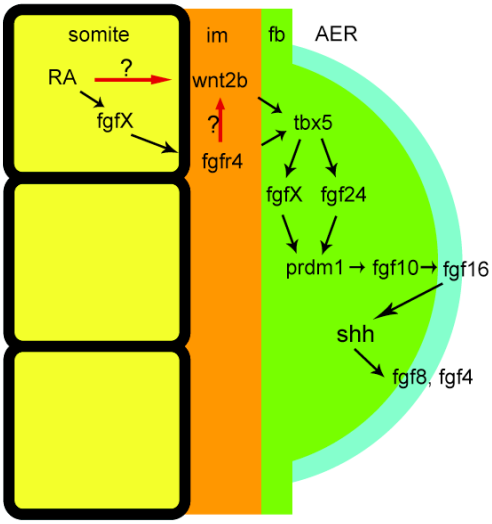

Figure 4.2 Current model of signaling cascade in pectoral fin induction
Fgfr4 is a novel Fgf signaling member in the cascade. It is unknown whether Fgfr4 acts epistatically upstream of the fin outgrowth factor, Wnt2a. It is also unclear, which ligands actively signal through Fgfr4 in fin field specification. Abbreviations: im – intermediate mesoderm, fb – fin bud, AER – apical ectodermal ridge.

4.12. Functions of Fgfrs in Fgf8a signaling and early development

Early during development Fgf8a is acting together with its paralog, Fgf24 and a member of the synexpression group, Fgf3. Together, Fgf8a and Fgf24 have been shown to promote posterior mesoderm development, and each gene separately is sufficient to do so (ace mutants displaying only a weak segmentation phenotype) (Reifers et al. 1998; Draper et al. 2003). The double knockdown of Fgfr1a and Fgfr1b to a certain extent resembles the loss of mesoderm seen in Fgf8a/Fgf24 double mutant. Based on phenotypic similarities, as well as comparable expression patterns, I conclude that Fgfr1a and Fgfr1b mediate Fgf8a and Fgf24 signals in mesoderm formation. However, other Fgf8/24 dependent tissues and organs, such as developing brain, heart, ear or pectoral fins may be dependent also on other receptors.

Fgf8 is also essential for the maintenance of the midbrain-hindbrain boundary. However, the double Fgfr1a and Fgfr1b knockdown did not affect the expression of MHB markers. Preliminary results suggest that there might be a redundancy between Fgfrs 1a, 1b and 4 in the maintenance of this organizer (data not shown). Interestingly, Fgfr3 and Fgfr4 are expressed in rhombomere 1 and Fgfr2 is expressed in the midbrain, both structures adjacent to MHB. Additionally, Fgfr3 has been shown to undergo expansion in the absence of Fgf8, which indicates a regulatory interaction (Sleptsova-Friedrich et al. 2001). It will be of great interest to investigate this issue closer by inducing e.g. triple knockdown situations with Fgfr1a, Fgfr1b and Fgfr3 or 4.

Another, Fgf8 related observation relates to limb induction, where the role of Fgf8 is still not clear for zebrafish development. However, the new evidence for the role of Fgfr4 in pectoral fin specification opens new possibilities for the early involvement of the Fgf ligands. Fgf8a is most likely involved in a redundant fashion together with other Fgfs. It would be worth investigating, which Fgf ligands act via Fgfr4 in the early fate determination within the lateral mesoderm.

4.13. TILLING as a method to generate knockout mutant fish

Targeted identification of the Fgfr mutants was, to a certain degree, disappointing. We did not recover any early nonsense mutations in fgfr1-3 genes (except for Fgfr1aIIIb isoform), and those we did recover in Fgfr4 were not disrupted, presumably due to alternative start of translation. The late nonsense mutations in turn, were difficult to interpret because of a complex genetic situation of the mutant fish. A combination of non-sense mediated decay and partial functional protein impairment is hard to interpret, because of problems in telling hypomorphs and null mutants apart.

Additionally, one is confronted with the accumulation of background mutations, which have to be eliminated through repeated and time-consuming rounds of outcrosses into wildtype backgrounds. Because the probability of obtaining null mutations is very low, it is challenging to prove allele specificity by complementation. Optimally, one needs to recover two presumptive null alleles in one gene or find a complementary mutant from the forward genetic screen. Control experiments with use of morpholinos may solve the question of specificity, however, only for early embryonic phenotypes.

Taken together, I found that the TILLING method can contribute to our understanding of gene function in development and adult homeostasis, however, it is beneficial to complement this approach with other, already established (e.g. morpholino) or newly discovered (e.g. zinc fingers) gene manipulation technologies.

5. Appendix

Appendix 1. Protein alignment of all zebrafish FGF receptors

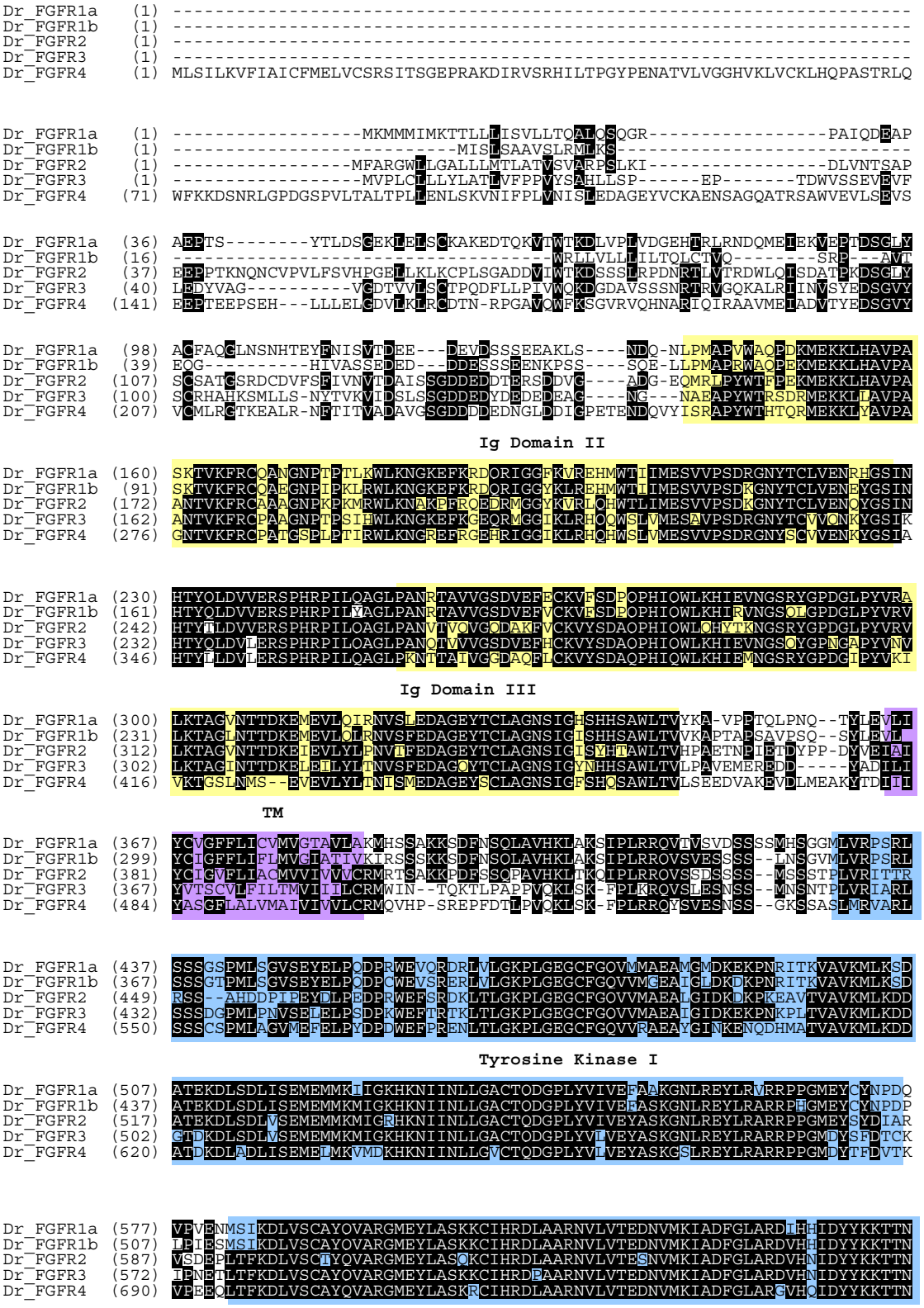

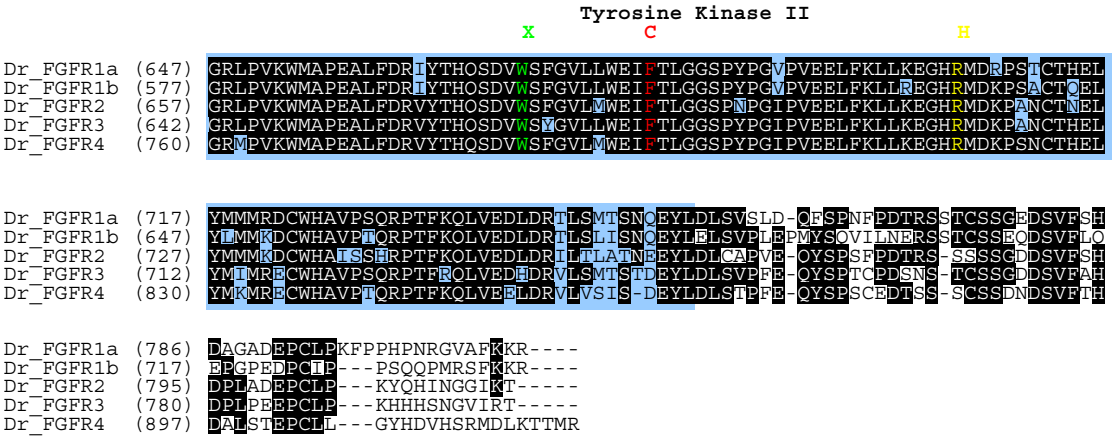

Appendix 2. Protein alignment of FGFR1a and b

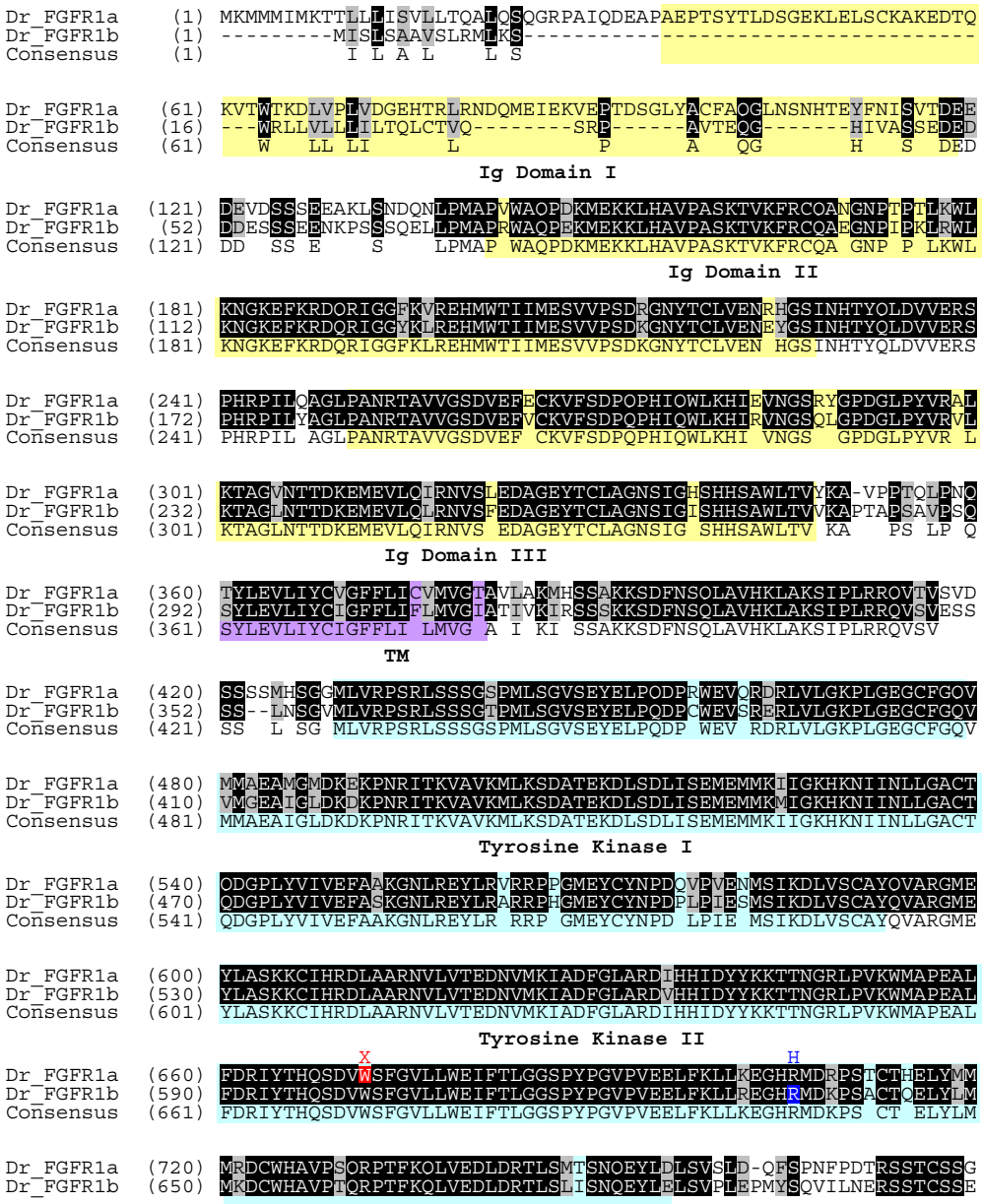

```
Consensus   (721) MKDCWHAVPSQRPTFKQLVEDLDRTLSL SNQEYLDLSV LD   FS       RSSTCSS

Dr_FGFR1a   (779) EDSVFSHDAGADEPCLPKFPPHPNRGVAFKKR
Dr_FGFR1b   (710) QDSVFLQEPGPEDPCIP---PSQQPMRSFKKR
Consensus   (781)  DSVF   D G DDPCIP    P  N    AFKKR
```

Appendix 3. Primer sequences for genotyping TILLING mutant fish

Fgfr primers TILLING mutants - annealing temp. 57ºC for all

304-zf-FGFR2-7-fwd-out	Tilling outer	TGATAAGACGAAGCTTGCAG	
305-zf-FGFR2-7-rev-out	Tilling outer	ATGCATGTGTGAATCCTGAG	434
306-zf-FGFR2-7-fwd-in	Tilling inner	**TGTAAAACGACGGCCAGT** TCAGCTGAGCAGGAAATAGG	
307-zf-FGFR2-7-rev-in	Tilling inner	**AGGAAACAGCTATGACCAT** CAGTTGGTTGTGTGGAACAG	288

308-zf-FGFR1-1819-fwd-out	TILLING outer	GCGGTCATAAAGGGATAAAG	
309-zf-FGFR1-1819-rev-out	TILLING outer	TGATGACACGTACAACTGGAG	692
310-zf-FGFR1-1819-fwd-in	Tilling inner	TGTAAAACGACGGCCAGT ATGTACTTTCATCCCAGCAG	
311-zf-FGFR1-1819-rev-in	Tilling inner	**AGGAAACAGCTATGACCAT** ACACACTCTCACCACACAAC	475

528-FGFR1-7-fwd-out	Tilling outer	AGAAATCAGAATCTGCCAAG	
529-FGFR1-7-rev-out	Tilling outer	AAAGGAGCGACGAGAAGAC	427
530-FGFR1-7-fwd-in	Tilling inner	**TGTAAAACGACGGCCAGT** CCACAGATTGTCCTAACCAG	
531-FGFR1-7-rev-in	Tilling inner	**AGGAAACAGCTATGACCAT** AGCTTGATTACCACCGTTTC	313

545-FGFR4-23-rev-out	Tilling outer	CCAATGGTTAACCTAGCTGAC	678
546-FGFR4-23-fwd-in	Tilling inner	**TGTAAAACGACGGCCAGT** AAACAGTGGTGATCTTTGTGAG	
547-FGFR4-23-rev-in	Tilling inner	AGGAAACAGCTATGACCAT ACCGCCCTGAAGATGAG	598
544-FGFR4-23-fwd-out	Tilling outer	TCCTTTGTTTGTGGCTTTG	

Appendix 4. Morpholino sequences

Fgfr1a
Translation blockers:
ATG Block: GCAGCAGCGTGGTCTTCATTATCAT
5' UTR1: ATCATCTTCATTATTATTATCAAAG
5' UTR2: CAAAGATCCTCTACATCTGAACTCC

Fgfr1b
Splice blocker:
E1/I1-2: CAAGAGAGCGCATGCTGCTTACGTA

Fgfr4
Translation blockers:
ATG: TGAAAACCTTTAAGATGCTCAACAT
5'UTR1: GATGCTCAACATCTTGCTGAGGTAA
5'UTR2: CAGCTTCAAATGCTGACTCCAGGCA

Splice blockers:
E6/I6-7: GGATATGTAGACCTGGTCATTTTCG
E8/I8-9: GCAAGCAGAAGCCCTCTTACCCAAC
E15/I15-16: GAAGCTAATTGAGCCCTTACTCTTT
E16/I16-17: TTTATAACTCACATTAGTTGTCTTC

p53
Standard: (Robu et al. 2007)

Appendix 5. Primers for morpholino validation

Fgfr1b
Forward: TGATCCTAACCCAGCTCTGC
Reverse: GGCATGAAGCTTTTTCTCCA

Fgfr4
FR4 e6 for 1: GTTTCAGAGGAGCCAACTGAG
FR4 e6 for 2: GAGGAACCATCAGAGCACCT
FR4 e6 rev1: TAGCTATCACTTTAAAACCGC
FR4 e6 rev 2: CCGCAAATTAATGGGAATG
FR4 e8 for 1: CACCATACTGGACTCACACTCA
FR4 e8 for 2: GGATGGAAAAGAAGCTGTATG
FR4 e8 rev 1: ATGTACAGCCTCGAGTGAACC
FR4 e8 rev 2: TGGTGCCTATGATGCAGC
FR4 e15 for 1: GCTGTACGTGCTGGTTGAA
FR4 e15 for 2: GCATCAAAAGGTAGCCTACG
FR4 e15 rev 1: GCTAGTAATACGATCCAGCGC
FR4 e15 rev 2: CGCCTGCTTGCTAACAGA
FR4 e16 for 1: GCATTCACAGAGATTTAGCCG
FR4 e16 for 2: GTTCTTGTGACAGAAGACAATGTG
FR4 e16 rev 1: CTGAAATTGGAAACAACAGGG
FR4 e16 rev 2: GCTGTGAGCGGGACAGTTAG

Appendix 6. Table of cloned constructs for this study

Number	Name	Gene	Vector
1	Fgfr1-GFP	Fgfr1a	pCS2+
2	Fgfr1-RFP	Fgfr1a	pCS2+
3	GFP-Fgfr1	Fgfr1a	pCS2+
4	Fgfr1-MYC	Fgfr1a	pCS2+
5	5'UTR-Fgfr1GFP	Fgfr1a	pCS2+
6	Fgfr1Y753STOP	Fgfr1a	pCS2+
7	Fgfr1Y753F	Fgfr1a	pCS2+
8	Fgfr1W671RFP	Fgfr1a	pCS2+
9	Fgfr1b full	Fgfr1b	pCR2TOPO
10	Fgfr1b_ish	Fgfr1b	pCR2TOPO
11	Fgfr2L545STOP	Fgfr2	pCS2+
12	Fgfr4 full	Fgfr4	pCR4TOPO
13	Grb2	Grb2	pCS2+
14	HA-Ub	Ubiquitin	pCDNA3.1

6. Software and websites

6.1. Software

Name of the application	Used for
Vector NTI for Mac	Sequence analysis, primer design, construct design, alignments
Finch TV 1.4.0	Sequencing chromatogram analysis
LAS AF 1.8.2	Confocal image acquisition and analysis
ImageJ	Confocal image/colocalization analysis
CellF	Stereomicroscope data acquisition
Adobe Photoshop CS2	Image analysis and preparation
Adobe Illustrator CS2	Figure assembly
EndNote 8.0	Literature library
Excel	Statistical analysis

6.2. Websites

URL	Used for
http://helix.wustl.edu/dcaps/dcaps.html	Primer design for single nucleotide polymorphism analysis
http://www.gene-tools.com/	Morpholino design and order
http://www.cbs.dtu.dk/services/SignalP/	Signal peptide prediction
http://vega.sanger.ac.uk/index.html	Zebrafish genomic DNA analysis, manual annotation data source
http://www.ensembl.org/Danio_rerio/index.html	Zebrafish genomic DNA analysis, automated annotation data source
http://zfin.org/	Zebrafish Research Database
http://www.expasy.org/sprot/	Protein structure prediction
http://www.proweb.org/input/ (CODDLE)	Codon Analysis For Predicting TILLING Lesions
http://limstill.niob.knaw.nl/	LIMSTILL for Identification of mutations by sequencing and TILLING, prediction tool
http://www.ihop-net.org/UniPub/iHOP/	Protein Interaction Network Prediction
http://fluorescence.nexus-solutions.net/frames6.htm	Chromophore Spectra Analysis
http://www.microscopyu.com/articles/livecellimaging/fpintro.html	Fluorescent Protein Properties
http://members.aol.com/_ht_a/lucatoldo/myhomepage/JaMBW/3/1/7/index.html	Antigenicity Plot for prediction of best peptides in antibody production

7. Literature

Alberts, B. (2002). Molecular biology of the cell. New York, Garland Science.

Albertson, R. C. and P. C. Yelick (2005). "Roles for fgf8 signaling in left-right patterning of the visceral organs and craniofacial skeleton." Dev Biol **283**(2): 310-21.

Allen, B. L. and A. C. Rapraeger (2003). "Spatial and temporal expression of heparan sulfate in mouse development regulates FGF and FGF receptor assembly." J Cell Biol **163**(3): 637-48.

Amaya, E., T. J. Musci, et al. (1991). "Expression of a dominant negative mutant of the FGF receptor disrupts mesoderm formation in Xenopus embryos." Cell **66**(2): 257-70.

Amsterdam, A. and N. Hopkins (2006). "Mutagenesis strategies in zebrafish for identifying genes involved in development and disease." Trends Genet **22**(9): 473-8.

Annaert, W. G., B. Becker, et al. (1997). "Export of cellubrevin from the endoplasmic reticulum is controlled by BAP31." J Cell Biol **139**(6): 1397-410.

Araki, I. and M. Brand (2001). "Morpholino-induced knockdown of fgf8 efficiently phenocopies the acerebellar (ace) phenotype." Genesis **30**(3): 157-9.

Arman, E., R. Haffner-Krausz, et al. (1998). "Targeted disruption of fibroblast growth factor (FGF) receptor 2 suggests a role for FGF signaling in pregastrulation mammalian development." Proc Natl Acad Sci U S A **95**(9): 5082-7.

Bellot, F., G. Crumley, et al. (1991). "Ligand-induced transphosphorylation between different FGF receptors." Embo J **10**(10): 2849-54.

Bokel, C. (2008). "EMS screens: from mutagenesis to screening and mapping." Methods Mol Biol **420**: 119-38.

Bottcher, R. T. and C. Niehrs (2005). "Fibroblast growth factor signaling during early vertebrate development." Endocr Rev **26**(1): 63-77.

Bottcher, R. T., N. Pollet, et al. (2004). "The transmembrane protein XFLRT3 forms a complex with FGF receptors and promotes FGF signalling." Nat Cell Biol **6**(1): 38-44.

Brand, M., C. P. Heisenberg, et al. (1996). "Mutations in zebrafish genes affecting the formation of the boundary between midbrain and hindbrain." Development **123**: 179-90.

Bryant, D. M., F. G. Wylie, et al. (2005). "Regulation of endocytosis, nuclear translocation, and signaling of fibroblast growth factor receptor 1 by E-cadherin." Mol Biol Cell **16**(1): 14-23.

Burgar, H. R., H. D. Burns, et al. (2002). "Association of the signaling adaptor FRS2 with fibroblast growth factor receptor 1 (Fgfr1) is mediated by alternative splicing of the juxtamembrane domain." J Biol Chem **277**(6): 4018-23.

Cabrita, M. A. and G. Christofori (2008). "Sprouty proteins, masterminds of receptor tyrosine kinase signaling." Angiogenesis **11**(1): 53-62.

Cao, H., J. Chen, et al. (2007). "Dynamin 2 mediates fluid-phase micropinocytosis in epithelial cells." J Cell Sci **120**(Pt 23): 4167-77.

Cao, Y., J. Zhao, et al. (2004). "fgf17b, a novel member of Fgf family, helps patterning zebrafish embryos." Dev Biol **271**(1): 130-43.

Casci, T., J. Vinos, et al. (1999). "Sprouty, an intracellular inhibitor of Ras signaling." Cell **96**(5): 655-65.

Chen, Y. A. and R. H. Scheller (2001). "SNARE-mediated membrane fusion." Nat Rev Mol Cell Biol **2**(2): 98-106.

Ciruna, B. G., L. Schwartz, et al. (1997). "Chimeric analysis of fibroblast growth factor receptor-1 (Fgfr1) function: a role for FGFR1 in morphogenetic movement through the primitive streak." Development **124**(14): 2829-41.

Colvin, J. S., B. A. Bohne, et al. (1996). "Skeletal overgrowth and deafness in mice lacking fibroblast growth factor receptor 3." Nat Genet **12**(4): 390-7.

Conner, S. D. and S. L. Schmid (2003). "Regulated portals of entry into the cell." Nature **422**(6927): 37-44.

Cross, M. J., L. Lu, et al. (2002). "The Shb adaptor protein binds to tyrosine 766 in the FGFR-1 and regulates the Ras/MEK/MAPK pathway via FRS2 phosphorylation in endothelial cells." Mol Biol Cell **13**(8): 2881-93.

Crossley, P. H., G. Minowada, et al. (1996). "Roles for FGF8 in the induction, initiation, and maintenance of chick limb development." Cell **84**(1): 127-36.

David, L., S. Blum, et al. (2003). "Recent duplication of the common carp (Cyprinus carpio L.) genome as revealed by analyses of microsatellite loci." Mol Biol Evol **20**(9): 1425-34.

De Moerlooze, L., B. Spencer-Dene, et al. (2000). "An important role for the IIIb isoform of fibroblast growth factor receptor 2 (FGFR2) in mesenchymal-epithelial signalling during mouse organogenesis." Development **127**(3): 483-92.

Deng, C., A. Wynshaw-Boris, et al. (1996). "Fibroblast growth factor receptor 3 is a negative regulator of bone growth." Cell **84**(6): 911-21.

Deng, C. X., A. Wynshaw-Boris, et al. (1994). "Murine FGFR-1 is required for early postimplantation growth and axial organization." Genes Dev **8**(24): 3045-57.

Dikic, I. (2003). "Mechanisms controlling EGF receptor endocytosis and degradation." Biochem Soc Trans **31**(Pt 6): 1178-81.

Draper, B. W., P. A. Morcos, et al. (2001). "Inhibition of zebrafish fgf8 pre-mRNA splicing with morpholino oligos: a quantifiable method for gene knockdown." Genesis **30**(3): 154-6.

Draper, B. W., D. W. Stock, et al. (2003). "Zebrafish fgf24 functions with fgf8 to promote posterior mesodermal development." Development **130**(19): 4639-54.

Dubrulle, J. and O. Pourquie (2004). "fgf8 mRNA decay establishes a gradient that couples axial elongation to patterning in the vertebrate embryo." Nature **427**(6973): 419-22.

Durai, S., M. Mani, et al. (2005). "Zinc finger nucleases: custom-designed molecular scissors for genome engineering of plant and mammalian cells." Nucleic Acids Res **33**(18): 5978-90.

Eisen, J. S. and J. C. Smith (2008). "Controlling morpholino experiments: don't stop making antisense." Development **135**(10): 1735-43.

Ekker, S. C. (2008). "Zinc finger-based knockout punches for zebrafish genes." Zebrafish **5**(2): 121-3.

Eswarakumar, V. P., I. Lax, et al. (2005). "Cellular signaling by fibroblast growth factor receptors." Cytokine Growth Factor Rev **16**(2): 139-49.

Fischer, S., B. W. Draper, et al. (2003). "The zebrafish fgf24 mutant identifies an additional level of Fgf signaling involved in vertebrate forelimb initiation." Development **130**(15): 3515-24.

Furthauer, M., C. Thisse, et al. (1997). "A role for FGF-8 in the dorsoventral patterning of the zebrafish gastrula." Development **124**(21): 4253-64.

Furutani-Seiki, M. and J. Wittbrodt (2004). "Medaka and zebrafish, an evolutionary twin study." Mech Dev **121**(7-8): 629-37.

Geisler, R., G. J. Rauch, et al. (2007). "Large-scale mapping of mutations affecting zebrafish development." BMC Genomics **8**: 11.

Gilbert, S. F. (2006). Developmental biology. Sunderland, Mass., Sinauer.

Grandel, H., K. Lun, et al. (2002). "Retinoic acid signalling in the zebrafish embryo is necessary during pre-segmentation stages to pattern the anterior-posterior axis of the CNS and to induce a pectoral fin bud." Development **129**(12): 2851-65.

Gruenberg, J. and F. R. Maxfield (1995). "Membrane transport in the endocytic pathway." Curr Opin Cell Biol **7**(4): 552-63.

Guy, G. R., E. S. Wong, et al. (2003). "Sprouty: how does the branch manager work?" J Cell Sci **116**(Pt 15): 3061-8.

Haffter, P., M. Granato, et al. (1996). "The identification of genes with unique and essential functions in the development of the zebrafish, Danio rerio." Development **123**: 1-36.

Haglund, K. and I. Dikic (2005). "Ubiquitylation and cell signaling." Embo J **24**(19): 3353-9.

Haglund, K., S. Sigismund, et al. (2003). "Multiple monoubiquitination of RTKs is sufficient for their endocytosis and degradation." Nat Cell Biol **5**(5): 461-6.

Halevy, O., E. Monsonego, et al. (1994). "A new avian fibroblast growth factor receptor in myogenic and chondrogenic cell differentiation." Exp Cell Res **212**(2): 278-84.

Hanover, J. A., M. C. Willingham, et al. (1984). "Kinetics of transit of transferrin and epidermal growth factor through clathrin-coated membranes." Cell **39**(2 Pt 1): 283-93.

Hashiguchi, Y. and M. Nishida (2005). "Evolution of vomeronasal-type odorant receptor genes in the zebrafish genome." Gene **362**: 19-28.

Haugsten, E. M., J. Malecki, et al. (2008). "Ubiquitination of fibroblast growth factor receptor 1 is required for its intracellular sorting but not for its endocytosis." Mol Biol Cell **19**(8): 3390-403.

Haugsten, E. M., V. Sorensen, et al. (2005). "Different intracellular trafficking of FGF1 endocytosed by the four homologous FGF receptors." J Cell Sci **118**(Pt 17): 3869-81.

Henikoff, S., B. J. Till, et al. (2004). "TILLING. Traditional mutagenesis meets functional genomics." Plant Physiol **135**(2): 630-6.

Henley, J. R., H. Cao, et al. (1999). "Participation of dynamin in the biogenesis of cytoplasmic vesicles." Faseb J **13 Suppl 2**: S243-7.

Henley, J. R., E. W. Krueger, et al. (1998). "Dynamin-mediated internalization of caveolae." J Cell Biol **141**(1): 85-99.

Horton, W. A., J. G. Hall, et al. (2007). "Achondroplasia." Lancet **370**(9582): 162-72.

Huang, F., L. K. Goh, et al. (2007). "EGF receptor ubiquitination is not necessary for its internalization." Proc Natl Acad Sci U S A **104**(43): 16904-9.

Hufnagel, L., J. Kreuger, et al. (2006). "On the role of glypicans in the process of morphogen gradient formation." Dev Biol **300**(2): 512-22.

Itoh, N. (2007). "The Fgf families in humans, mice, and zebrafish: their evolutional processes and roles in development, metabolism, and disease." Biol Pharm Bull **30**(10): 1819-25.

Itoh, N. and M. Konishi (2007). "The zebrafish fgf family." Zebrafish **4**(3): 179-86.

Itoh, N. and D. M. Ornitz (2004). "Evolution of the Fgf and Fgfr gene families." Trends Genet **20**(11): 563-9.

Jovelin, R., X. He, et al. (2007). "Duplication and divergence of fgf8 functions in teleost development and evolution." J Exp Zoolog B Mol Dev Evol **308**(6): 730-43.

Jukkola, T., L. Lahti, et al. (2006). "FGF regulated gene-expression and neuronal differentiation in the developing midbrain-hindbrain region." Dev Biol **297**(1): 141-57.

Kavsak, P., R. K. Rasmussen, et al. (2000). "Smad7 binds to Smurf2 to form an E3 ubiquitin ligase that targets the TGF beta receptor for degradation." Mol Cell **6**(6): 1365-75.

Keegan, B. R., J. L. Feldman, et al. (2005). "Retinoic acid signaling restricts the cardiac progenitor pool." Science **307**(5707): 247-9.

Kimmel, C. B., W. W. Ballard, et al. (1995). "Stages of embryonic development of the zebrafish." Dev Dyn **203**(3): 253-310.

Klock, A. and B. G. Herrmann (2002). "Cloning and expression of the mouse dual-specificity mitogen-activated protein (MAP) kinase phosphatase Mkp3 during mouse embryogenesis." Mech Dev **116**(1-2): 243-7.

Kondoh, K. and E. Nishida (2007). "Regulation of MAP kinases by MAP kinase phosphatases." Biochim Biophys Acta **1773**(8): 1227-37.

Kornberg, T. B. and A. Guha (2007). "Understanding morphogen gradients: a problem of dispersion and containment." Curr Opin Genet Dev **17**(4): 264-71.

Kurita, K. and N. Sakai (2004). "Functionally distinctive testicular cell lines of zebrafish to support male germ cell development." Mol Reprod Dev **67**(4): 430-8.

Kwiatkowski, B. A., I. Kirillova, et al. (2008). "FGFR4 and its novel splice form in myogenic cells: Interplay of glycosylation and tyrosine phosphorylation." J Cell Physiol **215**(3): 803-17.

Lawson, N. D., J. W. Mugford, et al. (2003). "phospholipase C gamma-1 is required downstream of vascular endothelial growth factor during arterial development." Genes Dev **17**(11): 1346-51.

Lin, X., E. M. Buff, et al. (1999). "Heparan sulfate proteoglycans are essential for FGF receptor signaling during Drosophila embryonic development." Development **126**(17): 3715-23.

Livak, K. J. and T. D. Schmittgen (2001). "Analysis of relative gene expression data using real-time quantitative PCR and the 2(-Delta Delta C(T)) Method." Methods **25**(4): 402-8.

Ma, A. C., R. Liang, et al. (2007). "The role of phospholipase C gamma 1 in primitive hematopoiesis during zebrafish development." Exp Hematol **35**(3): 368-73.

Marcelle, C., A. Eichmann, et al. (1994). "Distinct developmental expression of a new avian fibroblast growth factor receptor." Development **120**(3): 683-94.

Mariani, F. V., C. P. Ahn, et al. (2008). "Genetic evidence that FGFs have an instructive role in limb proximal-distal patterning." Nature **453**(7193): 401-5.

Marics, I., F. Padilla, et al. (2002). "FGFR4 signaling is a necessary step in limb muscle differentiation." Development **129**(19): 4559-69.

Marques, S. R., Y. Lee, et al. (2008). "Reiterative roles for FGF signaling in the establishment of size and proportion of the zebrafish heart." Dev Biol **321**(2): 397-406.

Martin, B. L. and D. Kimelman (2008). "Regulation of canonical Wnt signaling by Brachyury is essential for posterior mesoderm formation." Dev Cell **15**(1): 121-33.

Maves, L. and C. B. Kimmel (2005). "Dynamic and sequential patterning of the zebrafish posterior hindbrain by retinoic acid." Dev Biol **285**(2): 593-605.

McCullough, J., M. J. Clague, et al. (2004). "AMSH is an endosome-associated ubiquitin isopeptidase." J Cell Biol **166**(4): 487-92.

McMahon, H. T., Y. A. Ushkaryov, et al. (1993). "Cellubrevin is a ubiquitous tetanus-toxin substrate homologous to a putative synaptic vesicle fusion protein." Nature **364**(6435): 346-9.

Meng, X., M. B. Noyes, et al. (2008). "Targeted gene inactivation in zebrafish using engineered zinc-finger nucleases." Nat Biotechnol **26**(6): 695-701.

Mercader, N., S. Fischer, et al. (2006). "Prdm1 acts downstream of a sequential RA, Wnt and Fgf signaling cascade during zebrafish forelimb induction." Development **133**(15): 2805-15.

Meyers, E. N., M. Lewandoski, et al. (1998). "An Fgf8 mutant allelic series generated by Cre- and Flp-mediated recombination." Nat Genet **18**(2): 136-41.

Min, H., D. M. Danilenko, et al. (1998). "Fgf-10 is required for both limb and lung development and exhibits striking functional similarity to Drosophila branchless." Genes Dev **12**(20): 3156-61.

Mohammadi, M., I. Dikic, et al. (1996). "Identification of six novel autophosphorylation sites on fibroblast growth factor receptor 1 and elucidation of their importance in receptor activation and signal transduction." Mol Cell Biol **16**(3): 977-89.

Mohammadi, M., A. M. Honegger, et al. (1991). "A tyrosine-phosphorylated carboxy-terminal peptide of the fibroblast growth factor receptor (Flg) is a binding site for the SH2 domain of phospholipase C-gamma 1." Mol Cell Biol **11**(10): 5068-78.

Mohammadi, M., G. McMahon, et al. (1997). "Structures of the tyrosine kinase domain of fibroblast growth factor receptor in complex with inhibitors." Science **276**(5314): 955-60.

Monsonego-Ornan, E., R. Adar, et al. (2002). "FGF receptors ubiquitylation: dependence on tyrosine kinase activity and role in downregulation." FEBS Lett **528**(1-3): 83-9.

Moon, A. M. and M. R. Capecchi (2000). "Fgf8 is required for outgrowth and patterning of the limbs." Nat Genet **26**(4): 455-9.

Mori, S., L. Claesson-Welsh, et al. (1995). "Ligand-induced polyubiquitination of receptor tyrosine kinases." Biochem Biophys Res Commun **213**(1): 32-9.

Moss, M. L. (1961). "Osteogenesis of acellular teleost fish bone." American Journal of Anatomy **108**(1): 99-109.

Moss, M. L. (1963). "The biology of acellular teleost bone." Ann N Y Acad Sci **109**: 337-50.

Mousavi, S. A., L. Malerod, et al. (2004). "Clathrin-dependent endocytosis." Biochem J **377**(Pt 1): 1-16.

Myers, J. M., G. G. Martins, et al. (2003). "Nuclear trafficking of FGFR1: a role for the transmembrane domain." J Cell Biochem **88**(6): 1273-91.

Nakayama, Y., A. Miyake, et al. (2008). "Fgf19 is required for zebrafish lens and retina development." Dev Biol **313**(2): 752-66.

Naviglio, S., C. Mattecucci, et al. (1998). "UBPY: a growth-regulated human ubiquitin isopeptidase." Embo J **17**(12): 3241-50.

Nomura, R., E. Kamei, et al. (2006). "Fgf16 is essential for pectoral fin bud formation in zebrafish." Biochem Biophys Res Commun **347**(1): 340-6.

Ornitz, D. M. and N. Itoh (2001). "Fibroblast growth factors." Genome Biol **2**(3): REVIEWS3005.

Ornitz, D. M., J. Xu, et al. (1996). "Receptor specificity of the fibroblast growth factor family." J Biol Chem **271**(25): 15292-7.

Park, P. W., O. Reizes, et al. (2000). "Cell surface heparan sulfate proteoglycans: selective regulators of ligand-receptor encounters." J Biol Chem **275**(39): 29923-6.

Partanen, J., L. Schwartz, et al. (1998). "Opposite phenotypes of hypomorphic and Y766 phosphorylation site mutations reveal a function for Fgfr1 in anteroposterior patterning of mouse embryos." Genes Dev **12**(15): 2332-44.

Parton, R. G. and A. A. Richards (2003). "Lipid rafts and caveolae as portals for endocytosis: new insights and common mechanisms." Traffic **4**(11): 724-38.

Pelkmans, L., T. Burli, et al. (2004). "Caveolin-stabilized membrane domains as multifunctional transport and sorting devices in endocytic membrane traffic." Cell **118**(6): 767-80.

Pellegrini, L., D. F. Burke, et al. (2000). "Crystal structure of fibroblast growth factor receptor ectodomain bound to ligand and heparin." Nature **407**(6807): 1029-34.

Phillips, B. T., K. Bolding, et al. (2001). "Zebrafish fgf3 and fgf8 encode redundant functions required for otic placode induction." Dev Biol **235**(2): 351-65.

Picker, A. and M. Brand (2005). "Fgf signals from a novel signaling center determine axial patterning of the prospective neural retina." Development **132**(22): 4951-62.

Picker, A., C. Brennan, et al. (1999). "Requirement for the zebrafish mid-hindbrain boundary in midbrain polarisation, mapping and confinement of the retinotectal projection." Development **126**(13): 2967-78.

Pirvola, U., B. Spencer-Dene, et al. (2000). "FGF/FGFR-2(IIIb) signaling is essential for inner ear morphogenesis." J Neurosci **20**(16): 6125-34.

Praefcke, G. J., M. G. Ford, et al. (2004). "Evolving nature of the AP2 alpha-appendage hub during clathrin-coated vesicle endocytosis." Embo J **23**(22): 4371-83.

Raible, F. and M. Brand (2001). "Tight transcriptional control of the ETS domain factors Erm and Pea3 by Fgf signaling during early zebrafish development." Mech Dev **107**(1-2): 105-17.

Raiborg, C., L. Malerod, et al. (2008). "Differential functions of Hrs and ESCRT proteins in endocytic membrane trafficking." Exp Cell Res **314**(4): 801-13.

Raiborg, C., T. E. Rusten, et al. (2003). "Protein sorting into multivesicular endosomes." Curr Opin Cell Biol **15**(4): 446-55.

Rawls, J. F., M. R. Frieda, et al. (2003). "Coupled mutagenesis screens and genetic mapping in zebrafish." Genetics **163**(3): 997-1009.

Reifers, F., H. Bohli, et al. (1998). "Fgf8 is mutated in zebrafish acerebellar (ace) mutants and is required for maintenance of midbrain-hindbrain boundary development and somitogenesis." Development **125**(13): 2381-95.

Reifers, F., E. C. Walsh, et al. (2000). "Induction and differentiation of the zebrafish heart requires fibroblast growth factor 8 (fgf8/acerebellar)." Development **127**(2): 225-35.

Reilly, J. F., E. Mizukoshi, et al. (2004). "Ligand dependent and independent internalization and nuclear translocation of fibroblast growth factor (FGF) receptor 1." DNA Cell Biol **23**(9): 538-48.

Robu, M. E., J. D. Larson, et al. (2007). "p53 activation by knockdown technologies." PLoS Genet **3**(5): e78.

Rodriguez-Esteban, C., T. Tsukui, et al. (1999). "The T-box genes Tbx4 and Tbx5 regulate limb outgrowth and identity." Nature **398**(6730): 814-8.

Sambrook, J. and D. W. Russell (2001). Molecular cloning: a laboratory manual. Cold Spring Harbor, NY, Cold Spring Harbor Laboratory Press.

Schmahl, J., Y. Kim, et al. (2004). "Fgf9 induces proliferation and nuclear localization of FGFR2 in Sertoli precursors during male sex determination." Development **131**(15): 3627-36.

Scholpp, S. and M. Brand (2004). "Endocytosis controls spreading and effective signaling range of Fgf8 protein." Curr Biol **14**(20): 1834-41.

Scholpp, S., C. Groth, et al. (2004). "Zebrafish fgfr1 is a member of the fgf8 synexpression group and is required for fgf8 signalling at the midbrain-hindbrain boundary." Dev Genes Evol **214**(6): 285-95.

Shanmugalingam, S., C. Houart, et al. (2000). "Ace/Fgf8 is required for forebrain commissure formation and patterning of the telencephalon." Development **127**(12): 2549-61.

Sharrocks, A. D., A. L. Brown, et al. (1997). "The ETS-domain transcription factor family." Int J Biochem Cell Biol **29**(12): 1371-87.

Shimada, A., M. Yabusaki, et al. (2008). "Maternal-zygotic medaka mutants for fgfr1 reveal its essential role in the migration of the axial mesoderm but not the lateral mesoderm." Development **135**(2): 281-90.

Shiotsugu, J., Y. Katsuyama, et al. (2004). "Multiple points of interaction between retinoic acid and FGF signaling during embryonic axis formation." Development **131**(11): 2653-67.

Sigismund, S., E. Argenzio, et al. (2008). "Clathrin-mediated internalization is essential for sustained EGFR signaling but dispensable for degradation." Dev Cell **15**(2): 209-19.

Sigismund, S., T. Woelk, et al. (2005). "Clathrin-independent endocytosis of ubiquitinated cargos." Proc Natl Acad Sci U S A **102**(8): 2760-5.

Sivak, J. M., L. F. Petersen, et al. (2005). "FGF signal interpretation is directed by Sprouty and Spred proteins during mesoderm formation." Dev Cell **8**(5): 689-701.

Sleptsova-Friedrich, I., Y. Li, et al. (2001). "fgfr3 and regionalization of anterior neural tube in zebrafish." Mech Dev **102**(1-2): 213-7.

Sorensen, V., A. Wiedlocha, et al. (2006). "Different abilities of the four FGFRs to mediate FGF-1 translocation are linked to differences in the receptor C-terminal tail." J Cell Sci **119**(Pt 20): 4332-41.

Sorkin, A. and L. K. Goh (2008). "Endocytosis and intracellular trafficking of ErbBs." Exp Cell Res.

Sorokin, A., M. Mohammadi, et al. (1994). "Internalization of fibroblast growth factor receptor is inhibited by a point mutation at tyrosine 766." J Biol Chem **269**(25): 17056-61.

Soubeyran, P., K. Kowanetz, et al. (2002). "Cbl-CIN85-endophilin complex mediates ligand-induced downregulation of EGF receptors." Nature **416**(6877): 183-7.

Stern, H. M., R. D. Murphey, et al. (2005). "Small molecules that delay S phase suppress a zebrafish bmyb mutant." Nat Chem Biol **1**(7): 366-70.

Sugaya, N., H. Habuchi, et al. (2008). "6-O-sulfation of heparan sulfate differentially regulates various fibroblast growth factor-dependent signalings in culture." J Biol Chem **283**(16): 10366-76.

Summerton, J. and D. Weller (1997). "Morpholino antisense oligomers: design, preparation, and properties." Antisense Nucleic Acid Drug Dev **7**(3): 187-95.

Sun, X., F. V. Mariani, et al. (2002). "Functions of FGF signalling from the apical ectodermal ridge in limb development." Nature **418**(6897): 501-8.

Takeuchi, Y., K. Molyneaux, et al. (2005). "The roles of FGF signaling in germ cell migration in the mouse." Development **132**(24): 5399-409.

Tamimi, Y., J. M. Skarie, et al. (2006). "FGF19 is a target for FOXC1 regulation in ciliary body-derived cells." Hum Mol Genet **15**(21): 3229-40.

Tamura, K., S. Yonei-Tamura, et al. (1999). "Differential expression of Tbx4 and Tbx5 in Zebrafish fin buds." Mech Dev **87**(1-2): 181-4.

Thisse, B. and C. Thisse (2005). "Functions and regulations of fibroblast growth factor signaling during embryonic development." Dev Biol **287**(2): 390-402.

Thisse, B., C. Thisse, et al. (1995). "Novel FGF receptor (Z-FGFR4) is dynamically expressed in mesoderm and neurectoderm during early zebrafish embryogenesis." Dev Dyn **203**(3): 377-91.

Thummel, R., S. Bai, et al. (2006). "Inhibition of zebrafish fin regeneration using in vivo electroporation of morpholinos against fgfr1 and msxb." Dev Dyn **235**(2): 336-46.

Till, B. J., S. H. Reynolds, et al. (2003). "Large-scale discovery of induced point mutations with high-throughput TILLING." Genome Res **13**(3): 524-30.

Trokovic, N., R. Trokovic, et al. (2003). "Fgfr1 regulates patterning of the pharyngeal region." Genes Dev **17**(1): 141-53.

Trokovic, R., T. Jukkola, et al. (2005). "Fgfr1-dependent boundary cells between developing mid- and hindbrain." Dev Biol **278**(2): 428-39.

Trueb, B., S. C. Neuhauss, et al. (2005). "Fish possess multiple copies of fgfrl1, the gene for a novel FGF receptor." Biochim Biophys Acta **1727**(1): 65-74.

Tsang, M., R. Friesel, et al. (2002). "Identification of Sef, a novel modulator of FGF signalling." Nat Cell Biol **4**(2): 165-9.

Tsang, M., S. Maegawa, et al. (2004). "A role for MKP3 in axial patterning of the zebrafish embryo." Development **131**(12): 2769-79.

Ueda, Y., S. Hirai, et al. (1996). "Protein kinase C activates the MEK-ERK pathway in a manner independent of Ras and dependent on Raf." J Biol Chem **271**(38): 23512-9.

Ullrich, A. and J. Schlessinger (1990). "Signal transduction by receptors with tyrosine kinase activity." Cell **61**(2): 203-12.

Ullrich, O., S. Reinsch, et al. (1996). "Rab11 regulates recycling through the pericentriolar recycling endosome." J Cell Biol **135**(4): 913-24.

Vieira, C. and S. Martinez (2005). "Experimental study of MAP kinase phosphatase-3 (Mkp3) expression in the chick neural tube in relation to Fgf8 activity." Brain Res Brain Res Rev **49**(2): 158-66.

Wakioka, T., A. Sasaki, et al. (2001). "Spred is a Sprouty-related suppressor of Ras signalling." Nature **412**(6847): 647-51.

Wang, J. K., G. Gao, et al. (1994). "Fibroblast growth factor receptors have different signaling and mitogenic potentials." Mol Cell Biol **14**(1): 181-8.

Weinstein, M., X. Xu, et al. (1998). "FGFR-3 and FGFR-4 function cooperatively to direct alveogenesis in the murine lung." Development **125**(18): 3615-23.

Westerfield, M. (2000). The zebrafish book: a guide for the laboratory use of zebrafish (Danio rerio). [Eugene, OR], M. Westerfield.

White, R. J., Q. Nie, et al. (2007). "Complex regulation of cyp26a1 creates a robust retinoic acid gradient in the zebrafish embryo." PLoS Biol **5**(11): e304.

Winkler, S., A. Schwabedissen, et al. (2005). "Target-selected mutant screen by TILLING in Drosophila." Genome Res **15**(5): 718-23.

Wouters, F. S. and P. I. Bastiaens (1999). "Fluorescence lifetime imaging of receptor tyrosine kinase activity in cells." Curr Biol **9**(19): 1127-30.

Xie, M. H., I. Holcomb, et al. (1999). "FGF-19, a novel fibroblast growth factor with unique specificity for FGFR4." Cytokine **11**(10): 729-35.

Xu, X., M. Weinstein, et al. (1999). "Fibroblast growth factor receptors (FGFRs) and their roles in limb development." Cell Tissue Res **296**(1): 33-43.

Xu, X., M. Weinstein, et al. (1998). "Fibroblast growth factor receptor 2 (FGFR2)-mediated reciprocal regulation loop between FGF8 and FGF10 is essential for limb induction." Development **125**(4): 753-65.

Yamaguchi, T. P., K. Harpal, et al. (1994). "fgfr-1 is required for embryonic growth and mesodermal patterning during mouse gastrulation." Genes Dev **8**(24): 3032-44.

Yamaguchi, T. P. and J. Rossant (1995). "Fibroblast growth factors in mammalian development." Curr Opin Genet Dev **5**(4): 485-91.

Yan, D. and X. Lin (2007). "Drosophila glypican Dally-like acts in FGF-receiving cells to modulate FGF signaling during tracheal morphogenesis." Dev Biol **312**(1): 203-16.

Yokoi, H., A. Shimada, et al. (2007). "Mutant analyses reveal different functions of fgfr1 in medaka and zebrafish despite conserved ligand-receptor relationships." Dev Biol **304**(1): 326-37.

Yu, K., J. Xu, et al. (2003). "Conditional inactivation of FGF receptor 2 reveals an essential role for FGF signaling in the regulation of osteoblast function and bone growth." Development **130**(13): 3063-74.

Zerial, M. and H. McBride (2001). "Rab proteins as membrane organizers." Nat Rev Mol Cell Biol **2**(2): 107-17.

Zhang, X., O. A. Ibrahimi, et al. (2006). "Receptor specificity of the fibroblast growth factor family. The complete mammalian FGF family." J Biol Chem **281**(23): 15694-700.

8. List of publications

Part of this work has been included in the following manuscript:

Nicolas Rohner, Miklós Bercsényi, László Orbán, **Maria E. Kolanczyk**, Dirk Linke, Michael Brand, Christiane Nüsslein-Volhard, Matthew P. Harris (2009) “Fibroblast Growth Factor Signalling is a Target for Selection in Domestication” (submitted to Science)